A TWISTORIAL DESCRIPTION OF THE NULL DYNAMICS OF MAXWELL-DIRAC FIELDS

by

J.G. CARDOSO

THESIS SUBMITTED IN PARTIAL FULFILMENT OF THE REQUIREMENTS FOR THE DEGREE OF DOCTOR OF PHILOSOPHY

Department of Mathematics
Quaid-i-Azam University
Islamabad, Pakistan
1992

TABLE OF CONTENTS

ACKNOWLEDGMENTS

I am deeply indebted to Professor Roger Penrose for introducing me to the techniques upon which my thesis is essentially based. I am most grateful to Dr. Asghar Qadir for his continuous supervision during the period over which this work was elaborated. My warmest thanks go to both the World Laboratory and the Dr. Abdul Hafeez Khan Foundation for supporting my project financially. I should like to acknowledge also the Third World Academy of Sciences for a relevant travel grant.

LIST OF PAPERS COMING OUT OF THE THESIS

1. NULL DESCRIPTION OF THE DYNAMICS OF CLASSICAL MAXWELL-DIRAC FIELDS
2. A TWISTORIAL DESCRIPTION OF CLASSICAL MAXWELL-DIRAC FIELDS
3. CONSTRUCTION OF A NEW NULL-TWISTOR DIAGRAMMATIC STRUCTURE
4. NEW TWISTOR DIAGRAMS FOR MAXWELL-DIRAC FIELDS

ABSTRACT

Penrose's null initial data techniques are used to treat systematically the classical Maxwell-Dirac system in real Minkowski space. On the basis of the structure of the field equations a graphical device is constructed which enables one to label the distributional elements of the corresponding infinite invariant exact set in terms of colored graphs. Upon carrying out the actual evaluation of the elementary contributions, general prescriptions are provided whereby the trees may be completely specified. Each such tree turns out to be associated with a manifestly scaling invariant finite integral which is taken over a compact space of appropriate null Minkowski configurations. In particular, the integrals describing the processes of electromagnetic scattering of Dirac fields are taken over spaces of forked null zigzags that start at the origin and terminate at a fixed point lying in the interior of the future null cone of the origin. Subsequently, certain transcription techniques are employed to translate directly the entire basic set of scattering formulae into the framework of twistor theory. The contours over which the resulting twistor scattering integrals appear to be taken are defined explicitly. A simple correspondence between scattering diagrams and twistor diagrams is then suggested.

CHAPTER ONE

GENERAL INTRODUCTION

Penrose's null initial data (NID) techniques [1-3] constitute a general framework for describing the dynamics of sets of interacting spinor fields in both flat and curved space-times. This null approach was designed to treat a form of initial value problem in which the initial data for all fields are specified at non-singular points of null hypersurfaces. Roughly speaking, the elements of an NID set are defined as those components of the fields which are associated with the (null) directions of the generators of some NID hypersurface. In general, such initial data carry twice as much information per space-time point as those for the corresponding space-like hypersurface initial value problem since an arbitrary null datum is locally specified by a pair of real numbers. Hence the null-hypersurface initial data generally provide one-half the number of real-valued scalar functions that are required in the ordinary space-like approach. One of the key concepts upon which these techniques are based is that of an invariant exact set (IES). The striking feature of such a field set is that the (local) algebraic relations defining its exactness do not involve gauge-dependent quantities explicitly. All interactions thus appear as field equations or else as commutation relations involving covariant derivatives along with the fields themselves. Once we are given an IES, we can state that the field equations propagate the fields in a non-redundant way throughout the relevant space-time

domain. Likewise all the constraints which would occur in the space-like treatment are automatically eliminated from the basis of the theory.

According to the standard methods, the actual evaluation of the fields is carried out by using either power series expansions or integral devices. In the former case, one usually requires the fields to be analytic on their domain of definition. In the event that the fields constitute an IES, the knowledge of NID at some point of the domain thus enables one to evaluate the fields explicitly at any other relevant point. In the latter case, the analiticity requirement is not strictly necessary, but the fields have to form an IES on real Minkowski space ($\mathbb{RM}$) in addition to being well-behaved on two-real-dimensional space-like regions provided by intersections between NID hypersurfaces and appropriate null cones, whose topology is indeed S^2.

Actually, there are two types of integral expressions for the elements of an IES. One is the spinning generalization of the Kirchoff-D'Adhemar integrals for massless scalar fields proposed by Penrose (see, for instance, Ref.[3]). The Kirchoff-D'Adhemar-Penrose (KAP) field integrals can be looked upon as being linearly composed of proper Lorentz invariant distributional pieces whenever the NID for the fields are specified on a null cone. Their integrands are scaling invariant (SI) two-forms on two-spheres which appear to play a very important role in the null description of scattering processes. Each field integral of the other type arises in situations which involve also integrations along null geodesics of $\mathbb{RM}$. These latter field expressions carry SI three-volume forms, and appear as explicit convolutions taken

over NID hypersurfaces. Such features afford us an invariant method for treating IES's of interacting fields in a systematic way. The basic prescription consists in splitting the fields into an infinite number of elementary contributions that satisfy symbolic field density equations (FDE) on the interior of the NID cone which are essentially of the same form as those controlling the propagation of the system of interest. Towards achieving the recovery of the entire fields, we have first to set up general prescriptions for calculating explicitly an elementary distributional field of arbitrary order, and then to add appropriately all the pieces together. When scattering processes are effectively allowed for, the outgoing fields appear as SI expressions which generally involve both types of field integrals. Under these circumstances, the elementary contributions propagate for a while as massless free fields, but scatter off each other at suitable points lying in the interior of the NID cone. To any order, each of the corresponding field integrals involves, in effect, a KAP-differential form defined at the point at which the process giving rise to the outgoing field happens, together with SI volume forms which take into account the contributions coming from all the other relevant interior points as well as those emanating from the NID cone. Both the charge and the helicity of the incoming fields are preserved when electromagnetic scattering processes are considered alone. The NID hypersurfaces for higher-order scattering processes are actually defined as pieces of light cones of appropriate interior points. In the case of either integral pattern, the usually required normal and tangential derivatives at points of the initial data hypersurface are

combined and made into directional derivatives defined along (null) geodesics lying on NID hypersurfaces. It can therefore be said that the generators of NID hypersurfaces appear to play a double role. They first pick out those components of the fields which enter into the defining expressions for the relevant NID. Then they single out those space-time directions along which the derivatives, occurring explicitly in the integral expressions, are defined.

The explicit integral expression for any distributional field can always be thought of as being taken over an abstract space of suitably connected null graphs that start at the vertex of the NID cone and terminate at a fixed interior point. These graphs are equipped with forward spin basis sets whose elements contribute appropriate inner products to the relevant NID, the end-vertices being taken to coincide with the point at which the elementary field is to be evaluated. All the null data involved in the actual evaluation of the contribution in question are specified at those vertices of the graphs at which the relevant differential forms are set up. It appears that the expression for the null datum for any scattering process explicitly carries only internal edges of the relevant graphs. Furthermore, the spin-inner-product structures arising from the relevant calculations lead automatically to an unambiguous vertex configuration for each graph whence all the processes turn out to be specified by the edge-vertex structures of the scattering diagrams. The information about the NID for all the processes is totally carried by suitably contracted first derivatives of the elements of the spin bases.

These null methods were used earlier [4-6] for describing

completely the dynamics of classical Dirac fields, based upon the fact that the Van der Waarden form of the Dirac equation [7-10], in $\mathbb{RM}$, allows one to treat the Dirac pair as an IES of interacting spinor fields, the rest-mass of the fields playing the role of a coupling constant. In respect of the description of the mass-scattering processes [5,6], each of the entire fields is given as the sum of two infinite series of terms which appear as manifestly SI integrals taken over (compact) spaces of null zigzags in $\mathbb{RM}$ carrying adequate edge-vertex structures. The formal simplicity of the resulting scattering formulae was due to the choice of the future null cone $\mathscr{C}_o^+$ of an origin O of $\mathbb{RM}$ as the NID hypersurface for all the elementary fields. All the stages of the calculations involved were carried out straightforwardly insofar as the elementary distributional fields for this system might be labelled in a trivial (linear) way. Nevertheless, for an arbitrary IES, it is not generally possible to label the elements of its associated infinite set in this way. For such systems, we have to build up a colored-graph label device which enables us to actually work out the basic prescriptions in a consistent manner. In fact, this procedure not only makes the whole description more transparent even in cases where the distributional pieces may be labelled linearly, but can also be regarded as a characteristic part of the techniques. In any case, the colored-vertex configurations of the graphs are ultimately suggested by the structure of the relevant FDE.

The theory of twistor diagrams was introduced by Penrose [11,12] as an attempt to provide a divergence-free framework for describing elementary physical processes. Accordingly, each twistor

diagram represents the integral of a holomorphic SI differential form which is taken over a compact contour bearing a well-defined topology. Though the results arising from earlier computations [13,14] led to the same scattering amplitudes as those described by Feymann diagrams, the theory was deemed to be equivalent to a massless version of the conventional QED or to a high-energy limiting case of the theory of massive fields. It was necessary, then, to try to extend the theory so as to incorporate massive fields into the scheme without modifying the standard formalism. One trivial suggestion to solve this problem [12] was that the introduction of the infinity twistors into the structures occurring in the former theory would break the conformal invariance of the approach, thereby allowing the presence of rest-masses. An actual solution, due to Hodges [15], emerged as a suitable re-definition of the twistor functions and inner products entering explicitly into the contour integrals. However, these methods were not implemented in any natural way and, in fact, have not been considered entirely satisfactory. One important feature of NID techniques seems to be the fact that the entire set of scattering formulae arising out of the systematic treatment of an IES can be neatly transcribed into the framework of twistor theory. This fact has arisen [16] in an explicit twistorial translation of the mass-scattering processes referred to before.

The patterns of the twistor expressions associated with the geometric properties of the relevant RM-configurations appear to be intimately related to the edge-vertex structures involved. Moreover, the integrands of the resulting twistorial scattering integrals appear

as totally skew-symmetric (SI) holomorphic projective structures which are defined on products of subspaces of Riemann spheres that correspond to suitable vertices of the null graphs. All the contours partaking of the actual evaluation of any elementary field integral are specified naturally, their existence being assumed at the outset. This assumption is based only upon the nullity of the underlying Minkowskian structures. The S^2-topology involved in the integration of a KAP-form turns out to be replaced by the product of two S^1's when the twistorial transcription of the corresponding RM-pattern is carried through. As far as this situation is concerned, what really happens is that the twistor differential form coming into play "splits out" each of the two-sphere structures into two pieces which contribute contours lying in different subspaces. Such splitting appeared for the first time in a twistorial transcription of the generalized KAP-integrals [17]. One of the most important results arising in this twistor framework is the correspondence between the handedness of the fields and the valence of the twistors involved in the respective field integrals. The twistorial integral for any unprimed field carries, in effect, only twistors lying in the null portion $\mathbb{PN}^*$ of the dual projective twistor space whereas the twistors entering into the integrals for primed fields belong to the null subset $\mathbb{PN}$ of projective twistor space. This fact is relevant for twistor theory insofar as it brings out, in a non-trivial way, a clear relationship between the nullity of Minkowskian structures and the fundamental twistor particle hypothesis for massless free systems [18-22]. These transcription methods make manifest the reduction of symmetry that occurs due the introduction of the infinity twistors

[23-25], as was expected earlier. Hopefully, they may be useful to tackle the problem of naturally incorporating masses into twistor theory.

This thesis is primarily concerned with using NID methods to describe completely the dynamics of classical Maxwell-Dirac fields. It is another non-trivial generalization of the prescriptions provided by Penrose [3] in connection with the application of NID techniques to IES's. It is worth remarking that the Lorentz gauge condition is required to ensure the exacteness of the entire set [3], and is thus taken up from the beginning. A somewhat important property of this system is that, in order to recover the complete set, it suffices to build up the prescriptions for evaluating a finite number of basic null structures. Such configurations are clearly suggested by the pattern of the field equations along with the properties of the proper Lorentz invariant distributional splitting of KAP-integrals. Any element of the entire IES can then be recovered by adding together an infinite number of contributions which are obtained by combining these basic blocks appropriately. The relevant FDE are set upon the interior $\mathbb{V}_o^+$ of $\mathscr{E}_o^+$ whereupon the NID generating all the elementary contributions are specified. Each distributional piece is represented as a colored tree which is completely specified by the solution of the corresponding density equation. In the case of the potential contributions, the prescriptions for constructing the colored graphs lead to patterns which are somewhat different from those of the trees labelling the fields. To any order, this fact appears to be directly related to the structure of the solutions of the potential density equations which

actually give rise to the presence of loops in the associated RM-configurations. These solutions do not entail any "reduction" of the graphical calculational devices used for evaluating the relevant null structures. The colored graphs turn out to be associated with SI finite integrals which are taken over spaces of forked and crossed null zigzags that start at O and terminate at a fixed point lying in $\mathbb{V}^{+}_{o}$.

Subsequently, the methods are given whereby one may carry out in a straightforward way an explicit twistorial transcription of the RM-integral formulae that describe the processes of electromagnetic scattering of elementary Dirac fields. The procedures at this stage are based to a large extent upon those involved in the translation of the mass-scattering integrals for Dirac fields [16]. Accordingly, the contours occurring in each twistor field integral are defined on products of subspaces of Riemann spheres associated with adequate vertices of the (forked) null structures that enter into the corresponding RM-pattern. Particular use will be made of new generalized SI holomorphic volume differential forms which allow one to immediately write down the twistorial structure associated with the wedge-product of an arbitrary number of three-volume forms. It will be seen that the standard patterns emerge once again here. All the twistorial integrals arising from working out the relevant prescriptions carry only totally skew-symmetric holomorphic projective structures. Each such field expression turns out to be represented by a twistor diagram. This result gives rise at once to a diagrammatic correspondence involving the basic Minkowskian scattering patterns. A notable feature of the twistor diagrams is the fact that some of the

singularity lines connect vertices of the same type. This property is due to the presence of infinity-twistor inner products in the denominators of the integrands of the field integrals, and actually arose in an earlier situation [23] concerning a twistor-diagram representation of the Dirac fields. In general, the numerators also explicitly carry inner products of this type which play the role of connecting lines in the diagrams.

I believe that the material presented here will provide a concrete background for the construction of a manifestly null QED involving twistors explicitly. It is upon this belief along with the hope of obtaining fresh insights into the framework of twistor theory that the main motivation for elaborating this work rests. The relevance of the thesis lies in this fact and the feature that it exhibits the prescriptions for building up explicit twistor diagrams which involve the combination of new singularity-line configurations with the standard structures [11-15].

The thesis consists of six chapters and one appendix. It is organized as follows. Chapter 2 deals with some of the concepts involved in the two-spinor formulation of the theory, and introduces the relevant FDE along with a set of colored-graph prescriptions. Chapter 3 is concerned with the evaluation of the basic electromagnetic RM-configurations. In chapter 4, the diagrams that describe the scattering processes are explicitly calculated. There the description of pure mass-scattering processes does not play any crucial role, and will therefore be omitted. Chapter 5 is devoted to the twistor transcription of the basic scattering patterns, the corresponding

twistor-diagrammatic structures being then exhibited. In chapter 6, some concluding remarks on the entire set of field formulae are presented. In the appendix, explicit calculations yielding the relevant exacteness relations are carried out. The detailed outline of chapters 2 through 5 will be given in due course. Thoughout the work, use is made of all the two-spinor and twistor-diagram conventions given by Penrose [3,11,12]. The natural system of units ($c=\hbar=1$) will be used. Unprimed and primed fields will be referred to as left-handed and right-handed fields, respectively. It must be emphasized, however, that the elementary fields recovering the complete IES are generally non-analytic. Hence there will be no attempt to attribute any specific positive-negative frequency character to them. The usual definition of the charge-helicity conjugation operator [20,22] is adopted, but with the handedness of each of the Dirac fields being reversed under the action of the conjugation. This requirement not only facilitates the construction of the calculational devices, but also enhances some of the features of the scattering diagrams of chapter 4. Thus all the fields will be assumed to propagate to the future. The behaviour of null data at the vertex of $\mathscr{E}_o^+$ is discussed extensively by Penrose & Rindler [3]. Here, no analicity assumption will be explicitly made, but at the outset the elements of the basic NID set shall be required to be smooth functions at O.

CHAPTER TWO

MAXWELL-DIRAC SETS

2.1 Introduction

The main aim of this chapter is to set up a framework which will be used to obtain the prescriptions involved in the evaluation of the elementary Minkowskian structures. In Sec.2.2, a review of some facts concerning the two-spinor formulation of the Maxwell-Dirac theory [3] is presented without working out the pertinent variational principle explicitly [10,26,27]. The choice of $\mathscr{C}_o^+$ as the NID hypersurface for all the Maxwell-Dirac elements yields a particularly simple set of elementary NID for the system. At this stage, the same data set as that suggested by Penrose [3] is utilized to define the relevant $\hat{\pi}$-NID (Sec.2.3). These latter data involve certain spin operators that appear to be closely related to the conformal invariant form of the Penrose þ-operators [2,3,17]. Their relevance stems from the fact that they are the data which enter into any SI volume- and KAP-integral expressions. The symbolic FDE associated with the basic null configurations are introduced in Sec.2.4. In Sec.2.5, the rules for building up a set of colored graphs that label the elementary distributional pieces are explained. Nevertheless, the complete specification of the graphs will be achieved later when the explicit solutions of the FDE are obtained (chapters 3 and 4).

2.2 Maxwell-Dirac Theory

A Maxwell-Dirac system in $\mathbb{RM}$ is defined by

$$MDS = \{\phi_{AB}(x), \bar{\phi}_{A'B'}(x), \Phi_{AA'}(x), \psi_{A}(x), \chi_{A'}(x)\}. \qquad (2.1)$$

In this set, the conjugate quantities $\phi_{AB}(x)$, $\bar{\phi}_{A'B'}(x)$ are the so-called Maxwell spinors. They are both symmetric and normally taken to be dependent opposite-helicity massless uncharged fields of spin $\pm$ 1. Either of them describes completely [3] the six electromagnetic degrees of freedom at every $x^{AA'} \in \mathbb{RM}$. The vector $\Phi_{AA'}(x)$ is the electromagnetic potential. It is real and usually enters into the definition of the Maxwell bivector $F_{ab}(x)$ as

$$F_{AA'BB'}(x) = 2\,\nabla_{[AA'}\Phi_{BB']}(x), \qquad (2.2)$$

where $\nabla_{AA'}$ is the ordinary partial derivative operator $\partial/\partial x^{AA'}$. The quantities $\psi_{A}(x), \chi_{A'}(x)$ define the Dirac-field pair [3], and carry locally the information about eight real degrees of freedom. These latter objects are opposite-helicity massive charged spin $\pm$ 1/2 fields of the same rest-mass and charge. It is useful to define their charge-helicity conjugates $\bar{\psi}_{A'}(x)$, $\bar{\chi}_{A}(x)$ which similarly carry the opposite charge and reversed helicities, but bear the same rest-mass as the former fields. The conjugation operator, $\hat{\tau}$, is an antilinear involutory mapping which is not here taken to reverse the order of the factors involved in any field expression. It should be noticed that this assumption appears to agree with the classical character of the fields.

There are six gauge-invariant relationships between the Maxwell fields and potential which can be obtained by first splitting the right-hand side of (2.2) into symmetric and skew parts involving the index pairs AB and A'B', and then identifying

$$F_{AA'BB'}(x) = \varepsilon_{AB}\bar{\phi}_{A'B'}(x) + \varepsilon_{A'B'}\phi_{AB}(x). \tag{2.3}$$

This procedure yields

$$\phi_{AB}(x) = \nabla_{A'(A}\Phi^{A'}_{B)}(x),\ \bar{\phi}_{A'B'}(x) = \nabla_{A(A'}\Phi^{A}_{B')}(x), \tag{2.4}$$

which actually brings out the electromagnetic symmetry property. Clearly, using the Lorentz gauge condition

$$\nabla_{A'[A}\Phi^{A'}_{B]}(x) = 0 \Leftrightarrow \nabla_a\Phi^a(x) = 0 \Leftrightarrow \nabla_{A[A'}\Phi^{A}_{B']}(x) = 0, \tag{2.5}$$

we can drop the symmetrization brackets from the right-hand sides of (2.4) whence (2.5) reduces to

$$\phi^A_A(x) = 0 = \bar{\phi}^{A'}_{A'}(x). \tag{2.6}$$

This simplification is easily seen by using the splitting relation

$$\nabla_{A'A}\Phi^{A'}_{B}(x) = \nabla_{A'(A}\Phi^{A'}_{B)}(x) + \frac{1}{2}\varepsilon_{AB}\nabla_C\Phi^C(x), \tag{2.7}$$

and its complex conjugate, taking (2.4) into account. It should be stressed that the symmetry of the Maxwell fields makes the ordering of the relevant upper and lower indices immaterial. (This is why the indices occurring in (2.6) have not been staggered.) The structure of the defining expression (2.2) together with the (local) commutativity of the ∇-operators gives rise to a set of eight real gauge-invariant identities which constitute the first "half" of Maxwell's equations [3]. These statements can be thought of as constituting the Bianchi identities of the entire theory, and emerge from the simple computation

$$\nabla_{[a}F_{bc]}(x) = \nabla_{[a}\nabla_b\Phi_{c]}(x) = 0 \Rightarrow \nabla^{AA'}{}^*F_{AA'BB'}(x) = 0, \tag{2.8}$$

where ${}^*F_{ab}(x)$ is the dual electromagnetic bivector which is given by

$${}^*F_{AA'BB'}(x) = i[\varepsilon_{AB}\bar{\phi}_{A'B'}(x) - \varepsilon_{A'B'}\phi_{AB}(x)]\ . \tag{2.9}$$

Explicitly, we have

$$\nabla^{A'}_{B}\phi^{AB}(x) = \nabla^{A}_{B}\bar{\phi}^{A'B'}(x), \tag{2.10}$$

which are the identities referred to above.

The part of the complete theory that consists of the second "half" of Maxwell's equations together with the (covariant) Dirac equations arises as the equations of motion involving the following Lagrangian density

$$\mathscr{L}_{MD} = \mathscr{L}_{M} + \mathscr{L}_{D} + \mathscr{L}_{INT}, \tag{2.11}$$

where $\mathscr{L}_{M}$, $\mathscr{L}_{D}$ and $\mathscr{L}_{INT}$ stand, respectively, for the Maxwell, Dirac and interacting pieces of $\mathscr{L}_{MD}$ which are written out explicitly as [26]

$$\mathscr{L}_{M} = \frac{1}{8\pi}\,[\,\phi_{AB}(x)\phi^{AB}(x) + \bar{\phi}_{A'B'}(x)\bar{\phi}^{A'B'}(x)\,]\,, \tag{2.12a}$$

$$\begin{aligned}\mathscr{L}_{D} = i\{&\frac{1}{2}\,[\,\bar{\chi}_{A}(x)\nabla^{AA'}\chi_{A}(x) + \bar{\psi}_{A}(x)\nabla^{AA'}\psi_{A}(x)\,]\\ &- \frac{1}{2}\,[\,(\nabla^{AA'}\bar{\chi}_{A}(x))\chi_{A}(x) + (\nabla^{AA'}\bar{\psi}_{A}(x))\psi_{A}(x)\,]\\ &- \frac{m}{\sqrt{2}}\,[\,\bar{\chi}_{A}(x)\psi^{A}(x) + \bar{\psi}_{A}(x)\chi^{A}(x)\,]\,\},\end{aligned} \tag{2.12b}$$

and

$$\mathscr{L}_{INT} = j_{AA'}(x)\Phi^{AA'}(x), \tag{2.12c}$$

with m denoting the rest-mass of the Dirac fields and $j_{AA'}(x)$ being a real vector which plays the role of a source for the Maxwell fields and potential. This vector is called the Dirac current density, its explicit expression being

$$j_{AA'}(x) = e[\,\bar{\psi}_{A}(x)\psi_{A}(x) + \bar{\chi}_{A}(x)\chi_{A}(x)\,]\,, \tag{2.13}$$

where e denotes the charge of the elements of the former $\psi\chi$-pair. It should be emphasized that the full Lagrangian density as expressed in (2.11) is a real $SL(2,\mathbb{C})$-scalar function on $\mathbb{RM}$. The relevant equations of motion read [26]

$$\nabla^{A'}_{B}\frac{\partial\mathscr{L}_{M}}{\partial\phi_{AB}(x)} + \nabla^{A}_{B'}\frac{\partial\mathscr{L}_{M}}{\partial\bar{\phi}_{A'B'}(x)} + \frac{\partial\mathscr{L}_{INT}}{\partial\Phi_{AA'}(x)} = 0, \tag{2.14a}$$

$$\nabla^{AA'} \frac{\partial \mathcal{L}_D}{\partial(\nabla^{AB'}\bar{\psi}_B,(x))} - \frac{\partial(\mathcal{L}_D + \mathcal{L}_{INT})}{\partial\bar{\psi}_A,(x)} = 0, \tag{2.14b}$$

$$\nabla^{AA'} \frac{\partial \mathcal{L}_D}{\partial(\nabla^{BA'}\bar{\chi}_B(x))} - \frac{\partial(\mathcal{L}_D + \mathcal{L}_{INT})}{\partial\bar{\chi}_A(x)} = 0. \tag{2.14c}$$

Equation (2.14a) gives rise to the second "half" of Maxwell's equations which, when combined with (2.10) and (2.13), yield the gauge-invariant field equations

$$\nabla^B_A,\phi_{AB}(x) = 2\pi e[\bar{\psi}_A,(x)\psi_A(x) + \bar{\chi}_A(x)\chi_A,(x)] = \nabla^{B'}_A\bar{\phi}_A',_B,(x). \tag{2.15}$$

These statements constitute the Maxwell part of the theory. Equations (2.14b) and (2.14c) yield, in turn, the Dirac equations

$$\mathcal{D}^{AA'}\psi_A(x) = \mu\chi^{A'}(x),\ \mathcal{D}_{AA'}\chi^{A'}(x) = -\mu\psi_A(x), \tag{2.16}$$

where $\mu=m/\sqrt{2}$, and

$$\mathcal{D}_{AA'} = \nabla_{AA'} - ie\,\Phi_{AA'},(x). \tag{2.17}$$

The above operator is the covariant derivative operator for the entire theory. For any relevant quantity $\Upsilon^{\mathcal{E}\mathcal{F}'}(x)$, with $\mathcal{E}$ and $\mathcal{F}$ being arbitrary clumped spinor indices, we thus have the commutation relation

$$[\mathcal{D}_a,\mathcal{D}_b]\Upsilon^{\mathcal{E}\mathcal{F}'}(x) = -2ie[\nabla_{[a}(\Phi_{b]}(x)\Upsilon^{\mathcal{E}\mathcal{F}'}(x)) + \Phi_{[a}(x)\nabla_{b]}\Upsilon^{\mathcal{E}\mathcal{F}'}(x)]$$

$$= -ieF_{ab}(x)\Upsilon^{\mathcal{E}\mathcal{F}'}(x), \tag{2.18}$$

whence (2.3) can be looked upon as the "curvature" of the theory.

It is of some interest to notice at this stage that the Bianchi identities (2.8) arise directly from the straightforward computation

$$\mathcal{D}_{[a}\mathcal{D}_b\mathcal{D}_{c]}\Upsilon^{\mathcal{E}\mathcal{F}'}(x) = \mathcal{D}_{[a}\mathcal{D}_{[b}\mathcal{D}_{c]]}\Upsilon^{\mathcal{E}\mathcal{F}'}(x)$$

$$= -ie\mathcal{D}_{[a}[F_{bc]}(x)\Upsilon^{\mathcal{E}\mathcal{F}'}(x)] = -ie[(\nabla_{[a}F_{bc]}(x))\Upsilon^{\mathcal{E}\mathcal{F}'}(x)$$

$$+ F_{[ab}(x)\mathcal{D}_{c]}\Upsilon^{\mathcal{E}\mathcal{F}'}(x)] = \mathcal{D}_{[[a}\mathcal{D}_b]\mathcal{D}_{c]}\Upsilon^{\mathcal{E}\mathcal{F}'}(x)$$

$$= -ieF_{[ab}(x)\mathcal{D}_{c]}\Upsilon^{\mathcal{E}\mathcal{F}'}(x). \tag{2.19}$$

One important result emerging from this theory is the conservation of charge. There are several methods of establishing the corresponding statement as an identity [10,26,27], only one of which, involving the skew-symmetric operators [3,20]

$$\blacksquare_{AB} = \mathcal{D}_{A'[A}\mathcal{D}^{A'}_{B]} = \frac{1}{2}\varepsilon_{AB}\blacksquare, \quad \blacksquare_{A'B'} = \mathcal{D}_{A[A'}\mathcal{D}^{A}_{B']} = \frac{1}{2}\varepsilon_{A'B'}\blacksquare, \tag{2.20}$$

where $\blacksquare = \mathcal{D}_C\mathcal{D}^C$, is mentioned here. The basic procedure consists in letting these operators act upon the electromagnetic fields in such a way that the indices carried by the resulting structure are exhausted. After some explicit calculations involving particularly (2.15) and (2.17), we thus obtain

$$\blacksquare_{AB}\phi^{AB}(x) = 2\pi\nabla_{AA'}j^{AA'}(x) = \blacksquare_{A'B'}\bar{\phi}^{A'B'}(x) \equiv 0. \tag{2.21}$$

2.3 Null Initial Data Sets

The simplest NID set on $\mathscr{C}^+_o$ that generates all the field elements of (2.1) is defined by

$$\text{MDNID} = \{\phi_L{}^o(\overset{W}{o}{}^A;W),\ \bar{\phi}_R{}^o(\bar{\overset{W}{o}}{}^{A'};W),\ \psi_L{}^-(\overset{V}{o}{}^A;V),\ \chi_R{}^-(\bar{\overset{U}{o}}{}^{A'};U)\}. \tag{2.22}$$

Its elements are explicitly expressed as

$$\phi_L{}^o(\overset{W}{o}{}^A;W) = \overset{W}{o}{}^A\overset{W}{o}{}^B\phi_{AB}(W),\quad \bar{\phi}_R{}^o(\bar{\overset{W}{o}}{}^{A'};W) = \bar{\overset{W}{o}}{}^{A'}\bar{\overset{W}{o}}{}^{B'}\bar{\phi}_{A'B'}(W), \tag{2.23a}$$

$$\psi_L{}^-(\overset{V}{o}{}^A;V) = \overset{V}{o}{}^A\psi_A(V),\quad \chi_R{}^-(\bar{\overset{U}{o}}{}^{A'};U) = \bar{\overset{U}{o}}{}^{A'}\chi_{A'}(U), \tag{2.23b}$$

with $W^{AA'}$, $V^{AA'}$ and $U^{AA'}$ belonging all to $\mathscr{C}^+_o$. The spinors carried by the arguments of the elements of (2.22) enter into the definition of the (real) flag poles specifying the (null) directions of the relevant generators of $\mathscr{C}^+_o$. Each such spinor is chosen to be covariantly constant along the respective generator, the (conjugate) expressions associated with this choice being [3,20]

$$\overset{S}{o}{}^A\bar{\overset{S}{o}}{}^{A'}\overset{S}{\nabla}_{AA'}\overset{S}{o}{}^B = 0,\quad \overset{S}{o}{}^A\bar{\overset{S}{o}}{}^{A'}\overset{S}{\nabla}_{AA'}\bar{\overset{S}{o}}{}^{B'} = 0, \tag{2.24}$$

where the letter "S" stands for either W, V or U and $\overset{S}{\nabla}_{AA'} = \partial/\partial S^{AA'}$. The data $\phi_L o(\overset{WA}{o};W)$ and $\overline{\phi}_R o(\overset{\bar{A}'}{o};W)$ are, respectively, the (uncharged) left-handed and right-handed electromagnetic null data, whereas $\psi_L\text{-}(\overset{VA}{o};V)$ and $\chi_R\text{-}(\overset{\bar{A}'}{o};U)$ are similarly the left-handed and right-handed Dirac null data. These data are spread over the whole of $\mathscr{E}^+_o$, and appear to be formally the same as those for spinning massless free fields [3,11,12,17,28]. Each of them is a complex-valued scalar function of eight real variables. All the elementary potentials are also generated by them. Thus there will be no distributional potential contribution arising from potential data on $\mathscr{E}^+_o$. This fact agrees with the Penrose procedure [3] whereby, upon treating the system (2.1), one chooses a potential-data set whose elements are all taken to vanish on $\mathscr{E}^+_o$. A further point concerning this procedure will be made in chapter 6.

To define the $\hat{\pi}$-NID set, it is convenient to think of $\overset{SA}{o}$ and $\overset{\bar{A}'}{o}$ as elements of conjugate spin bases $\{\overset{SA}{o},\overset{KA}{o}\}$, $\{\overset{\bar{A}'}{o},\overset{\bar{A}'}{o}\}$ set up at $S^{AA'}$. The other spinors making up the bases are also taken to be covariantly constant along the generator of the future null cone $\mathscr{E}^+_S$ of $S^{AA'}$ that passes through some point $K^{AA'}$. These latter spinors are chosen in such a way that the flag pole associated with them points in a future null direction through $S^{AA'}$, with the conjugate spin inner products at $S^{AA'}$

$$z_S = \overset{SA}{o}\overset{K}{o}_A, \quad \bar{z}_S = \overset{\bar{A}'}{o}\overset{\bar{}}{o}_{KA'}, \tag{2.25}$$

being held fixed. Let γ_S denote the generator of $\mathscr{E}^+_o$ through $S^{AA'}$, and r_{OS} be a positive affine parameter on γ_S such that

$$S^{AA'} = r_{OS}\overset{SA}{o}\overset{\bar{A}'}{o}, \quad \mathbb{D} = \overset{SA}{o}\overset{\bar{A}'}{o}\overset{S}{\nabla}_{AA'}. \tag{2.26}$$

The latter quantity is the directional derivative operator $\partial/\partial r_{OS}$ at

$S^{AA'}$ in the direction of γ_S. Upon acting on the elements of (2.22), the relevant $\hat{\pi}$-operators are defined at the appropriate points as follows

$$\hat{\pi}_{W1-} = \frac{r_{OW}}{(z_W)^2}\,\{\mathbb{D} - 3\,\overset{W}{\overset{O}{\rho}}(W)\},\quad \hat{\pi}_{W1+} = \frac{r_{OW}}{(\bar{z}_W)^2}\,\{\mathbb{D} - 3\,\overset{W}{\overset{O}{\rho}}(W)\}, \tag{2.27}$$

$$\hat{\pi}_{V1/2-} = \frac{r_{OV}}{z_V}\,\{\mathbb{D} - 2\,\overset{V}{\overset{O}{\rho}}(V)\},\quad \hat{\pi}_{U1/2+} = \frac{r_{OU}}{\bar{z}_U}\,\{\mathbb{D} - 2\,\overset{U}{\overset{O}{\rho}}(U)\}, \tag{2.28}$$

where $\overset{O}{\rho}(S)$ is the (real) convergence of the generators of $\mathscr{E}^{+}_{o}$ at $S^{AA'}$ whose defining expression is written as [2,3,5]

$$\overset{O}{\rho}(S) = (\overset{SAK}{o\ o\ o_A})^{-1} \overset{S}{o_B}\ \overset{KC-C'}{o\ o}\ \nabla_{CC'}\ \overset{SB}{o}\ , \tag{2.29}$$

whence $\overset{O}{\rho}(S) = -1/r_{OS}$. We thus have the NID set

$$\hat{\pi}\text{-NID}=\{\hat{\pi}_{W1-}\phi_L{}^{o}(\overset{WA}{o};W),\hat{\pi}_{W1+}\bar{\phi}_R{}^{o}(\bar{o}^{A'}_{W};W),\hat{\pi}_{V1/2-}\psi_L{}^{-}(\overset{VA}{o};V),\hat{\pi}_{U1/2+}\chi_R{}^{-}(\bar{o}^{A'}_{U};U)\}. \tag{2.30}$$

It is worth remarking explicitly that, read from left to right, the data entering into (2.30) are of the types {0,-2;0,0}, {0,0;-2,0}, {0,-1;0,0} and {0,0;-1,0}. At this stage I have made use of the terminology of the compacted spin coefficient formalism of Geroch, Penrose and Held [29], but my complex-conjugation convention involves "reflecting" the number pair appearing on either side of a curl-bracket piece in the vertical that "passes" through the respective semicolon. In fact, the pattern of the above $\hat{\pi}$-NID constitutes a particular case of that used earlier [17] to treat an SI version of the KAP-integral expressions for massless free fields of arbitrary spin. It is worthwhile to introduce the conjugate Dirac $\hat{\pi}$-data. We have,

$$\hat{\tau}\,\hat{\pi}_{V1/2-}\psi_L{}^{-}(\overset{VA}{o};V) = \hat{\pi}_{V1/2+}\bar{\psi}_R{}^{+}(\bar{o}^{A'}_{V};V), \tag{2.31a}$$

$$\hat{\tau}\,\hat{\pi}_{U1/2+}\chi_R{}^{-}(\bar{o}^{A'}_{U};U) = \hat{\pi}_{U1/2-}\bar{\chi}_L{}^{+}(\overset{UA}{o};U). \tag{2.31b}$$

The construction of the elements of (2.30) is illustrated in Fig.1. All the left-handed and right-handed data with which I will be dealing in

what follows are, respectively, represented by white and black spots bearing suitable charge-helicity labels. In particular, the work of Sec. 2.4 involves Dirac $\hat{\pi}$-data defined at points lying on generators of (future) null cones of suitable points of $\mathbb{V}^{+}_{o}$.

2.4 Distributional Field Density Equations

The FDE associated with the basic field-potential configurations are now introduced. It will become apparent that the construction of these statements rests only upon the structure of the theory. The null configurations constructed here will be used in chapters 3 and 4 as calculational devices for working out the FDE. In particular, when obtaining the explicit solutions of the FDE for

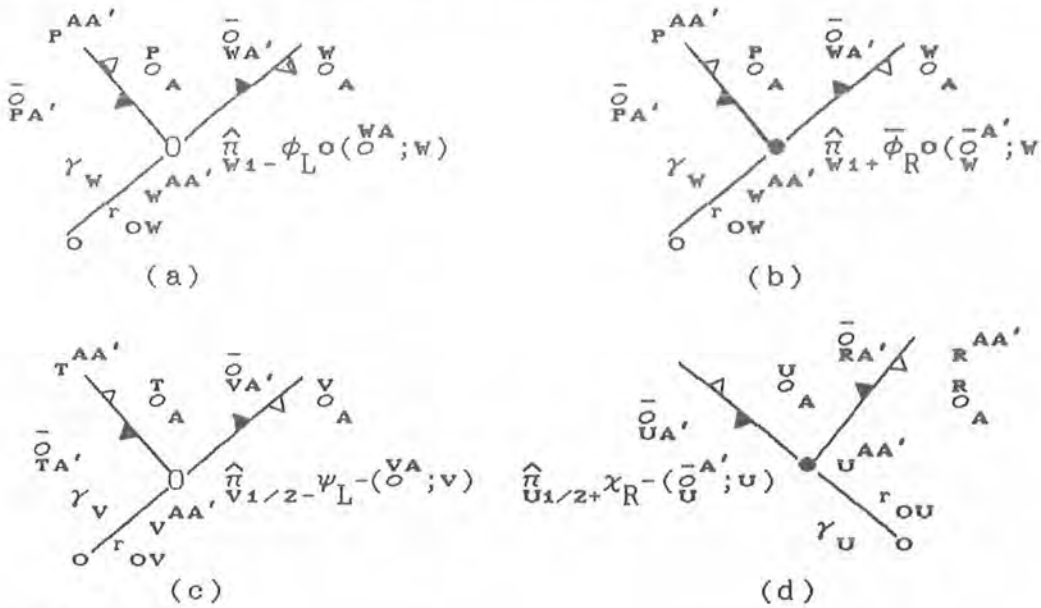

Figure 1.

Diagram illustrating the construction of the $\hat{\pi}$-data on $\mathscr{E}^{+}_{o}$ for the elements of the Maxwell-Dirac set. The left-handed (resp. right-handed) data are shown in (a) and (c) (resp. (b) and (d)), and are represented by white (resp. black) spots.

"higher-order" electromagnetic contributions (Sec.3.2), we will see that the reality is lost. For this reason, henceforth another kernel letter will be used in place of $\overline{\phi}$ to indicate that the corresponding left-handed and right-handed fields are independent of one another.

For the electromagnetic fields, one has to build up six basic FDE. Two of these involve the SI free densities $\langle L^{O}(M);\phi_{AB}(x)\rangle$ and $\langle R^{O}(M);\theta_{A'B'}(x)\rangle$ which are produced by electromagnetic data centred at some $M^{AA'} \in \mathscr{E}^{+}_{O}$. The relevant FDE are written at some $x^{AA'}$ lying in the interior of $\mathscr{E}^{+}_{M}$ as

$$\overset{x}{\nabla}{}^{AA'} \langle L^{O}(M);\phi_{AB}(x)\rangle = 0, \quad \overset{x}{\nabla}{}^{AA'} \langle R^{O}(M);\theta_{A'B'}(x)\rangle = 0. \tag{2.32}$$

It must be observed that the statements (2.32) are associated with the standard splitting of the KAP-integrals [3,5,17] for fields of spin ± 1. This KAP-splitting involves shifting the origin to $M^{AA'}$ in such a way that $x^{AA'}$ appears as a future time-like vector given by the sum of two future null vectors, $r_{MR}\,\overset{MA-A'}{o\ o}_{M}$ and $r_{RX}\,\overset{KA-A'}{o\ o}_{K}$. The RM-configurations involved can be readily constructed by adequately transporting the flag poles $\overset{MA-A'}{o\ o}_{M}$ and $\overset{KA-A'}{o\ o}_{K}$ (Fig.2). Thus $x^{AA'}$ is future-null separated from both $K^{AA'}$ and $R^{AA'}$ which are, in turn, future-null separated from $M^{AA'}$, the latter point lying on $\mathscr{E}^{+}_{O}$. This construction rests upon the fact that the explicit field densities entering into (2.32) involve a distributional field [3] whose (non-compact) support is identified with $\mathscr{E}^{+}_{M}$. The potential densities $\langle L^{O}(M);\Phi_{AA'}(x)\rangle$ and $\langle R^{O}(M);\Phi_{AA'}(x)\rangle$ associated with (2.32) satisfy the density equations

$$\overset{x}{\nabla}_{AA'} \langle L^{O}(M);\Phi_{B}{}^{A'}(x)\rangle = \langle L^{O}(M);\phi_{AB}(x)\rangle = \overset{x}{\nabla}_{AA'} \langle R^{O}(M);\Phi_{B}{}^{A'}(x)\rangle, \tag{2.33a}$$

$$\overset{x}{\nabla}_{AA'} \langle R^{O}(M);\Phi_{B}{}^{A}(x)\rangle = \langle R^{O}(M);\theta_{A'B'}(x)\rangle = \overset{x}{\nabla}_{AA'} \langle L^{O}(M);\Phi_{B}{}^{A}(x)\rangle. \tag{2.33b}$$

It will be shown later (see Sec.3.2) that the solutions of the above equations are the only real electromagnetic densities, whence $\theta = \overline{\phi}$ and $\langle L^{O}(M);\Phi_{AA'}(x)\rangle = \langle R^{O}(M);\Phi_{AA'}(x)\rangle$.

The densities involved in the other electromagnetic FDE are actually produced by $\hat{\pi}$-data generating elementary Dirac current pieces of the types $(L^{-}R^{+})$ and $(R^{-}L^{+})$. Such data are centred at points $N^{AA'}$ and $P^{AA'}$ which lie in either $\mathscr{E}_{o}^{+}$ or $\mathbb{V}_{o}^{+}$. In this latter case, the Dirac datum spots are actually produced by scattering data. The patterns of the configurations involved in the formation of such data are the same as those constructed in chapters 3 and 4 and will therefore be specified later. For simplicity, and without any loss of generality, assume that the data carrying the same charge are set up at the same point whence the current pieces appear as $(L^{-}(N)R^{+}(P))$ and $(R^{-}(N)L^{+}(P))$. The procedure for constructing the relevant null configurations is essentially the same as that giving rise to Fig.2 since the fields emanating from $N^{AA'}$ and $P^{AA'}$ have once again to be split

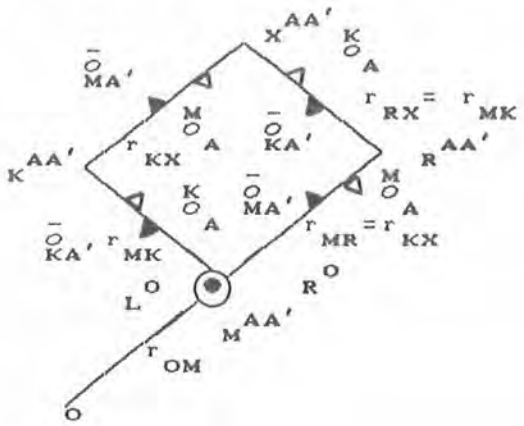

Figure 2.

Planar configuration involved in the SI splitting of the KAP-integrals that gives rise to the real electromagnetic densities.

into their KAP-distributional pieces. Let $Z^{AA'}$ and $T^{AA'}$ be points lying on $\mathscr{E}^{+}_{N}$ and $\mathscr{E}^{+}_{P}$, with the corresponding null poles being $\overset{Z}{o}_{A}\bar{o}_{A}$, and $\overset{T}{o}_{A}\bar{o}_{A}$, respectively. The generators γ_{Z} and γ_{T} are taken to intersect each other at a "middle" point $M^{AA'}$ while $x^{AA'}$ is now a point lying in the two-plane of $N^{AA'}$, $P^{AA'}$ and $M^{AA'}$ that is future-null separated from both $Z^{AA'}$ and $T^{AA'}$. Thus $x^{AA'}$ belongs to the interior of both $\mathscr{E}^{+}_{N}$ and $\mathscr{E}^{+}_{P}$, the inner products $z_{N}=o^{N}o^{AZ}o_{A}$, $z_{P}=o^{P}o^{AT}o_{A}$ being held fixed along with their complex conjugates and $z_{M}=o^{Z}o^{AT}o_{A}$, $\bar{z}_{M}=o^{\bar{Z}}o^{\bar{A}'}\bar{o}_{TA}$, (see Fig.3). Invoking (2.15), we then write the symbolic FDE

$$\overset{x}{\nabla}{}^{B}_{A},\langle L^{-}(N)R^{+}(P);\phi_{AB}(x)\rangle = 2\pi e\langle L^{-}(N);\psi_{A}(x)\rangle\langle R^{+}(P);\bar{\psi}_{A},(x)\rangle$$
$$= \overset{x}{\nabla}{}^{B'}_{A}\langle L^{-}(N)R^{+}(P);\Theta_{A',B},(x)\rangle, \qquad (2.34)$$

where $\langle L^{-}(N);\psi_{A}(x)\rangle$ and $\langle R^{+}(P);\bar{\psi}_{A},(x)\rangle$ denote, respectively, the conjugate ψ-distributional densities coming from $N^{AA'}$ and $P^{AA'}$. In a similar way, the FDE for the densities produced by the $(R^{-}(N)L^{+}(P))$-piece are written as

$$\overset{x}{\nabla}{}^{B}_{A},\langle R^{-}(N)L^{+}(P);\phi_{AB}(x)\rangle = 2\pi e\langle R^{-}(N);\chi_{A},(x)\rangle\langle L^{+}(P);\bar{\chi}_{A}(x)\rangle$$
$$= \overset{x}{\nabla}{}^{B'}_{A}\langle R^{-}(N)L^{+}(P);\Theta_{A',B},(x)\rangle. \qquad (2.35)$$

The potentials associated with (2.34) and (2.35) are subject to the density equations

$$\overset{x}{\nabla}_{AA},\langle L^{-}(N)R^{+}(P);\Phi^{A'}_{B}(x)\rangle = \langle L^{-}(N)R^{+}(P);\phi_{AB}(x)\rangle, \qquad (2.36a)$$

$$\overset{x}{\nabla}_{AA},\langle L^{-}(N)R^{+}(P);\Phi^{A}_{B},(x)\rangle = \langle L^{-}(N)R^{+}(P);\Theta_{A',B},(x)\rangle, \qquad (2.36b)$$

and

$$\overset{x}{\nabla}_{AA},\langle R^{-}(N)L^{+}(P);\Phi^{A'}_{B}(x)\rangle = \langle R^{-}(N)L^{+}(P);\phi_{AB}(x)\rangle, \qquad (2.37a)$$

$$\overset{x}{\nabla}_{AA},\langle R^{-}(N)L^{+}(P);\Phi^{A}_{B},(x)\rangle = \langle R^{-}(N)L^{+}(P);\Theta_{A',B},(x)\rangle. \qquad (2.37b)$$

A block diagram illustrating the production of the distributional electromagnetic densities is shown in Fig.4.

When combined with the electromagnetic structures constructed above, the field equations (2.16) give rise to six basic FDE for the Dirac fields. As the entire theory stands, the corresponding explicit statements appear to control the interaction between elementary Dirac fields and electromagnetic potentials. The configurations associated

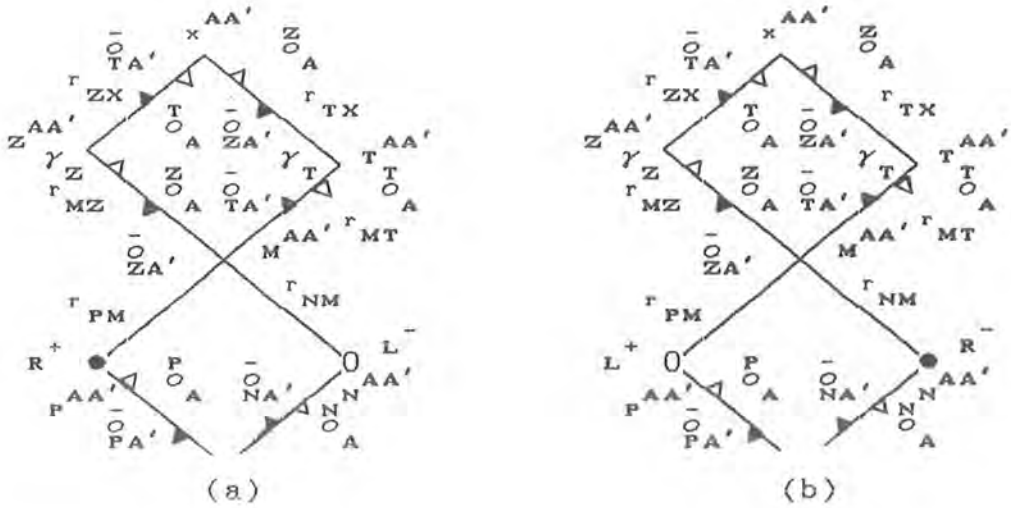

Figure 3

Null planar configurations associated with the FDE for the distributional electromagnetic densities produced by elementary current pieces. The generators of $\mathscr{C}^{+}_{N}$ *and* $\mathscr{C}^{+}_{\mathcal{P}}$ *through* $Z^{AA'}$ *and* $T^{AA'}$ *meet at a "middle" point* $M^{AA'}$ *. The point* $x^{AA'}$ *lies on the plane of* $N^{\mathcal{A}}$, $P^{\mathcal{A}}$ *and* $M^{\mathcal{A}}$, *and is defined by transporting parallelly the flag poles* $\overset{Z}{\circ}\overset{A-A'}{\circ}_{Z}$ *and* $\overset{T}{\circ}\overset{A-A'}{\circ}_{T}$ *along the generators* γ_{T} *and* γ_{Z}, *respectively. This transport yields at once the equalities* $r_{TX}=r_{MZ}$ *and* $r_{MT}=r_{ZX}$. *The generators "incoming" at* $N^{\mathcal{A}}$ *and* $P^{\mathcal{A}}$ *appear in the structures that give rise to the formation of the* $\hat{\pi}$*-data involved, and are not required to lie in the plane of* $N^{\mathcal{A}}$, $P^{\mathcal{A}}$ *and* $M^{\mathcal{A}}$: *(a)* $(L^{-}R^{+})$*-configuration; (b)* $(R^{-}L^{+})$*-configuration.*

with such FDE can be built up by suitably coupling the structures of Figs.2 and 3 with those corresponding to incoming distributional Dirac fields. It will be seen in chapter 4 that this "suitability" is intimately related to the fact that the scattering structures have to carry electromagnetic-field branches which bear the same handedness as that of the incoming and outgoing fields. The procedure leading to this feature amounts to replacing the potential vector kernels associated with the former configurations without violating the relevant FDE, but the former potential poles are always brought back when the latter configurations "collapse" so as to restore the former structures. In particular, the handedness feature implies that there are only two appropriate "dual" configurations for each current piece.

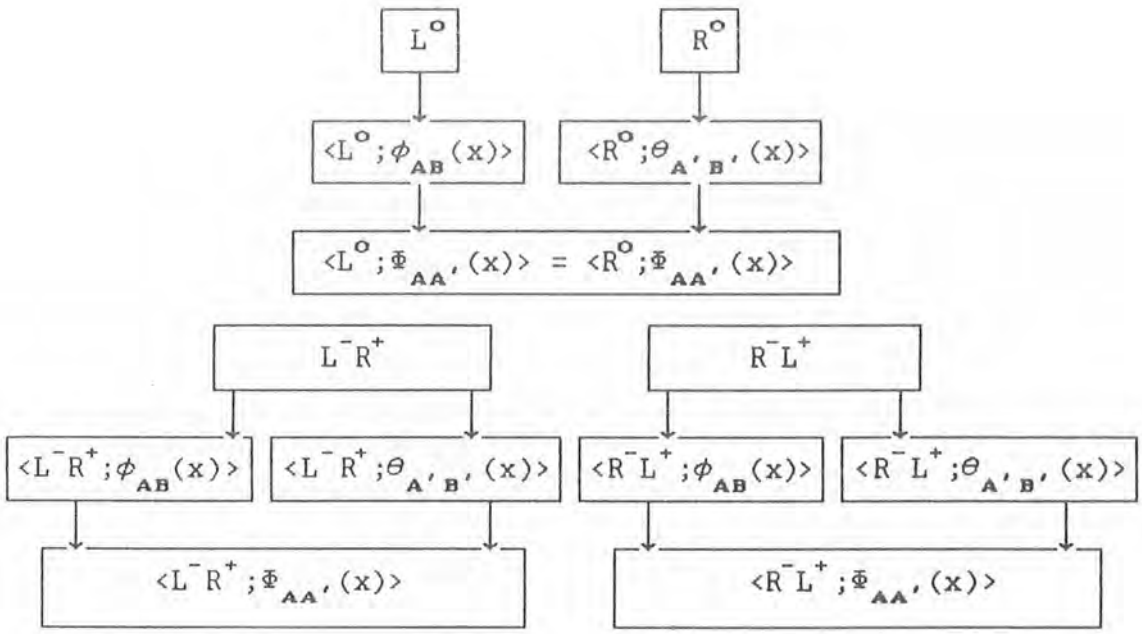

Figure 4

Block diagram showing the production of the basic electromagnetic densities. For simplicity the N's and P's have been deleted.

The structures under consideration are shown in Figs.5 and 6. In Fig.5, the incoming fields emanate from $\hat{\pi}$-data set up at a point $D^{AA'}$ which does not in general lie on $\mathcal{E}^{+}_{O}$, but is taken to belong to the plane spanned by $M^{AA'}$, $K^{AA'}$ and $x^{AA'}$. One of the generators of $\mathcal{E}^{+}_{D}$ lying in this plane contains a point $S^{AA'}$ which is past-null separated from $x^{AA'}$, and thus intersects the geodesic passing through $M^{AA'}$ and $K^{AA'}$ at $m^{AA'}$. At this stage, the affine parameter r_{OM} is no longer required to lie in the main plane of the configurations. The inner products at $m^{AA'}$ and $D^{AA'}$ are set as $z_m = {}^{SAK}_{O\ O\ A}$, $\bar{z}_m = {}^{-A'\ -}_{O\ O\ KA'}$, and $z_D = {}^{DAS}_{O\ O\ A}$, $\bar{z}_D = {}^{-A'\ -}_{O\ O\ SA'}$. The corresponding FDE are written as follows

$$\overset{x}{\nabla}{}^{AA'} \langle \bar{L}(D) L^{O}(M); \psi_{A}(x) \rangle = ie \langle L^{O}(M); \Phi^{AA'}(x) \rangle \langle \bar{L}(D); \psi_{A}(x) \rangle, \quad (2.38)$$

$$\overset{x}{\nabla}{}^{AA'} \langle \bar{R}(D) R^{O}(M); \chi_{A'}(x) \rangle = ie \langle R^{O}(M); \Phi^{AA'}(x) \rangle \langle \bar{R}(D); \chi_{A'}(x) \rangle. \quad (2.39)$$

Operating on these equations with ∇^{B}_{A}, and $\nabla^{B'}_{A}$, and using the Lorentz gauge condition for the potential density, after some elementary

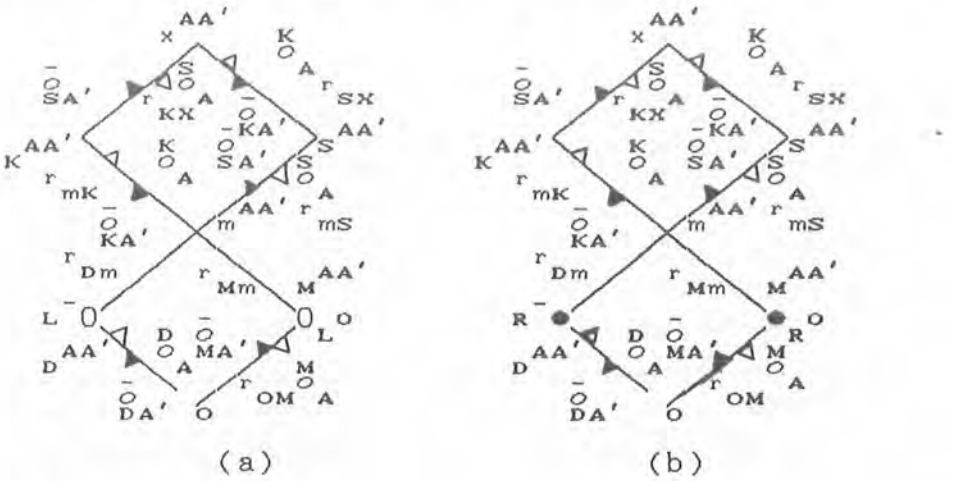

Figure 5

Configurations for the FDE describing the interaction between Dirac fields and "zero-order" potentials: (a) left-handed structure; (b) right-handed structure.

manipulations we get the wave equations (with $\Box_x = \nabla^{X}_{a} \nabla^{Xa}$)

$$\Box_x \langle L^-(D) L^O(M); \psi^A(x)\rangle = -ie\,[\,\langle L^O(M); \phi^{AB}(x)\rangle \langle L^-(D); \psi_B(x)\rangle - \langle L^O(M); \Phi^{A'}_{B}(x)\rangle \nabla^{X}_{(A} \langle L^-(D); \psi^{B)}(x)\rangle\,], \quad (2.40)$$

$$\Box_x \langle R^-(D) R^O(M); \chi^{A'}(x)\rangle = -ie\,[\,\langle R^O(M); \theta^{A'B'}(x)\rangle \langle R^-(D); \chi_{B'}(x)\rangle - \langle R^O(M); \Phi^{A}_{B'}(x)\rangle \nabla^{X}_{(A'} \langle R^-(D); \chi^{B')}(x)\rangle\,]. \quad (2.41)$$

The construction of Fig.6 is carried out in a similar way. Now, the scatterer branches involve the current pieces of Fig.3. The incoming fields are produced by data specified at two points $D^{AA'}$ and $B^{AA'}$, the generators of $\mathcal{E}^+_D$ and $\mathcal{E}^+_B$ intersecting the branches at $F^{AA'}$ and $G^{AA'}$, respectively. In the case of either pair of "dual" structures, the intersection takes place in such a way that these latter points appear to be past-null separated from two points $R^{AA'} \in \mathcal{E}^+_N$ and $K^{AA'} \in \mathcal{E}^+_P$ which lie, therefore, in the planes of $N^{AA'}$, $F^{AA'}$, $D^{AA'}$ and $P^{AA'}$, $G^{AA'}$, $B^{AA'}$, respectively. Furthermore, $x^{AA'}$ lies in both of these planes, and is future-null separated not only from $R^{AA'}$ and $K^{AA'}$, but also from two other points $\Sigma^{AA'} \in \mathcal{E}^+_D$ and $\sigma^{AA'} \in \mathcal{E}^+_B$ which are, respectively, taken to be future-null separated from $F^{AA'}$ and $G^{AA'}$. The generators of $\mathcal{E}^+_N$ and $\mathcal{E}^+_P$ passing through $R^{AA'}$ and $K^{AA'}$ now meet at $m^{AA'}$, which accordingly belongs to both planes. Evidently, as the configurations stand, the intersection between the two planes is the line passing through $m^{AA'}$ and $x^{AA'}$. The relevant inner products will be defined later (see chapter 4). For the corresponding FDE, we have

$$\nabla^{X}_{AA'} \langle L^-(D) R^+(P) L^-(N); \psi_A(x)\rangle = ie \langle L^-(N) R^+(P); \Phi^{AA'}(x)\rangle \langle L^-(D); \psi_A(x)\rangle, \quad (2.42)$$

$$\nabla^{X}_{AA'} \langle R^-(B) L^-(N) R^+(P); \chi_{A'}(x)\rangle = ie \langle L^-(N) R^+(P); \Phi^{AA'}(x)\rangle \langle R^-(B); \chi_{A'}(x)\rangle, \quad (2.43)$$

$$\overset{x}{\nabla}{}^{AA'} \langle R^{-}(D)L^{+}(P)R^{-}(N);\chi_{A},(x)\rangle = ie\langle R^{-}(N)L^{+}(P);\Phi^{AA'}(x)\rangle\langle R^{-}(D);\chi_{A},(x)\rangle, \tag{2.44}$$

$$\overset{x}{\nabla}{}^{AA'} \langle L^{-}(B)R^{-}(N)L^{+}(P);\psi_{A}(x)\rangle = ie\langle R^{-}(N)L^{+}(P);\Phi^{AA'}(x)\rangle\langle L^{-}(B);\psi_{A}(x)\rangle. \tag{2.45}$$

The procedure yielding (2.40) and (2.41) leads also to wave equations associated with (2.42)-(2.45) which can be immediately obtained from

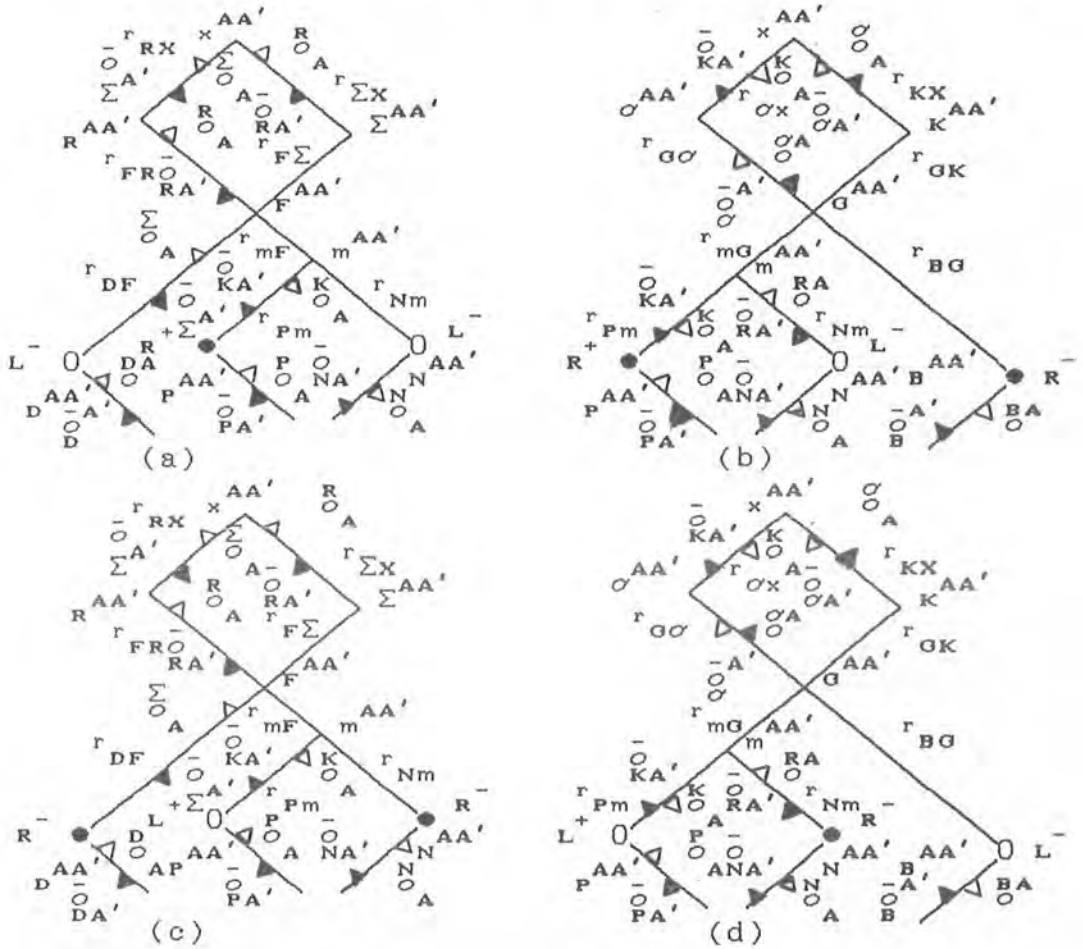

Figure 6

"Dual" configurations describing the interaction between Dirac and potential densities. In (a), (b) (resp.(c), (d)) two Dirac densities propagate in a region of potential density produced by a $\psi\overline{\psi}$- (resp.$\chi\overline{\chi}$-) current piece.

the former statements by replacing L^{o} and R^{o} by appropriate current pieces. For (2.42), for instance, we have

$$\Box_{x}\langle L^{-}(D)R^{+}(P)L^{-}(N);\psi^{A}(x)\rangle = -ie\,[\,\langle L^{-}(N)R^{+}(P);\phi^{AB}(x)\rangle\langle L^{-}(D);\psi_{B}(x)\rangle - \langle L^{-}(N)R^{+}(P);\Phi^{A'}_{B}(x)\rangle\overset{x}{\nabla}{}^{(A}_{A'}\langle L^{-}(D);\psi^{B)}(x)\rangle\,] \,. \tag{2.46}$$

It should be emphasized that each differentiated Dirac density with which we have been dealing corresponds to an elementary contribution that arises as the result of the interaction between an incoming field and a potential density. Indeed, the solutions of the FDE are to be regarded as densities for new contributions arising in this way. Some block diagrams illustrating these processes are given in Fig.7. The formation of the datum spots involves appropriately combining the configurations that arise from the actual evaluation of the above structures. In accordance with this fact, each contribution appears as an RM-integral whose integrand involves the wedge-product of differential forms set up at the datum spots.

2.5 Colored Graphs

The distributional pieces which recover each of the elements of (2.1) can not be labelled in a trivial way. It becomes necessary to design a graphical label device whereby each elementary contribution may be unambiguously identified. Thus each graph will represent an integral expression corresponding to a distributional field or potential. Such a set of graphs should also facilitate the construction of the explicit integral associated with any contribution. The graphical representation to be constructed now also enables one to re-

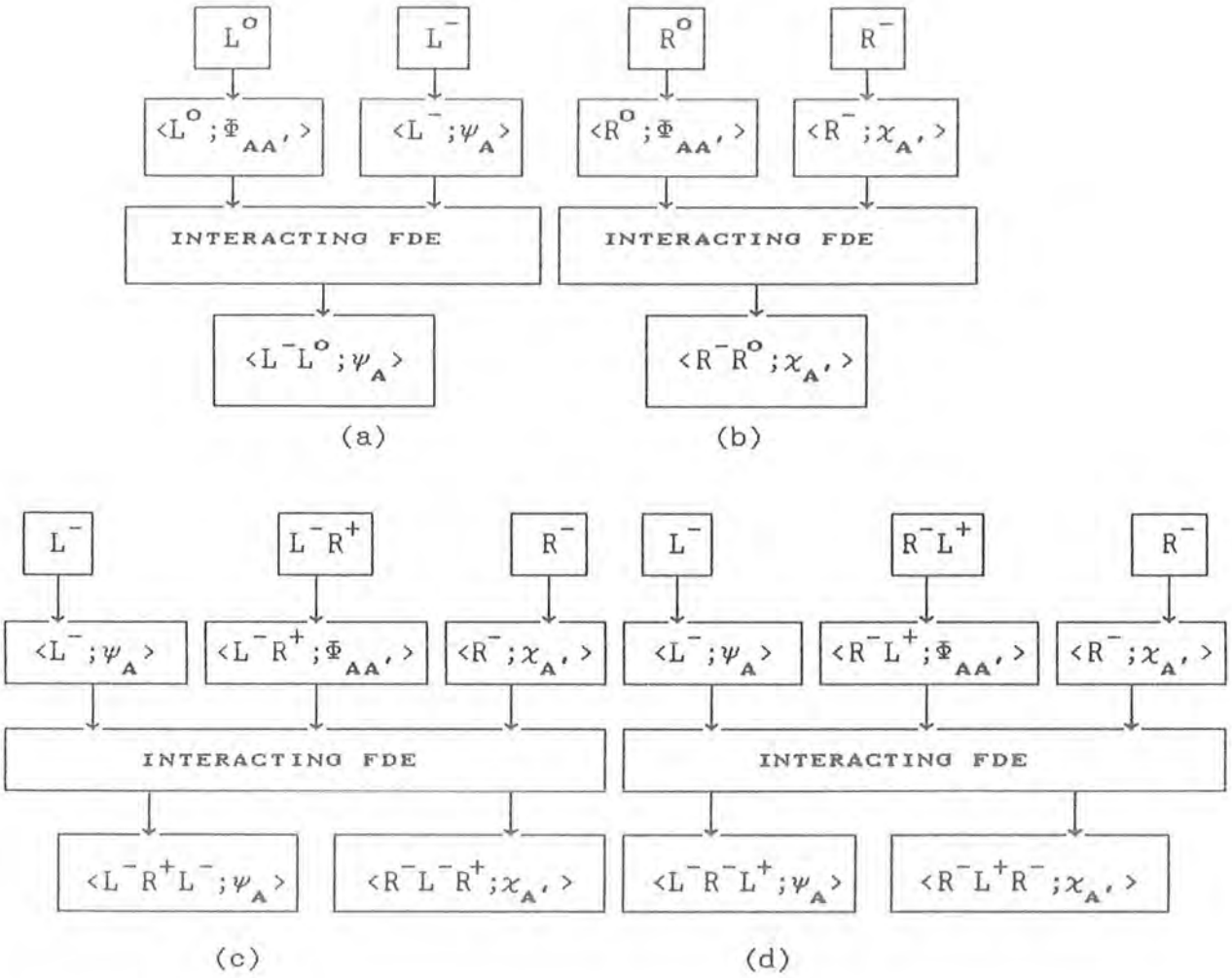

Figure 7

Block diagrams showing how new Dirac densities arise from the interaction between Dirac and potential densites. In (a) and (b), the incoming Dirac densities interact with the "zero-order" potential density. In either case, the relevant potential piece is produced by the electromagnetic datum that carries the same handedness as the incoming and outgoing densities. In (c) and (d), the interaction processes described by the dual configurations are controlled by the first-order FDE.

express the mass-scattering zigzag patterns in a simpler manner. This point will be touched upon again in chapter 6.

The device used here consists of planar trees carrying uncolored and colored vertices connected by solid straight, dashed and wavy lines. The uncolored vertices bear no meaning, but merely appear as end-points of external lines. In any graph, each colored vertex denotes a datum spot. It thus bears the white color or the black color depending upon whether the corresponding spot is left- or right-handed. Such a vertex also carries a charge label which effectively removes the charge-helicity ambiguity, and always contributes a specific differential form to the relevant integrand. The wavy lines appear as external lines starting at colored vertices. Each of them represents a proper Lorentz invariant distributional field [3,5,6,30,31], and carries a number referring to the "degree" of the distribution. Moreover, all the vertices from which they emanate actually contribute volume differential forms to the integral, each distribution being defined with the origin displaced to the RM-point associated with the vertex bearing the respective line. Colored vertices which do not involve wavy lines contribute KAP-like two-forms, and are always carried by graphs representing explicit outgoing fields. For an arbitrary scattering graph, there is only one colored vertex of this latter type while all the colored vertices occurring in graphs which do not represent scattering processes are of the former type. The solid straight and dashed lines can be both internal and external. Each of these lines really starts at a colored vertex. Internal dashed lines just play the role of connecting pieces, not contributing anything to

the integrands. External dashed lines always start at colored vertices which do not correspond to datum spots lying on $\mathscr{E}_o^+$. In this case, the line represents the whole $\hat{\pi}$-datum involved in the formation of the respective RM-spot. In the other case, the colored vertex does not bear such a line, but carries also the contribution due to a datum centred at a point of $\mathscr{E}_o^+$ unless it is connected with another colored vertex without bearing a wavy line. Of course, this latter rule has to be adequately extended when the external dashed lines are replaced by the corresponding sub-graphs. In the first instance, if a vertex carries an external dashed line it also carries a wavy line, but the converse is not true in any case. We can have vertices carrying wavy lines without bearing external dashed lines and also vertices carrying neither type of line. Indeed, a colored vertex which does not carry both external dashed and wavy lines appears as either the only vertex in a graph or the KAP-vertex of a scattering graph. The internal solid straight lines connect colored vertices which do not bear necessarily the same color. Each such line represents a typical inner-product affine-parameter structure carried explicitly by an integral expression. It is worth observing at this stage that the affine parameters involved are always carried by the denominators of the integrands, but the inner products are allowed to enter also into the numerators. Each external solid straight line denotes an explicit outgoing spinor carried by the integrand of an integral, the spinor being unprimed or primed according as the vertex from which the line comes is white or black. Two vertices of different colors can be "stuck" together to form a double-color vertex. Each such composite vertex bears a wavy line and carries the

information associated with a "shrunk" internal straight line. It really counts as one element to the relevant vertex-set, but corresponds to two datum spots centred at a common point of $\mathscr{C}_o^+$. The handedness of the datum entering into the associated integral is the same as that of the spot corresponding to the part of the vertex from which the wavy line emanates. These patterns appear to be useful only when we consider the real potential contributions. For these elementary pieces, it is convenient to atribute an upper-lower end-point character to the external solid straight lines which enables us to decide whether the corresponding spinors leave or enter the datum spots associated with those colored-vertex parts at which the lines start. Notice that this end-point rule actually breaks the invariance of the pieces carried by the elementary contributions when the graphs undergo arbitrary reflections and rotations. In general, the order of the colored vertices in a graph is irrelevant because the conjugation ambiguity has been eliminated from the beginning. Nevertheless, it seems to be worthwhile in any case to place the vertices in such a way that they bring about the structure of the symbolic expression for the corresponding integral. It appears that, when taken along any edge, the sum of the charges equals either zero, $\pm$ e or $\pm$ 2e. The values - e and - 2e actually arise in subgraphs representing conjugate Dirac branches. Explicit colored graphs will be exhibited later in chapters 3 and 4.

CHAPTER THREE

EVALUATION OF ELECTROMAGNETIC GRAPHS

3.1 Introduction

In this chapter, the explicit evaluation of the basic null diagrams associated with the elementary electromagnetic contributions is presented. It will be seen that, in the case of the fields, the configurations shown in Figs.2 and 3 turn out to be "reduced" because of the presence of Δ_1-functions in the solutions of the FDE (2.32), (2.34) and (2.35). For the corresponding potential densities, however, the null-loop pattern of the underlying configurations is retained since the solutions of (2.33), (2.36) and (2.37) all involve step functions for the relevant spotted vertices. One important feature of the solutions of the electromagnetic FDE is the correspondence between the handedness of the field densities and that of the datum spots with respect to which the Δ_1-functions are defined. This feature appears, in turn, to be intimately related to the structure of the flag poles entering into the solutions for the corresponding potential densities. In the particular case of the null configurations of Fig.3, these latter densities appear as sums of suitably contracted first derivatives of appropriate spinors, which are identitifed with the gradient of certain (scalar) functions whose definition comes directly from the structures of the RM-patterns. Such facts entail a remarkably simple form of the colored trees associated with the integral expressions. The basic procedure for solving the density equations was

used earlier for treating pure Dirac fields [4-6]. Essentially, it is equivalent to working out the geometric relations for each basic configuration. Section 3.2 deals with the construction of the integrals for the fields. In Sec.3.3, the integral expressions for the potentials are presented. Henceforth a distribution of "degree" k defined with the origin displaced to some point $R^{AA'}$ will be denoted by $\overset{R}{\Delta}_k(x)$.

3.2 Field Integrals

As was pointed out previously, the SI solutions of the free FDE (2.32) constitute the standard distributional splitting of the KAP-integrals for fields of spin $\pm$ 1. These are given by [3,5,6,17]

$$\langle L^{O}(M);\phi_{AB}(x)\rangle = \frac{1}{2\pi}\, \overset{K}{o}_{A}\overset{K}{o}_{B}\, \overset{M}{\Delta}_1(x)\hat{\pi}_{M1-}\phi_L o(\overset{MC}{o};M), \tag{3.1}$$

$$\langle R^{O}(M);\theta_{A'B'}(x)\rangle = \frac{1}{2\pi}\, \bar{o}_{KA'}\bar{o}_{KB'}\overset{M}{\Delta}_1(x)\hat{\pi}_{M1+}\bar{\phi}_R o(\bar{o}^{C'}_{M};M). \tag{3.2}$$

To see how the above solutions actually arise, one has first to derive the expressions for the derivatives of the spinors and affine parameters involved in Fig.2. We have, in effect,

$$x^{AA'} = M^{AA'} + r_{MR}\, \overset{MA-A'}{o\ o}_{M} + r_{RK}\, \overset{KA-A'}{o\ o}_{K}, \tag{3.3}$$

with $M^{AA'}$ and the flag pole $\overset{MA-A'}{o\ o}_{M}$ being both held fixed. Thus, differentiating (3.3) and making suitable contractions, we obtain the simple relations

$$\overset{x}{\nabla}_{AA'}\overset{K}{o}_{B} = -\frac{1}{\bar{z}_M z_M r_{MK}}\, \overset{K}{o}_{AMA'}\bar{o}^{M}_{B}, \tag{3.4}$$

$$\overset{x}{\nabla}_{AA'}r_{MR} = \frac{1}{\bar{z}_M z_M}\, \overset{K}{o}_{AKA'}\bar{o}, \quad \overset{x}{\nabla}_{AA'}r_{RK} = \frac{1}{\bar{z}_M z_M}\, \overset{M}{o}_{AMA'}\bar{o}, \tag{3.5}$$

together with the conjugate of (3.4). Hence, using the above relations and invoking the SI distributional expression

* The question concerning the convergence of the series giving the complete fields is not discussed here. This still constitutes an open problem which was referred to much earlier in Refs.[3,5]. We mention, however, that this problem can be easily treated by using the techniques provided in Ref.[35]. Of course, these are matters which would repay further investigation.

$$\nabla_{AA'}{}^{X}\,{}^{M}\Delta_1(x) = r_{RX}\,{}^{K}o_{AKA'}\,{}^{M}\Delta_2(x) - \frac{1}{\bar{z}_M z_M r_{RX}}\,{}^{M}o_{AMA'}\,{}^{M}\Delta_1(x), \tag{3.6}$$

we immediately arrive at Eqs.(2.32). The electromagnetic free-field contributions are then written as the conjugate KAP integrals

$$\langle\langle L^{o}(M);\phi_{AB}(x)\rangle\rangle = \frac{1}{2\pi}\int_{\mathbb{K}}{}^{1}\!\mathcal{K}\; o^{X}_{A}\,o^{X}_{B}\,\hat{\pi}_{M1-}\,\phi_{L}\,o(o^{MC};M), \tag{3.7}$$

$$\langle\langle R^{o}(M);\theta_{A'B'}(x)\rangle\rangle = \frac{1}{2\pi}\int_{\mathbb{K}}{}^{1}\!\mathcal{K}\; \bar{o}_{XA'}\,\bar{o}_{XB'}\,\hat{\pi}_{M1+}\,\bar{\phi}_{R}\,o(\bar{o}_{M}^{C'};M), \tag{3.8}$$

where ${}^{1}\!\mathcal{K}$ is an SI two-form on the space ${}^{1}\mathbb{K} \cong S^2$ of null graphs that start at O and terminate at $x^{AA'}$ (see Ref.[17]). It should be stressed that the Δ_1-function occurring in (3.1) and (3.2) really implies a "reduction" of Fig.2 so as to make $x^{AA'}$ coincide with $K^{AA'}$. The corresponding graphical representations are depicted as follows

$\langle\langle L^{o}(M);\phi_{AB}(x)\rangle\rangle =$  , $\langle\langle R^{o}(M);\theta_{A'B'}(x)\rangle\rangle =$  . (3.9)

There is an important geometric property of Fig.3 which arises immediately from the fact that the points $N^{AA'}$ and $P^{AA'}$ are held fixed as $x^{AA'}$ varies suitably. This property amounts to stating that the (real) SI vector

$$K^{AA'} = r_{NM}\,o^{ZA}\,\bar{o}^{A'}_{Z} - r_{PM}\,o^{TA}\,\bar{o}^{A'}_{T}, \tag{3.10}$$

remains constant. Upon transvection with $o^{N}_{AP}\,\bar{o}_{A'}$, we get the scalar

$$K = \bar{z}_P(o^{TAN}o_{TA})r_{PM} - z_N(o^{ZA'}\bar{o}_{PA'})r_{NM}, \tag{3.11}$$

which is referred to as the K-scalar for the configurations involved. This scalar quantity will play a significant role in Sec.3.3 and chapter 4. The explicit derivatives of the relevant spinors and affine parameters are given by

$$\overset{\times}{\nabla}_{\dot{B}\dot{B}'}\overset{ZA}{O} = -\frac{r_{PM}}{z_N\bar{z}_M(r_{MZ}r_{MT}-r_{NZ}r_{PT})}\overset{Z}{O}\bar{O}_{\dot{B}T\dot{B}'}\overset{NA}{O}, \tag{3.12}$$

$$\overset{\times}{\nabla}_{\dot{B}\dot{B}'}r_{NZ} = \frac{1}{z_M\bar{z}_M}\{\overset{T}{O}\bar{O}_{\dot{B}T\dot{B}'} + \frac{r_{NZ}r_{PM}}{z_N\bar{z}_N(r_{MZ}r_{MT}-r_{NZ}r_{PT})} \times [\bar{z}_N(\overset{NAT}{O}\overset{}{O}_A)\overset{Z}{O}\bar{O}_{\dot{B}T\dot{B}'} + C.C.]\}, \tag{3.13}$$

$$\overset{\times}{\nabla}_{\dot{B}\dot{B}'}r_{MZ} = \frac{1}{z_M\bar{z}_M}\{\overset{T}{O}\bar{O}_{\dot{B}T\dot{B}'} + \frac{r_{MZ}r_{PM}}{z_N\bar{z}_N(r_{MZ}r_{MT}-r_{NZ}r_{PT})} \times [\bar{z}_N(\overset{NAT}{O}\overset{}{O}_A)\overset{Z}{O}\bar{O}_{\dot{B}T\dot{B}'} + C.C.]\}, \tag{3.14}$$

$$\overset{\times}{\nabla}_{\dot{B}\dot{B}'}r_{NM} = \frac{1}{z_M\bar{z}_M}\{\frac{r_{NM}r_{PM}}{z_N\bar{z}_N(r_{MZ}r_{MT}-r_{NZ}r_{PT})}[\bar{z}_N(\overset{NAT}{O}\overset{}{O}_A)\overset{Z}{O}\bar{O}_{\dot{B}T\dot{B}'} + C.C.]\}, \tag{3.15}$$

along with the conjugate of (3.12) and the relations obtained from those given above by interchanging N$\longleftrightarrow$P and Z$\longleftrightarrow$T. Notice that the piece involving a difference between products of parameters in the denominators is invariant under these interchanges. The entire set of expressions can be derived by differentiating the relations

$$x^{AA'} = N^{AA'} + r_{NZ}\overset{ZA-A'}{O\ O}_{Z} + r_{ZX}\overset{TA-A'}{O\ O}_{T} = P^{AA'} + r_{PT}\overset{TA-A'}{O\ O}_{T} + r_{TX}\overset{ZA-A'}{O\ O}_{Z}, \tag{3.16}$$

and making appropriate contractions. When deriving these expressions, it is convenient to use the trivial affine-parameter identities

$$r_{NZ}r_{PM} + r_{NM}r_{MT} \equiv r_{NM}r_{PT} + r_{MZ}r_{PM} \equiv -(r_{MZ}r_{MT} - r_{NZ}r_{PT}).$$

To write out the middle blocks of Eqs. (2.34) and (2.35) explicitly, we use the KAP-splitting relations for the Dirac current densities

$$\langle L^-(N);\psi_A(x)\rangle\langle R^+(P);\bar{\psi}_{A'}(x)\rangle = e/4\pi^2(\overset{Z}{O}_A\overset{N}{\Delta}_1(x)\hat{\pi}_{N1/2-}\psi_L - (\overset{NB}{O};N))$$
$$\times(\bar{O}_{TA'}\overset{P}{\Delta}_1(x)\hat{\pi}_{P1/2+}\bar{\psi}_R + (\bar{O}^{B'}_{P};P)), \tag{3.17}$$

$$\langle R^-(N);\chi_{A'}(x)\rangle\langle L^+(P);\bar{\chi}_A(x)\rangle = e/4\pi^2(\bar{O}_{ZA'}\overset{N}{\Delta}_1(x)\hat{\pi}_{N1/2+}\chi_R - (\bar{O}^{B'}_{N};N))$$
$$\times(\overset{T}{O}_A\overset{P}{\Delta}_1(x)\hat{\pi}_{P1/2-}\bar{\chi}_L + (\overset{PB}{O};P)). \tag{3.18}$$

The procedure for obtaining the solution of the equation occurring in (2.34) that involves the left-handed field density is now developed. The solutions of the other FDE will then be achieved by making trivial replacements. In accordance with the general prescription given in Refs.[4-6], one seeks a solution of the form

$$\langle \bar{L}(N)R^{+}(P);\phi_{AB}(x)\rangle = \alpha_A\beta_B \overset{N}{\Delta}_j(x)\overset{P}{\Delta}_k(x) \times \hat{\pi}_{N1/2-}\psi_L(\overset{NC}{o};N)\hat{\pi}_{P1/2+}\bar{\psi}_R(\overset{\bar{C}'}{o};P), \tag{3.19}$$

where α_A and β_B are spinors to be determined along with j and k. Thus, operating on (3.19) with $\overset{X}{\nabla}^{BA'}$ and making use of the generalized SI derivative

$$\overset{X}{\nabla}^{BA'}\overset{N}{\Delta}_j(x) = r_{NZ}\overset{ZB-A'}{o}\overset{N}{\Delta}_{j+1}(x) - \frac{j}{z_M\bar{z}_M r_{NZ}}\overset{TB-A'}{o}\overset{N}{\Delta}_j(x), \tag{3.20}$$

together with the expression that arises from applying the NP-ZT interchange rule to (3.20), we obtain after some calculations

$$\alpha_A\beta_B = \lambda\, \overset{Z}{o}_A\overset{Z}{o}_B, \quad \lambda = \frac{e}{2\pi}\frac{r_{NZ}}{z_M(r_{MZ}r_{MT} - r_{NZ}r_{PT})}, \quad j=1,\ k=0. \tag{3.21}$$

Hence the solution sought is uniquely given by

$$\langle \bar{L}(N)R^{+}(P);\phi_{AB}(x)\rangle = -\frac{e}{2\pi z_M r_{PM}}\overset{Z}{o}_A\overset{Z}{o}_B\overset{N}{\Delta}_1(x)\overset{P}{\Delta}_o(x) \times \hat{\pi}_{N1/2-}\psi_L(\overset{NC}{o};N)\hat{\pi}_{P1/2+}\bar{\psi}_R(\overset{\bar{C}'}{o};P), \tag{3.22}$$

provided that

$$\overset{X}{\nabla}^{BA'}(\lambda\,\overset{Z}{o}_A\overset{Z}{o}_B) = -\frac{e}{2\pi}\frac{\overset{Z}{o}_A\overset{\bar{A}'}{o}_T}{z_M\bar{z}_M(r_{MZ}r_{MT} - r_{NZ}r_{PT})}. \tag{3.23}$$

In fact, the terms involving $\overset{N}{\Delta}_1(x)$ and $\overset{P}{\Delta}_o(x)$ cancel when (3.22) is inserted into the density equation under consideration, the remaining terms thus reinstating the relevant right-hand side. The field contribution is then symbolically expressed as

$$\langle\langle L^-(N)R^+(P);\phi_{AB}(x)\rangle\rangle = \int_{\mathbb{E}_L} \langle L^-(N)R^+(P);\phi_{AB}(x)\rangle \underset{\sim}{\Delta}_I^- \wedge \underset{\sim}{\Omega}_N^- \wedge \underset{\sim}{\Delta}_{II}^+ \wedge \underset{\sim}{\Omega}_P^+, \quad (3.24)$$

where the charged Δ-forms are those associated with the contributions of the spotted vertices occurring in the configurations that give rise to the formation of the current spots. The Ω-forms are associated with the explicit contributions emanating from $N^{AA'}$ and $P^{AA'}$. These latter forms are SI volume forms of the type

$$\underset{\sim}{\Omega}_W = \frac{dr_{HW}}{r_{HW}} \wedge \overset{W}{\underset{\sim}{\mathcal{S}}}, \quad (3.25)$$

where the affine parameter involved lies on the generator of the future null cone of an appropriate vertex $H^{AA'}$ that appears in the underlying configuration, and $\overset{W}{\underset{\sim}{\mathcal{S}}}$ stands for the SI element of two-surface area of the (space-like) intersection between $\mathcal{E}_Y^-$ and $\mathcal{E}_H^+$, with $Y^{AA'}$ denoting a suitable point lying to the future of $N^{AA'}$ or $P^{AA'}$ (see Ref.[6]). The integration is taken over the space $\mathbb{E}_L$ of structures of the type shown in Fig.8a. Once again, we see clearly that the former calculational structure (Fig.3a) is "reduced" because of the presence of the $\overset{N}{\Delta}_1$-function. Thus for (3.24) we have the graph

$$\langle\langle L^-(N)R^+(P);\phi_{AB}(x)\rangle\rangle =$$

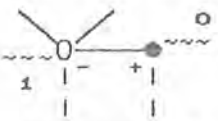

. (3.26)

It is evident that the relevant (typical) structure associated with the internal line occurring in the above graph is $\frac{-e/2\pi}{z_M r_{PM}}$. When worked out explicitly, the prescription yielding (3.22) shows us that the solution for the right-handed density involved in Eq.(2.34) can be obtained from (3.22) by first applying the NP-ZT interchange rule to the distributions, replacing the explicit $\overset{Z}{o}_A$-spinors by $\bar{o}_{TA'}, \bar{o}_{TB'}$, , and then taking a complex conjugation of the inner product at $M^{AA'}$, the overall

sign being also changed. We thus have

$$\langle L^{-}(N)R^{+}(P);\theta_{A',B'}(x)\rangle = \frac{e}{2\pi\bar{z}_{M}r_{NM}}\,\bar{o}_{\dot{T}A'}\,\bar{o}_{\dot{T}B'}\,\overset{P}{\Delta}_{1}(x)\overset{N}{\Delta}_{0}(x)$$
$$\times\,\hat{\pi}_{N1/2-}\psi_{L}^{-}(\overset{NC}{o};N)\hat{\pi}_{P1/2+}\bar{\psi}_{R}^{+}(\bar{o}_{P}^{C'};P), \qquad (3.27)$$

whence the corresponding contribution is written as

$$\langle\langle L^{-}(N)R^{+}(P);\theta_{A',B'}(x)\rangle\rangle = \int_{\mathbb{E}_{R}}\langle L^{-}(N)R^{+}(P);\theta_{A',B'}(x)\rangle\underset{\sim}{\Delta}_{I}^{-}\wedge\underset{\sim}{\Omega}_{N}^{-}\wedge\underset{\sim}{\Delta}_{II}^{+}\wedge\underset{\sim}{\Omega}_{P}^{+}, \qquad (3.28)$$

with the integral taken over the space of null configurations of the type exhibited in Fig.8b. The corresponding colored-graph representation is then given by

$$\langle\langle L^{-}(N)R^{+}(P);\theta_{A',B'}(x)\rangle\rangle =$$

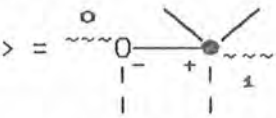

. (3.29)

To the FDE (2.35) with the current density (3.18), the standard prescription yields the solutions

$$\langle R^{-}(N)L^{+}(P);\phi_{AB}(x)\rangle = \frac{e}{2\pi z_{M}r_{NM}}\,\overset{T}{o}_{A}\,\overset{T}{o}_{B}\,\overset{P}{\Delta}_{1}(x)\overset{N}{\Delta}_{0}(x)$$
$$\times\,\hat{\pi}_{N1/2+}\chi_{R}^{-}(\bar{o}_{N}^{C'};N)\hat{\pi}_{P1/2-}\bar{\chi}_{L}^{+}(\overset{PC}{o};P), \qquad (3.30)$$

$$\langle R^{-}(N)L^{+}(P);\theta_{A',B'}(x)\rangle = -\frac{e}{2\pi\bar{z}_{M}r_{PM}}\,\bar{o}_{\dot{Z}A'}\,\bar{o}_{\dot{Z}B'}\,\overset{N}{\Delta}_{1}(x)\overset{P}{\Delta}_{0}(x)$$
$$\times\,\hat{\pi}_{N1/2+}\chi_{R}^{-}(\bar{o}_{N}^{C'};N)\hat{\pi}_{P1/2-}\bar{\chi}_{L}^{+}(\overset{PC}{o};P), \qquad (3.31)$$

the associated SI field integrals thus being

$$\langle\langle R^{-}(N)L^{+}(P);\phi_{AB}(x)\rangle\rangle = \int_{\mathcal{S}_{L}}\langle R^{-}(N)L^{+}(P);\phi_{AB}(x)\rangle\underset{\sim}{\delta}_{I}^{-}\wedge\underset{\sim}{\Omega}_{N}^{-}\wedge\underset{\sim}{\delta}_{II}^{+}\wedge\underset{\sim}{\Omega}_{P}^{+}, \qquad (3.32)$$

$$\langle\langle R^{-}(N)L^{+}(P);\theta_{A',B'}(x)\rangle\rangle = \int_{\mathcal{S}_{R}}\langle R^{-}(N)L^{+}(P);\theta_{A',B'}(x)\rangle\underset{\sim}{\delta}_{I}^{-}\wedge\underset{\sim}{\Omega}_{N}^{-}\wedge\underset{\sim}{\delta}_{II}^{+}\wedge\underset{\sim}{\Omega}_{P}^{+}. \qquad (3.33)$$

Notice that the latter integrands can be constructed from (3.22) and (3.27) by using the NP-ZT rule and supplying the $\hat{\pi}$-data. The configurations which are relevant for the integrations are depicted in

Figs. 8c and 8d. Accordingly, a simple white-black interchange rule yields the graphical representations

$$\langle\langle R^{-}(N)L^{+}(P);\phi_{AB}(x)\rangle\rangle = \quad , \tag{3.34}$$

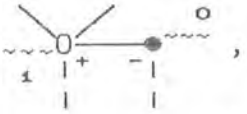

$$\langle\langle R^{-}(N)L^{+}(P);\theta_{A'B'}(x)\rangle\rangle = \quad . \tag{3.35}$$

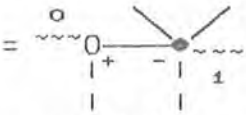

The differential forms entering explicitly into (3.32) and (3.33) bear essentially the same meaning as in (3.24) and (3.28). It should be emphasized at this stage that the Δ_1-function "reduction" yielding the patterns of Fig.8 implies in each case the identification of $x^{AA'}$ with either $Z^{AA'}$ or $T^{AA'}$.

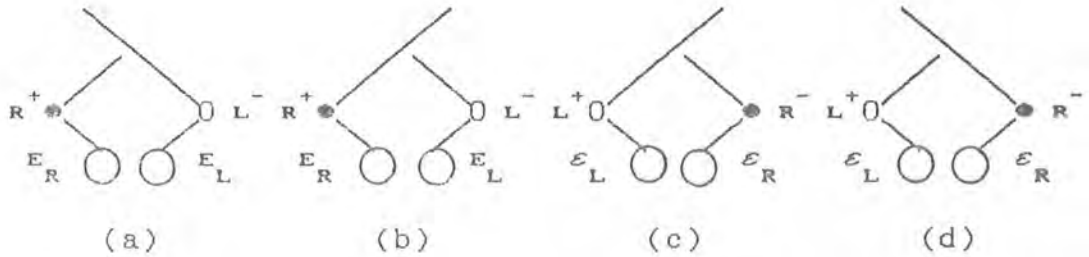

Figure 8

Minkowskian configurations involved in the integrations for the basic electromagnetic-field contributions produced by current pieces. The loops denote the branches that give rise to the formation of the current datum spots: (a) and (c) structures for left-handed fields; (b) and (d) structures for right-handed fields.

3.3 Potential Integrals

Upon working out the prescription for deriving the basic potential densities, one has to solve simultaneously the equations that enter into each of the pairs of FDE (2.33), (2.36) and (2.37). The explicit form of Eqs.(2.33) is achieved by simply using the field densities (3.1) and (3.2). We thus have

$$\overset{x}{\nabla}_{AA'}\langle L^{o}(M);\Phi^{A'}_{B}(x)\rangle = \frac{1}{2\pi}\,\overset{K}{o}_{A}\overset{K}{o}_{B}\overset{M}{\Delta}_{1}(x)\hat{\pi}_{M1-}\phi_{L}o(\overset{MC}{o};M), \tag{3.36}$$

$$\overset{x}{\nabla}_{AA'}\langle R^{o}(M);\Phi^{A}_{B'}(x)\rangle = \frac{1}{2\pi}\,\bar{o}_{KA'}\bar{o}_{KB'}\overset{M}{\Delta}_{1}(x)\hat{\pi}_{M1+}\bar{\phi}_{R}o(\bar{o}^{C'}_{M};M). \tag{3.37}$$

It follows that, invoking the basic procedure of which we made use in the preceeding section and using the formulae (3.4)-3.6), we obtain the expression

$$\langle L^{o}(M);\Phi_{AA'}(x)\rangle = \frac{1}{2\pi}\left[\frac{1}{\bar{z}_{M}r_{RX}}\overset{M}{\Delta}_{o}(x)\overset{K}{o}_{AMA'}\bar{o}_{A'}\hat{\pi}_{M1-}\phi_{L}o(\overset{MC}{o};M) + C.C.\right]$$

$$= \langle R^{o}(M);\Phi_{AA'}(x)\rangle. \tag{3.38}$$

This is the real ("zero-order") potential density referred to before. Notice that it can be re-expressed as

$$\langle L^{o}(M);\Phi_{AA'}(x)\rangle = \frac{1}{2\pi}\left[\overset{M}{\Delta}_{o}(x)o^{KB}\overset{x}{\nabla}_{AA'}\overset{K}{o}_{B}\hat{\pi}_{M1-}\phi_{L}o(\overset{MC}{o};M) + C.C.\right]$$

$$= \langle R^{o}(M);\Phi_{AA'}(x)\rangle. \tag{3.39}$$

The corresponding SI integral is written as

$$\langle\langle L^{o}(M);\Phi_{AA'}(x)\rangle\rangle = \int_{\mathcal{V}_{5}}\langle\mathscr{R}^{o}(M);\Phi_{AA'}(x)\rangle\Omega^{o}_{\sim M} = \langle\langle R^{o}(M);\Phi_{AA'}(x)\rangle\rangle, \tag{3.40}$$

where the letter $\mathscr{R}$ stands for either L or R, and the configuration over which the integral is taken is that shown in Fig.9. It should be emphasized, also, that the presence of the step function does not entail any collapse of the null loop of Fig.2. The corresponding graphical representation is thus depicted as follows

$$\langle\langle L^{\circ}(M);\Phi_{AA'}(x)\rangle\rangle = \quad + \quad = \langle\langle R^{\circ}(M);\Phi_{AA'}(x)\rangle\rangle. \qquad (3.41)$$

Recall that, for the potential contribution just calculated, it is convenient to use the upper-lower end-vertex convention. In fact, the conjugate graphical pieces can be easily constructed from one another by reflecting the lines in the vertical that "contains" the "interface" between the two colored parts, keeping the vertex fixed.

To calculate the potential density that enters into the pair of FDE (2.36), it is convenient (but not strictly necessary) to use the whole expression for $\alpha_A\beta_B$ as given by (3.21) in conjunction with the one associated with the right-handed field density (3.27). Thus, Eqs. (2.36) take the explicit form

$$\overset{x}{\nabla}_{AA'}\langle L^{-}(N)R^{+}(P);\Phi_{B}^{A'}(x)\rangle = \frac{e}{2\pi}\,\frac{r_{NZ}^{\;N}\Delta_1^{\;P}(x)\Delta_o(x)}{z_M(r_{MZ}r_{MT}-r_{NZ}r_{PT})}\,\overset{Z}{o}_A\,\overset{Z}{o}_B$$

$$\times\,\hat{\pi}_{N1/2-}\psi_L^{-}(\overset{NC}{o};N)\hat{\pi}_{P1/2+}\bar{\psi}_R^{+}(\bar{\overset{C'}{o}};P), \qquad (3.42)$$

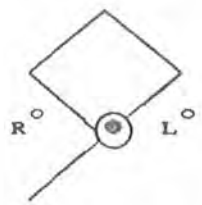

Figure 9

Five-edge null configuration involved in the integration of the real potential density. The presence of an overall step function in the whole integrand does not entail any collapse of the null loop.

and

$$\overset{\times}{\nabla}_{AA'}\langle L^{-}(N)R^{+}(P);\Phi^{A}_{B'}(x)\rangle = -\frac{e}{2\pi}\frac{r_{PT}\overset{P}{\Delta}_{i}(x)\overset{N}{\Delta}_{O}(x)}{\bar{z}_{M}(r_{MZ}r_{MT}-r_{NZ}r_{PT})}\bar{o}_{TA'}\bar{o}_{TB'}$$

$$\times\hat{\pi}_{N1/2-}\psi_{L}(\overset{NC}{o};N)\hat{\pi}_{P1/2+}\bar{\psi}_{R}(\bar{o}^{C'}_{P};P). \qquad (3.43)$$

Therefore, when replaced into (3.42) and (3.43), a common solution of the form

$$\langle L^{-}(N)R^{+}(P);\Phi_{AA'}(x)\rangle = \mu\,\xi_{A}\eta_{A'}\overset{P}{\Delta}_{j}(x)\overset{N}{\Delta}_{k}(x)$$

$$\times\hat{\pi}_{N1/2-}\psi_{L}(\overset{NC}{o};N)\hat{\pi}_{P1/2+}\bar{\psi}_{R}(\bar{o}^{C'}_{P};P), \qquad (3.44)$$

leads us uniquely to

$$\mu = -\frac{e}{2\pi}\frac{1}{z_{M}\bar{z}_{M}(r_{MZ}r_{MT}-r_{NZ}r_{PT})},\quad \xi_{A}\eta_{A'} = \overset{Z}{o}_{ATA'},\ ,\ j=k=0, \qquad (3.45)$$

where the relation (3.20) and its "ZT-dual" have been used. It follows that the pertinent potential contribution is written as

$$\langle\langle L^{-}(N)R^{+}(P);\Phi_{AA'}(x)\rangle\rangle = \int_{\mathcal{S}_{\psi\bar{\psi}}}\langle L^{-}(N)R^{+}(P);\Phi_{AA'}(x)\rangle\underset{\sim}{\Delta}^{-}_{I}\underset{\sim}{\Omega}^{-}_{N}\underset{\sim}{\Delta}^{+}_{II}\underset{\sim}{\Omega}^{+}_{P}, \qquad (3.46)$$

with the (SI) density involved being explicitly given by

$$\langle L^{-}(N)R^{+}(P);\Phi_{AA'}(x)\rangle = -\frac{e}{2\pi}\frac{\overset{Z}{o}_{ATA'}\overset{P}{\Delta}_{O}(x)\overset{N}{\Delta}_{O}(x)}{z_{M}\bar{z}_{M}(r_{MZ}r_{MT}-r_{NZ}r_{PT})}$$

$$\times\hat{\pi}_{N1/2-}\psi_{L}(\overset{NC}{o};N)\hat{\pi}_{P1/2+}\bar{\psi}_{R}(\bar{o}^{C'}_{P};P). \qquad (3.47)$$

The integral (3.46) is taken over the space $\mathcal{S}_{\psi\bar{\psi}}$ of null patterns of the type shown in Fig.10a, its graphical representation being

$$\langle\langle L^{-}(N)R^{+}(P);\Phi_{AA'}(x)\rangle\rangle = \quad . \qquad (3.48)$$

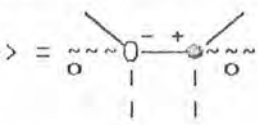

Thus, for the structure (3.48), the internal line represents the factor $-e/2\pi z_{M}\bar{z}_{M}(r_{MZ}r_{MT}-r_{NZ}r_{PT})$. In verifying that (3.47) does indeed satisfy Eqs.(3.42) and (3.43), one can make use of the relations

$$\overset{\times}{\nabla}_{AA'}[\, z_M \bar{z}_M (r_{MZ} r_{MT} - r_{NZ} r_{PT})] = -(r_{NM} \overset{Z}{O}_{AZA'} \bar{O} + r_{PM} \overset{T}{O}_{ATA'} \bar{O}), \quad (3.48)$$

and

$$\overset{\times}{\nabla}_{BB'}[\, \overset{ZA-A'}{O\ T}\ \overset{P}{\Delta}_O(x)\overset{N}{\Delta}_O(x)] = (z_N \bar{z}_M r_{NM} \overset{ZA-A'}{O\ P} - z_M \bar{z}_P r_{PM} \overset{NA-A'}{O\ T})$$

$$\times \frac{\overset{Z}{O}_{BTB'} \bar{O}\ \overset{P}{\Delta}_O(x)\overset{N}{\Delta}_O(x)}{z_N z_M \bar{z}_M \bar{z}_P (r_{MZ} r_{MT} - r_{NZ} r_{PT})} + [\, r_{NZ} \overset{Z}{O}_{BZB'} \bar{O}\ \overset{N}{\Delta}_1(x)\overset{P}{\Delta}_O(x)$$

$$+ r_{PT} \overset{T}{O}_{BTB'} \bar{O}\ \overset{P}{\Delta}_1(x)\overset{N}{\Delta}_O(x)]\ \overset{ZA-A'}{O\ T}, \quad (3.50)$$

which imply that

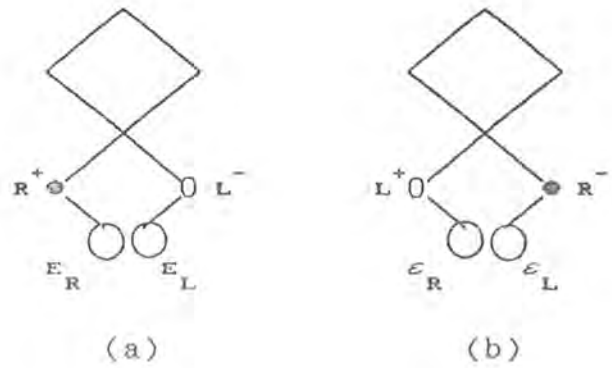

Figure 10

Configurations involved in the explicit integral expressions for the potential densities produced by elementary current densities. The fact that the integrands carry only the step functions for the points at which the datum spots are centred implies the preservation of the structures associated with the patterns of the former calculational devices. The loops have the same meaning as before; (a): structure involving a $\psi\bar{\psi}$-current piece; (b) structure involving a $\chi\bar{\chi}$-current piece.

$$\overset{X}{\nabla}_{BB'}\langle \bar{L}(N)R^{+}(P);\Phi_{AA'}(x)\rangle = -\frac{e}{2\pi}\{\overset{N}{\Delta}_{0}(x)\overset{P}{\Delta}_{0}(x)[\,(\frac{\bar{z}_{M}r_{NM}\overset{Z}{o}_{A}\overset{\bar{o}}{}_{PA'}}{\bar{z}_{P}}$$

$$-\frac{z_{M}r_{PM}\overset{N}{o}_{A}\overset{\bar{o}}{}_{TA'}}{z_{N}})\overset{Z}{o}_{BTB'}+(r_{NM}\overset{Z}{o}_{BZB'}+r_{PM}\overset{T}{o}_{BTB'})\overset{Z}{o}_{ATA'}\,]$$

$$+z_{M}\bar{z}_{M}(r_{MZ}r_{MT}-r_{NZ}r_{PT})[\,r_{NZ}\overset{Z}{o}_{BZB'}\overset{N}{\Delta}_{1}(x)\overset{P}{\Delta}_{0}(x)$$

$$+r_{PT}\overset{T}{o}_{BTB'}\overset{P}{\Delta}_{1}(x)\overset{N}{\Delta}_{0}(x)]\overset{Z}{o}_{ATA'}\}\frac{\hat{\pi}_{N1/2-}\psi_{L}(\overset{NC}{o};N)\hat{\pi}_{P1/2+}\bar{\psi}_{R}(\overset{\bar{C}'}{o}_{P};P)}{[z_{M}\bar{z}_{M}(r_{MZ}r_{MT}-r_{NZ}r_{PT})]^{2}}. \quad (3.51)$$

Consequently, making suitable contractions over the indices AB and A'B', yields the expressions (3.22) and (3.27) along with the divergencelessness of $\langle \bar{L}(N)R^{+}(P);\Phi_{AA'}(x)\rangle$. It should be pointed out that the densities (3.22), (3.27) and (3.47) differ by an overall sign from those exhibited in Penrose & Rindler [3]. This is due only to the choice of sign convention involved in the definition of the inner products at $M^{AA'}$.

There is another property of the configurations shown in Fig.3 which gives rise to an important alternative expression for the potential density (3.47). The property in question is that the SI quantity $z_{M}\bar{z}_{M}r_{PM}r_{NM}$ remains constant when the relevant integration is performed. A simple way of seeing this is to invoke the formulae (3.12)-(3.15) together with their (Z⟷T)-counterparts. This procedure yields the formal relations

$$\overset{X}{\nabla}_{AA'}(\log(z_{M}r_{PM})) = \frac{1}{z_{M}\bar{z}_{M}}(\bar{z}_{M}\overset{T}{o}_{B}\overset{X}{\nabla}_{AA'}\overset{ZB}{o} + z_{M}\overset{\bar{o}}{}_{ZB'}\overset{X}{\nabla}_{AA'}\overset{\bar{B}'}{o}_{T}), \quad (3.52)$$

$$\overset{X}{\nabla}_{AA'}(\log(\bar{z}_{M}r_{NM})) = \frac{1}{z_{M}\bar{z}_{M}}(\bar{z}_{M}\overset{TB}{o}\overset{X}{\nabla}_{AA'}\overset{Z}{o}_{B} + z_{M}\overset{\bar{B}'}{o}_{Z}\overset{X}{\nabla}_{AA'}\overset{\bar{o}}{}_{TB'}), \quad (3.53)$$

whence $\overset{X}{\nabla}_{AA'}(\log(z_{M}\bar{z}_{M}r_{PM}r_{NM})) = 0$. Thus, the density (3.47) reduces to

$$\langle L^{-}(N)R^{+}(P);\Phi_{AA'}(x)\rangle = -\frac{e}{2\pi}\,\frac{z_N^{\ N}\bar{z}_P^{\ P}\Delta_{\dot{C}}^{N}(x)\Delta_{\dot{C}}^{P}(x)}{K}\times\nabla_{AA'}(\log(z_M r_{PM}))$$
$$\times\,\hat{\pi}_{N1/2-}\psi_L^{-}(\overset{NC}{o};N)\hat{\pi}_{P1/2+}\bar{\psi}_R^{+}(\bar{o}_P^{C'};P), \qquad (3.54)$$

where K is the scalar quantity defined in (3.11). Similar calculations show us that the potential density produced by a $(R^{-}L^{+})$-current piece (see Eqs.(2.37)) can be directly obtained from (3.54) by replacing the $\hat{\pi}$-data and taking a complex conjugation of the remaining factor. Using (3.52) and (3.53), we thus get

$$\langle R^{-}(N)L^{+}(P);\Phi_{AA'}(x)\rangle = \frac{e}{2\pi}\,\frac{z_P^{\ P}\bar{z}_N^{\ N}\Delta_{\dot{C}}^{P}(x)\Delta_{\dot{C}}^{N}(x)}{\bar{K}}\times\nabla_{AA'}(\log(z_M r_{NM}))$$
$$\times\,\hat{\pi}_{N1/2+}\chi_R^{-}(\bar{o}_N^{C'};N)\hat{\pi}_{P1/2-}\bar{\chi}_L^{+}(\overset{PC}{o};P). \qquad (3.55)$$

Therefore, the SI integral for the contribution corresponding to this latter density is written as

$$\langle\langle R^{-}(N)L^{+}(P);\Phi_{AA'}(x)\rangle\rangle = \int_{\mathcal{S}_{\chi\bar{\chi}}} \langle R^{-}(N)L^{+}(P);\Phi_{AA'}(x)\rangle \delta_{\sim I}^{-}\wedge\Omega_{\sim N}^{-}\wedge\delta_{\sim II}^{+}\wedge\Omega_{\sim P}^{+}, \qquad (3.56)$$

with the integration being taken over the space of null patterns of the form shown in Fig.10b. For the graphical structure associated with (3.56), we have

$$\langle\langle R^{-}(N)L^{+}(P);\Phi_{AA'}(x)\rangle\rangle =$$

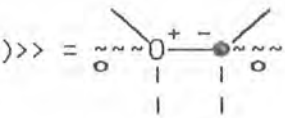

. (3.57)

CHAPTER FOUR

ELECTROMAGNETIC SCATTERING OF DIRAC FIELDS

4.1 Introduction

This chapter is concerned with the evaluation of the null configurations that describe the processes of electromagnetic scattering of Dirac fields. The relevant prescriptions are based upon the fact that, whenever the structures for the basic potential densities are coupled with the branches corresponding to the KAP-splitting of incoming Dirac fields, all the density equations associated with the former configurations remain formally unaffected. This fact allows one to carry out the actual calculation of the diagrams shown in Figs.5 and 6 in a systematic way. The coupling prescriptions involve modifying the (complex) potential flag poles in such a way that the blocks carried by the right-hand side of each of the equations governing the propagation of Dirac densities in regions with potential are "annihilated" if the handedness of the electromagnetic-field branch involved is different from that of the relevant incoming field. Thus, an incoming field of one handedness contributes a spinor to the modified potential kernels which carries the other handedness, but the "strong" relations (3.39), (3.54) and (3.55) still hold, with the formal labels Z and T carried by (3.52) and (3.53) being replaced by R and K, respectively. In the case of Fig.5, in particular, either of the incoming fields then picks out the piece of the real potential density that involves the electromagnetic datum

of the same handedness as that of the associated incoming density. Accordingly, each configuration of Fig.6 involves a Maxwell-field structure that possesses the same handedness as that of the corresponding incomig field. The spinor that emanates from the current spot carrying the other handedness becomes a "dummy" in the sense that it is taken over by one of the spinors involved in the incoming flag pole. The former spinor is the one whose flag pole lies on the main plane of the "dual" configuration, the structures of either pair having to be dealt with in this way. In any case, the standard potential kernel is brought back when the incoming Dirac branch is dropped from the relevant structure. For Fig.6, the main planes of each pair of "dual" configurations coincide, the NP-ZT interchange rule that emerges from the evaluation of Fig.3 appearing merely as an NP-RK rule. This feature of the RM-diagrams comes from the wave equations for the Dirac densities exhibited in chapter 2.

The explicit expressions for the NID for the scattering processes naturally arise from the solutions of the relevant FDE. The distributional structure of the solutions of the FDE as provided by Penrose & Rindler [3] will be used here. Each of these solutions carries two pieces which appear as a phase-shift and a scattering distributional term. Both of these terms vanish when the respective incoming field propagates far away from the scatterer branch. Due to this circumstance, each incoming field propagates as if it were free. All the phase-shift terms involve step functions for the scatterer spots along with Δ_1-functions for the spots from which the incoming fields emanate. Each of these pieces also carries a scalar function

multiplied by the spinor involved in the KAP-splitting of the incoming field. The phase-shift scalar functions appear to be constant on $\mathscr{E}_{D}^{+}$ and $\mathscr{E}_{B}^{+}$ with respect to those derivative operators which are defined in the direction of the propagation of the incoming densities. Such functions play a significant role in the determination of the null data for the processes in that they contribute pieces of elementary data which couple suitably with those coming directly from the right-hand sides of the FDE, thereby leading to useful (non-vanishing) scattering $\hat{\pi}$-data. Each scattering term involves only the product of a massless free charged spin $\pm$ 1/2 field with the step functions for the spotted points of the corresponding configuration. These "electron neutrinos" are required to satisfy certain specific relations set upon the future null cones of the spots involved in the scatterer branches.

The organization of the chapter is as follows. In Sec.4.2, the calculation of the diagrams of Fig.5 is carried out. The structures of Fig.6 are evaluated in Sec.4.3. The procedures for calculating explicitly just one pattern of each of the figures are completed. The integral expressions for the other patterns will then be constructed on the basis of simple interchange and conjugation rules. Most of the relations involving the derivatives of the spinors and affine parameters occurring in the structures under consideration can be obtained from those associated with Fig.3 by making trivial replacements. For this reason, the entire set of formulae that arise from the geometric properties of the scattering diagrams will not be written out explicitly.

4.2 Scattering by $\langle L^{o}(M);\Phi_{AA'}(x)\rangle$ and $\langle R^{o}(M);\Phi_{AA'}(x)\rangle$

In order to write down the explicit right-hand sides of the FDE (2.38) and (2.39), we first have to replace the complex vector kernels and inner products that enter into the derivatives of Eq.(3.39) by those for Fig.5. The corresponding modification of the formulae (3.12)-(3.15) amounts simply to replacing N,Z,P,T by M,K,D,S, respectively. Thus, using the relations for the latter null structures (see (3.49))

$$\overset{x}{\nabla}_{AA'}(\overset{KL}{o}\,\overset{x}{\nabla}^{A'}_{B}\,\overset{K}{o}_{L}) = \frac{1}{2}\,\varepsilon_{AB}\,\overset{KL}{o}\square_{x}\overset{K}{o}_{L} = 0, \tag{4.1a}$$

$$\overset{x}{\nabla}_{AA'}(\overset{KL}{o}\,\overset{x}{\nabla}^{A}_{B'}\,\overset{K}{o}_{L}) = \frac{1}{2}\,\varepsilon_{A'B'}\,\overset{KL}{o}\square_{x}\overset{K}{o}_{L} = 0, \tag{4.1b}$$

along with their conjugates, we obtain the density equation

$$\overset{x}{\nabla}_{AA'}\langle L^{o}(M);\Phi^{A'}_{B}(x)\rangle = \frac{1}{2\pi}\overset{M}{\Delta}_{1}(x)r_{MK}\,\overset{K}{o}_{A}\overset{-}{o}_{KA'}(\overset{KL}{o}\,\overset{x}{\nabla}^{A'}_{B}\,\overset{K}{o}_{L})\hat{\pi}_{M1-}\phi_{L}o(\overset{MC}{o};M), \tag{4.2}$$

together with the one that involves the right-handed electromagnetic datum. Hence, the expressions for the electromagnetic field densities that emerge from the SI distributional splitting of the free contributions hold on $\mathscr{C}^{+}_{M}$. It is worth emphasizing that the datum spots producing the incoming Dirac densities do not contribute at all to the integral expressions for the Maxwell quantities that enter into Eqs. (2.33). Thus, the Dirac branches of Fig.5 cease to play any role when the electromagnetic integrals are actually performed. It follows that Eqs.(2.38) and (2.39) can be re-written as

$$\overset{x}{\nabla}^{AA'}\langle L^{-}(D)L^{o}(M);\psi_{A}(x)\rangle = -\frac{ie}{4\pi^{2}}\,\frac{z_{m}r_{Dm}\overset{M}{\Delta}_{o}(x)\overset{D}{\Delta}_{1}(x)\overset{-A'}{o}_{S}}{\overset{-}{z}_{m}(r_{Dm}r_{MK}+r_{mS}r_{Mm})}$$

$$\times\,\hat{\pi}_{M1-}\phi_{L}o(\overset{MC}{o};M)\hat{\pi}_{D1/2-}\psi_{L}\text{-}(\overset{DM}{o};D), \tag{4.3}$$

$$\overset{X}{\nabla}{}^{AA'} \langle \bar{R}(D)R^{o}(M);\chi_{A'}(x)\rangle = -\frac{ie}{4\pi^2}\frac{\bar{z}_m r_{Dm}\overset{M}{\Delta}_{o}(x)\overset{D}{\Delta}_{1}(x)\overset{SA}{o}}{z_m(r_{Dm}r_{MK}+r_{mS}r_{Mm})}$$

$$\times \hat{\pi}_{M1+}\bar{\phi}_{R}{}^{o}(\overset{\bar{C}'}{o}_{M};M)\hat{\pi}_{D1/2+}\chi_{R}{}^{-}(\overset{\bar{M}'}{o}_{D};D). \qquad (4.4)$$

The standard pattern of the solution of Eq.(4.3) is given by

$$\langle \bar{L}(D)L^{o}(M);\psi_{A}(x)\rangle = \langle \bar{L}(D)L^{o}(M);\pi_{A}(x)\rangle\overset{M}{\Delta}_{o}(x)\overset{D}{\Delta}_{1}(x)$$

$$+ \langle \bar{L}(D)L^{o}(M);\mathcal{P}_{A}(x)\rangle\overset{M}{\Delta}_{o}(x)\overset{D}{\Delta}_{o}(x). \qquad (4.5)$$

In (4.5), the first term on the right-hand side constitutes the SI density of phase-shift that occurs due to the presence of the potential density in (2.38). Its bracked piece is explicitly written here as the SI expression

$$\langle \bar{L}(D)L^{o}(M);\pi_{A}(x)\rangle = U(x)\overset{S}{o}_{A}\,\hat{\pi}_{M1-}\phi_{L}{}^{o}(\overset{MC}{o};M)\hat{\pi}_{D1/2-}\psi_{L}{}^{-}(\overset{DM}{o};D), \qquad (4.6)$$

where U(x) is a well-behaved scalar function of the type {0,2;0,0}, the relevant rescaling acting on the $\overset{K}{o}_{A}$-spinors (see (4.10) below). The bracked piece of the second term is a massless free-field density of spin -1/2 which actually describes the propagation of the outgoing field. By definition, this latter term satisfies the following relation on $\mathcal{E}^{+}_{M}$

$$\langle \bar{L}(D)L^{o}(M);\mathcal{P}_{A}(x)\rangle\overset{KA}{o} = 0. \qquad (4.7)$$

Thus, replacing (4.5) into (4.3), and using the SI pattern of the expressions for the derivatives of the distributions together with (4.7) and the massless-free property

$$\overset{X}{\nabla}{}^{AA'} \langle \bar{L}(D)L^{o}(M);\mathcal{P}_{A}(x)\rangle = 0, \qquad (4.8)$$

yields the "reduced" scalar function at $S^{AA'}$

$$\langle \bar{L}(D)L^{o}(M)\bar{L}(S)\rangle \doteq \langle \bar{L}(D)L^{o}(M);\mathcal{P}_{A}(S)\rangle\overset{SA}{o}$$

$$= -\frac{ie}{4\pi^2}\frac{z_m\,\hat{\pi}_{M1-}\phi_{L}{}^{o}(\overset{MC}{o};M)\hat{\pi}_{D1/2-}\psi_{L}{}^{-}(\overset{DM}{o};D)}{\bar{z}_m r_{Mm}r_{DS}}, \qquad (4.9)$$

along with the "strong" requirement (see also (4.34))

$$\overset{S}{\underset{A}{O}}\nabla^{AA'}U(x) = -U(x)\,\frac{r_{Dm}r_{mK}\,\overset{-A'}{O}_{K}}{\bar{z}_m r_{DS}(r_{Dm}r_{MK} + r_{mS}r_{Mm})}$$

$$+\frac{ie}{4\pi^2}\,\frac{z_m r_{mS}\overset{-A'}{O}_{S}}{\bar{z}_m(r_{Dm}r_{MK} + r_{mS}r_{Mm})}. \qquad (4.10)$$

Hence, the function U(x) is constant on $\mathcal{C}_D^+$ with respect to $\partial/\partial r_{DS} = \overset{SA-A'}{O\ O\ S}\,\nabla_{AA'}^{X}$, whence a suitable displacement of the "reduced" form of Fig.5a leads to

$$\frac{\partial}{\partial r_{DS}}U(x) = 0. \qquad (4.11)$$

It is of some interest to re-define the phase-shift function as $U(x) = \frac{W(x)}{z_m r_{Mm}}$, with W(x) satisfying (4.11). In this connection, it should be noticed that the quantity $z_m r_{Mm}$ is also constant along generators of $\mathcal{C}_D^+$. In fact, the latter form exhibits the desirable behaviour of (4.6). The phase-shift integral is therefore written as

$$\langle\langle L^-(D)L^O(M);\pi_A(x)\rangle\rangle = \int_{\mathcal{P}_L}\langle L^-(D)L^O(M);\pi_A(x)\rangle \overset{M}{\Delta}_0(x)\overset{D}{\Delta}_1(x)\Omega^O_{\sim M}\wedge\omega^-_{\sim I}\wedge\Omega^-_{\sim D}, \qquad (4.12)$$

which is taken over the space $\mathcal{P}_L$ of null patterns of the type shown in Fig.11a. Its graphical representation is depicted as

$$\langle\langle L^-(D)L^O(M);\pi_A(x)\rangle\rangle = \ \underset{0}{\sim\sim\sim O}\overset{O}{\text{——}}\underset{1}{O\sim\sim\sim}, \qquad (4.13)$$

with the internal line thus denoting the whole U-function. The scalar function (4.9) is indeed the {1,0;0,0}-null datum at $S^{AA'}$ for the scattering process controlled by Eq.(2.38). Now, using the $\hat{\pi}$-operator

$$\hat{\pi}_{S1/2-} = \frac{r_{DS}}{z_S}\{\mathbb{D} + \frac{2}{r_{DS}}\overset{S}{}\}, \qquad (4.14)$$

and setting $z_S = \overset{SAX}{O\ O}_A$, we obtain the {0,-1;0,0}-datum for the process

$$\langle\langle L^{-}(D)L^{o}(M)L^{-}(S)\rangle\rangle = -\frac{ie}{4\pi^{2}}\,\frac{z_{m}\,\hat{\pi}_{M1-}\phi_{L}o(\overset{MC}{o};M)\hat{\pi}_{D1/2-}\psi_{L}{}^{-}(\overset{DM}{o};D)}{\bar{z}_{m}z_{S}r_{Mm}r_{DS}}. \qquad (4.15)$$

Consequently, the relevant scattering integral becomes

$$\langle\langle L^{-}(D)L^{o}(M)L^{-}(S);\mathcal{P}_{A}(x)\rangle\rangle = \int_{\Sigma_{L}} \overset{x}{o}_{A}\langle\langle L^{-}(D)L^{o}(M)L^{-}(S)\rangle\rangle \overset{M}{\Delta}_{o}(x)\overset{D}{\Delta}_{o}(x) \times \Omega^{o}_{\sim M}\wedge\omega^{-}_{\sim I}\wedge\Omega^{-}_{\sim D}\wedge\mathcal{K}^{-}_{\sim S}, \qquad (4.16)$$

with $\mathcal{K}^{-}_{\sim S}$ being the KAP-form at $S^{AA'}$, and the space Σ_{L} of null structures over which the integration is to be performed consisting of configurations of the type exhibited in Fig.11b. Graphically, for (4.16), we have

$$\langle\langle L^{-}(D)L^{o}(M)L^{-}(S);\mathcal{P}_{A}(x)\rangle\rangle = \qquad (4.17)$$

with the internal solid line representing the entire inner-product affine-parameter block carried explicitly by (4.15).

(a) (b)

Figure 11

Null patterns involved in the evaluation of the elementary contribution arising from the interaction between an incoming left-handed Dirac field density and the real potential density. The loop denotes the IRM*-pattern involved in the formation of the Dirac spot producing the incoming density: (a) phase-shift; (b) scattering.*

The contributions associated with the entire solution of Eq. (2.39) can be readily constructed from those obtained above by first replacing the relevant null data, and then taking a complex conjugation of the inner products appearing explicitly in (4.15). This result amounts to changing the color of the vertices carried by the graphs (4.13) and (4.17). Thus, the corresponding phase-shift expression is depicted as

$$\langle\langle \bar{R}(D)R^{o}(M);\Pi_{A},(x)\rangle\rangle = \tag{4.18}$$

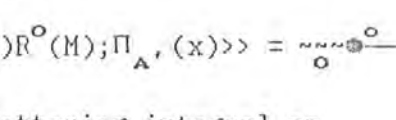

and the scattering integral as

$$\langle\langle \bar{R}(D)R^{o}(M)\bar{R}(S);S_{A},(x)\rangle\rangle = \tag{4.19}$$

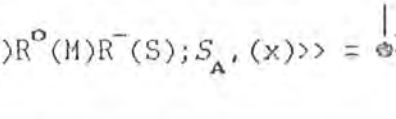

with the $\hat{\pi}$-datum involved in the latter structure being

$$\langle\langle \bar{R}(D)R^{o}(M)\bar{R}(S)\rangle\rangle = -\frac{ie}{4\pi^{2}}\frac{\bar{z}_{m}\hat{\pi}_{M1+}\bar{\phi}_{R}{}^{o}(\bar{\varrho}_{M}^{C'};M)\hat{\pi}_{D1/2+}\chi_{R}{}^{-}(\bar{\varrho}_{D}^{M'};D)}{z_{m}\bar{z}_{S}r_{Mm}r_{DS}}. \tag{4.20}$$

The configurations for the integrals represented by (4.18) and (4.19) are shown in Fig.12.

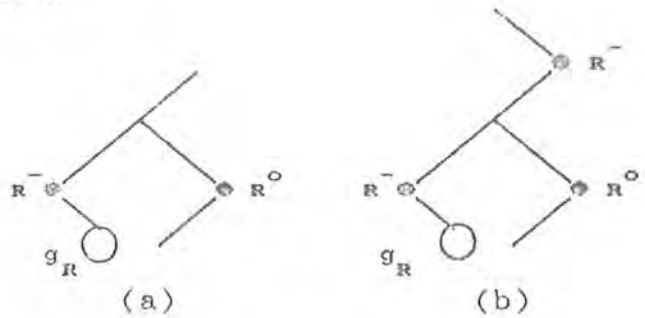

Figure 12

Null patterns involved in the evaluation of the elementary contribution arising from the interaction between an incoming right-handed Dirac field density and the real potential density. The loop denotes the underlying configuration g_R that gives rise to the formation of the Dirac spot: (a) phase-shift; (b) scattering.

4.3 Scattering by Higher-Order Elementary Potentials

We have seen that the colored graphs representing the scattering terms that come from the evaluation of Fig.5 do not involve any splitting of the null data for the processes. This feature comes from the fact that each of the scatterer structures partaking of the processes carries only a single spotted vertex. Thus, as the situation stands, the graphs do not carry any specific information concerning the individual pieces of the relevant null data. We shall now see that the graphs associated with the scattering pieces of the elementary contributions arising from the calculation of Fig.6 bring out naturally such a splitting of the null data. In accordance with this latter fact, the internal solid lines that join the (colored) vertices corresponding to the current spots appear as the contributions of the scatterer branches to the inner-product affine-parameter structures occurring in the scattering data, while the contributions due to the incoming branches are carried by the internal solid lines that connect the current blocks and the colored vertices associated with the KAP-forms. The pattern of the explicit distributional statements coming into play here is the same as that of the structures used in the previous section, but each piece of the solutions of the FDE now involves three distributions.

Only the calculation of the RM-structure associated with Eq.(2.42) will be explicitly carried out, but it is convenient to introduce the inner products for the configurations associated with Eqs.(2.43)-(2.45). We have

$$z_N = {}^{NAR}_{O\ O}{}_{A}, \quad z_P = {}^{PAK}_{O\ O}{}_{A}, \quad z_m = {}^{RAK}_{O\ O}{}_{A}, \tag{4.21a}$$

$$z_D = o^{DA\Sigma}\,o_A\,,\quad z_F = o^{RA\Sigma}\,o_A\,,\quad z_B = o^{BA\sigma}\,o_A\,,\quad z_G = o^{KA\sigma}\,o_A\,, \tag{4.21b}$$

along with their conjugates. At this stage all the procedures rest crucially upon the fact that statements of the type (4.1) involving the basis spinors of Fig.6 are also true. The relevant K-scalar is readily obtained from that for Fig.3 by replacing the labels Z and T by R and K, respectively, but the SI real vector $\alpha^{AA'} = r_{NF}\,o^{RA-A'}_{\;\;R\;\;o}\,o - r_{DF}\,o^{\Sigma A-A'}_{\;\;\Sigma\;\;o}\,o$ is also held fixed as $x^{AA'}$ varies in a suitable way. For the relations defining the position of $x^{AA'}$, we have

$$x^{AA'} = N^{AA'} + r_{NR}\,o^{RA-A'}_{\;\;R\;\;o}\,o + r_{RX}\,o^{\Sigma A-A'}_{\;\;\Sigma\;\;o}\,o\,, \tag{4.22a}$$

$$x^{AA'} = P^{AA'} + r_{Pm}\,o^{KA-A'}_{\;\;K\;\;o}\,o + r_{mR}\,o^{RA-A'}_{\;\;R\;\;o}\,o + r_{RX}\,o^{\Sigma A-A'}_{\;\;\Sigma\;\;o}\,o\,, \tag{4.22b}$$

$$x^{AA'} = D^{AA'} + r_{D\Sigma}\,o^{\Sigma A-A'}_{\;\;\Sigma\;\;o}\,o + r_{\Sigma X}\,o^{RA-A'}_{\;\;R\;\;o}\,o\,. \tag{4.22c}$$

Thus, differentiating out (4.22) and making appropriate contractions, we derive the relations

$$\overset{x}{\nabla}_{AA'}\,o^{KB} = -\,\frac{z_m r_{Nm} r_{DF}}{\bar{z}_m z_P z_F r_{Pm}(r_{NF}r_{D\Sigma} + r_{FR}r_{DF})}\,o^{\Sigma}_{\;ARA'}\,o^{FB}\,, \tag{4.23}$$

$$\overset{x}{\nabla}_{AA'} r_{Pm} = \left(\frac{r_{Nm}r_{DF}}{z_m\bar{z}_m}\right)\left[\frac{z_P z_F \bar{z}_m (o^{\bar{B}'}_{\;R}\,o_{FB'})\,o^{R}_{\;A\Sigma A'} + \text{C.C.}}{z_P z_F \bar{z}_P \bar{z}_F (r_{NF}r_{D\Sigma} + r_{FR}r_{DF})}\right], \tag{4.24}$$

$$\overset{x}{\nabla}_{AA'} r_{Nm} = \left(\frac{r_{Nm}r_{DF}}{z_m\bar{z}_m}\right)\left[\frac{z_N z_m \bar{z}_F (o^{\bar{B}'}_{\;K}\,o_{NB'})\,o^{\Sigma}_{\;ARA'} + \text{C.C.}}{z_N z_F \bar{z}_N \bar{z}_F (r_{NF}r_{D\Sigma} + r_{FR}r_{DF})}\right], \tag{4.25}$$

together with the conjugate of (4.23) and those expressions which can be obtained from (3.12)-(3.15) by making the replacement NZMPT$\longleftrightarrow$ NRFDΣ. It should be noticed that, as regards (4.24) and (4.25), the NP-RK interchange rule applies only to the spin inner products. This is because the standard flag poles $\{o^{RA-A'}_{\;\;K\;\;o}\,o\,,\,o^{KA-A'}_{\;\;R\;\;o}\,o\}$ actually enter into the picture only when the null patterns of either pair of "dual" configurations are appropriately combined together.

To write out the explicit right-hand side of Eq.(2.42), one has first to re-instate the expression (3.22) by adapting the pattern of either of the potential densities (3.47) and (3.54) to the situation depicted in Fig.6a. This task can be easily carried out by taking the derivative of the SI vector associated with the K-scalar for the configuration in question as well as suitably contracted second derivatives of $\overset{RA}{o}$ and $\overset{-A'}{\underset{K}{o}}$. Thus, making use of the derivative relations arising from (4.22), after some manipulations we obtain the statements

$$\frac{z_m}{\bar{z}_m}(\overset{x}{\nabla}_{AA'},\underset{RM'}{\bar{o}})(\overset{x}{\nabla}^{A'}_{B}\overset{-M'}{\underset{K}{o}}) + (\overset{x}{\nabla}_{AA'},\overset{K}{o}_{M})(\overset{x}{\nabla}^{A'}_{B}\overset{RM}{o})$$

$$-\frac{z_m}{\bar{z}_m}(\underset{RM'}{\bar{o}},\overset{x}{\nabla}^{A'}_{B}\overset{-M'}{\underset{K}{o}})(\underset{KN'}{\bar{o}},\overset{x}{\nabla}_{AA'},\overset{-N'}{\underset{R}{o}})+\frac{1}{z_m}(\overset{K}{o}_{M}\overset{x}{\nabla}^{A'}_{B}\overset{RM}{o})(\overset{R}{o}_{N}\overset{x}{\nabla}_{AA'},\overset{KN}{o}) = 0, \quad (4.26)$$

$$\overset{K}{o}_{M}\overset{x}{\nabla}_{A'}[\overset{x}{\nabla}^{A'}_{B}]\overset{RM}{o} = 0 = \frac{1}{2}\varepsilon_{AB}\overset{K}{o}_{M}\Box_{x}\overset{RM}{o}, \quad (4.27)$$

and

$$\underset{RM'}{\bar{o}}\overset{x}{\nabla}_{A'}[\overset{x}{\nabla}^{A'}_{B}]\overset{-M'}{\underset{K}{o}} = 0 = \frac{1}{2}\varepsilon_{AB}\underset{RM'}{\bar{o}}\Box_{x}\overset{-M'}{\underset{K}{o}}. \quad (4.28)$$

Hence, invoking the modified RK-version of (3.52), we get the equations

$$\overset{x}{\nabla}_{A'}[\overset{x}{\nabla}^{A'}_{B}](\log(z_m r_{Pm})) = 0 \Leftrightarrow \Box_x(\log(z_m r_{Pm})) = 0, \quad (4.29)$$

which, when combined with $\overset{x}{\nabla}_{AA'}\overset{P}{\Delta}_{O}(x)=0$ on $\mathscr{E}^{+}_{N}$, yield the SI statement

$$\overset{x}{\nabla}_{AA'}\langle L^{-}(N)R^{+}(P);\Phi^{A'}_{B}(x)\rangle = -\frac{e}{2\pi}\overset{R}{o}_{A}\overset{R}{o}_{B}\frac{\overset{N}{\Delta}_{1}(x)\overset{P}{\Delta}_{O}(x)}{z_m r_{Pm}}$$

$$\times\hat{\pi}_{N1/2-}\psi_{L}(\overset{NC}{o};N)\hat{\pi}_{P1/2+}\bar{\psi}_{R}(\overset{-M'}{\underset{P}{o}};P). \quad (4.30)$$

We have therefore been led to the solution (3.22). It turns out that Eq.(2.42) takes the explicit form

$$\overset{x}{\nabla}^{AA'}\langle L^{-}(D)R^{+}(P)L^{-}(N);\psi_{A}(x)\rangle = -\frac{ie^2}{4\pi^2}\frac{z_F r_{DF}\overset{N}{\Delta}_{O}(x)\overset{P}{\Delta}_{O}(x)\overset{D}{\Delta}_{1}(x)\overset{-A'}{\Omega}_{\Sigma}}{z_m\bar{z}_F r_{Pm}(r_{NF}r_{D\Sigma}+r_{FR}r_{DF})}$$

$$\times\hat{\pi}_{N1/2-}\psi_{L}(\overset{NC}{o};N)\hat{\pi}_{P1/2+}\bar{\psi}_{R}(\overset{-M'}{\underset{P}{o}};P)\hat{\pi}_{D1/2-}\psi_{L}(\overset{DC}{o};D). \quad (4.31)$$

Now, replacing into (4.31) the expression

$$\langle L^-(D)R^+(P)L^-(N);\psi_A(x)\rangle = \langle L^-(D)R^+(P)L^-(N);\mathcal{P}_A(x)\rangle \overset{N}{\Delta_0}(x)\overset{P}{\Delta_0}(x)\overset{D}{\Delta_1}(x) + \langle L^-(D)R^+(P)L^-(N);\Sigma_A(x)\rangle \overset{N}{\Delta_0}(x)\overset{P}{\Delta_0}(x)\overset{D}{\Delta_0}(x), \tag{4.32}$$

along with the defining relations

$$\overset{x}{\nabla}{}^{AA'}\langle L^-(D)R^+(P)L^-(N);\Sigma_A(x)\rangle = 0, \tag{4.33a}$$

$$\langle L^-(D)R^+(P)L^-(N);\Sigma_A(x)\rangle \overset{RA}{O} = 0, \tag{4.33b}$$

$$\langle L^-(D)R^+(P)L^-(N);\Sigma_A(x)\rangle \overset{KA}{O} = 0, \tag{4.33c}$$

and invoking once again the generalized pattern of derivatives of distributions, we require the following SI expression

$$\overset{x}{\nabla}{}^{AA'}\langle L^-(D)R^+(P)L^-(N);\mathcal{P}_A(x)\rangle - \langle L^-(D)R^+(P)L^-(N);\mathcal{P}_A(x)\rangle \frac{\overset{RA-A'}{O}\overset{}{R}}{z_F\bar{z}_F r_{D\Sigma}} + \langle L^-(D)R^+(P)L^-(N);\Sigma_A(x)\rangle r_{D\Sigma}\overset{\Sigma A-A'}{O}\overset{}{\Sigma}$$

$$= -\frac{ie^2}{4\pi^2}\frac{z_F r_{DF}\overset{-A'}{Q}}{z_m\bar{z}_F r_{Pm}(r_{NF}r_{D\Sigma} + r_{FR}r_{DF})} \times \hat{\pi}_{N1/2-}\psi_L{}^-(\overset{NC}{O};N)\hat{\pi}_{P1/2+}\bar{\psi}_R{}^+(\overset{-M'}{Q};P)\hat{\pi}_{D1/2-}\psi_L{}^-(\overset{DC}{O};D). \tag{4.34}$$

Strictly speaking, the statement associated with (4.34) holds on $\mathcal{E}_D^+$, whence the expression involved in the general situation actually carries the "reduced" form of the denominator occurring explicitly in the piece that bears the coupling constant. It follows that, writing

$$\langle L^-(D)R^+(P)L^-(N);\mathcal{P}_A(x)\rangle = \frac{1}{z_m r_{Pm} r_{NF}} V(x)\overset{\Sigma}{O}{}_A \hat{\pi}_{D1/2-}\psi_L{}^-(\overset{DC}{O};D) \times \hat{\pi}_{N1/2-}\psi_L{}^-(\overset{NC}{O};N)\hat{\pi}_{P1/2+}\bar{\psi}_R{}^+(\overset{-M'}{Q};P), \tag{4.35}$$

we obtain the following expression at $\Sigma^{AA'}$:

$$\langle L^-(D)R^+(P)L^-(N)L^-(\Sigma)\rangle \doteq \langle L^-(D)R^+(P)L^-(N);\Sigma_A(\Sigma)\rangle \overset{\Sigma A}{O} = -\frac{ie^2}{4\pi^2}\frac{z_F}{z_m\bar{z}_F r_{Pm}r_{NF}r_{D\Sigma}} \hat{\pi}_{N1/2-}\psi_L{}^-(\overset{NC}{O};N)\hat{\pi}_{P1/2+}\bar{\psi}_R{}^+(\overset{-M'}{Q};P)\hat{\pi}_{D1/2-}\psi_L{}^-(\overset{DC}{O};D), \tag{4.36}$$

provided that

$$\overset{\circ}{\Sigma}_{A}\,\overset{\times}{\nabla}^{AA'}W(x) = W(x)\,\frac{r_{FR}r_{DF}\overset{\circ}{R}^{-A'}}{\bar{z}_F r_{D\Sigma}(r_{NF}r_{D\Sigma} + r_{FR}r_{DF})} + \frac{ie^2}{4\pi^2}\,\frac{z_F r_{F\Sigma}\overset{\circ}{\Sigma}^{-A'}}{z_m\bar{z}_F r_{Pm}(r_{NF}r_{D\Sigma} + r_{FR}r_{DF})}, \tag{4.37}$$

with $W(x)=\frac{1}{z_m r_{Pm} r_{NF}}\,V(x)$. Equation (4.35) defines the explicit SI phase-shift density for the configuration under consideration. The scalar function W(x) can carry only spin weights for $\overset{\circ}{R}^{RA}$ and $\overset{\circ}{K}^{-A'}$ as a quantity of the type {1,0;1,0}. It clearly satisfies $\partial/\partial r_{D\Sigma}W(x) = 0$ on $\mathscr{E}^{+}_{D}$, and therefore so does V(x), since $\partial/\partial r_{D\Sigma}(\frac{1}{z_m r_{Pm} r_{NF}})=0$. Thus, the phase-shift integral is written as

$$\langle\langle L^{-}(D)R^{+}(P)L^{-}(N);\mathcal{P}_{A}(x)\rangle\rangle = \int_{\pi_L}\langle L^{-}(D)R^{+}(P)L^{-}(N);\mathcal{P}_{A}(x)\rangle \overset{N}{\Delta}_{0}(x)\overset{P}{\Delta}_{0}(x)\overset{D}{\Delta}_{1}(x) \times \tilde{\vartheta}^{-}_{I}\wedge\tilde{\Omega}^{-}_{N}\wedge\tilde{\vartheta}^{+}_{II}\wedge\tilde{\Omega}^{+}_{P}\wedge\tilde{\vartheta}^{-}_{III}\wedge\tilde{\Omega}^{-}_{D}, \tag{4.38}$$

where π_L denotes the space of null configurations of the type depicted in Fig.13a. For the corresponding graph, we have

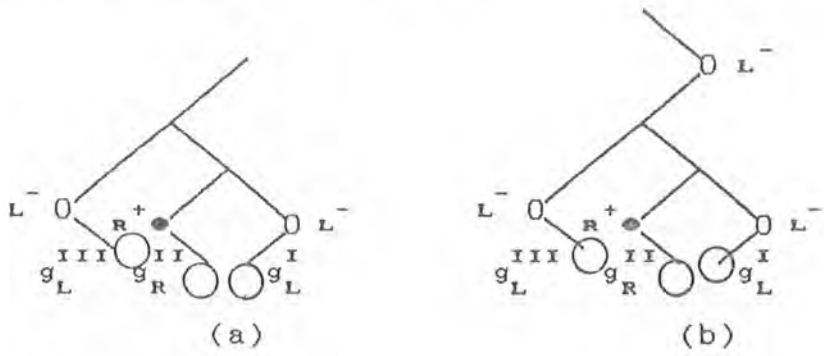

Figure 13

Null configurations associated with the integrations giving rise to the solution of equation 2.42. The loops denote the structures involved in the formation of the datum spots occurring in Fig.6a.

$$\langle\langle L^{-}(D)R^{+}(P)L^{-}(N);\mathcal{P}_{A}(x)\rangle\rangle = $$ 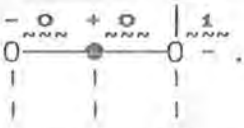 . (4.39)

For convenience, the internal solid line that connects the vertices associated with the current spots has been arbitrarily taken to represent the quantity $\frac{1}{z_m r_{Pm} r_{NF}}$. The reason for this convention is the fact that it may eventually be useful to ascribe a standard internal structure to the current branches of Fig.6. The function V(x) is represented by the line which connects the blocks associated with the incoming field and scatterer. When the incoming Dirac branch is disconnected from the structure, the contribution involving r_{NF} "evaporates", and the step function $\overset{N}{\Delta}_{0}(x)$ is replaced by $\overset{N}{\Delta}_{1}(x)$. We can easily see that the first term on the right-hand side of (4.37) actually cancels that coming from the combination of the derivatives of $\overset{\Sigma A}{o}$ and $\overset{D}{\Delta}_{1}(x)$. The second piece couples together with the right-hand side of Eq.(4.31), yielding the appropriate null-datum expression. It now becomes clear that if the former potential flag pole were utilized for calculating the scattering diagram, the information about the null datum for the process would be lost since the spinors $\overset{RA}{o}$, $\overset{KA}{o}$ and $\overset{\Sigma A}{o}$ and their conjugates are taken to be independent. Obviously, something similar occurs in the case of (4.15). In fact, (4.36) is the expression for the {1,0;0,0}-datum for the process. Setting $z_{\Sigma}=\overset{\Sigma A}{o}\overset{X}{o}_{A}$, we thus obtain the following expression for the corresponding $\hat{\pi}$-datum:

$$\langle\langle L^{-}(D)R^{+}(P)L^{-}(N)L^{-}(\Sigma)\rangle\rangle = -\frac{ie^{2}}{4\pi^{2}}\frac{z_{F}}{z_m \bar{z}_F z_{\Sigma} r_{Fm} r_{NF} r_{D\Sigma}}$$

$$\times \hat{\pi}_{N1/2-}\psi_{L}^{-}(\overset{NC}{o};N)\hat{\pi}_{P1/2+}\bar{\psi}_{R}^{+}(\overset{\bar{M}'}{o};P)\hat{\pi}_{D1/2-}\psi_{L}^{-}(\overset{DC}{o};D), \quad (4.40)$$

whence the relevant scattering integral turns out to be given by

$$<<L^{-}(D)R^{+}(P)L^{-}(N)L^{-}(\Sigma);\Sigma_{A}(x)>> = \int \overset{\times}{O}_{A} <<L^{-}(D)R^{+}(P)L^{-}(N)L^{-}(\Sigma)>>$$
$$\mathcal{X}_{L} \times \overset{N}{\Delta_{O}}(x)\overset{P}{\Delta_{O}}(x)\overset{D}{\Delta_{O}}(x)\mathcal{N}_{\sim N}^{-}\sim\mathcal{N}_{\sim P}^{+}\sim\mathcal{N}_{\sim D}^{-}\sim\mathcal{K}_{\sim\Sigma}^{-}. \tag{4.41}$$

Here $\vartheta_{\sim\mathcal{A}}\sim\Omega_{\sim Y}$ has been denoted by $\mathcal{N}_{\sim Y}$, with the letter Y ($\mathcal{A}$) standing for either N, P or D (I,II or III), the integral being taken over the space $\mathcal{X}_{L}$ of the configurations shown in Fig.13b. The associated graph is depicted as

$<<L^{-}(D)R^{+}(P)L^{-}(N)L^{-}(\Sigma);\Sigma_{A}(x)>>$ = 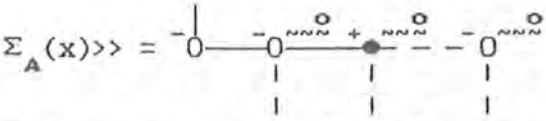 , (4.42)

with the internal solid line that connects the "wavy-line-free" vertex denoting the datum piece $z_{F}/\bar{z}_{F}z_{\Sigma}r_{D\Sigma}$. It must be emphasized that a term without a distribution for $D^{AA'}$ also arises here, when we perform the electromagnetic integrals associated with Eqs.(3.42) and (3.43). Thus, the incoming Dirac densities appear to be meaningful only when the scattering processes are explicitly considered.

The prescriptions for evaluating the other configurations of Fig.6 are essentially the same as those worked out before. All the quantities entering into the integrals for Fig.6b can be immediately obtained from those for Fig.6a by first applying the simultaneous interchanges $\Sigma\longleftrightarrow\sigma$, $F\longleftrightarrow G$, $D\longleftrightarrow B$, $N\longleftrightarrow P$, along with a complex conjugation, and then replacing the $\hat{n}$-datum that generates the incoming density. This constitutes the interchange rule which enables us to write down the field integral for one configuration on the basis of that for the corresponding "dual" structure. Roughly speaking, the integrals for Fig.6c can be constructed from (4.38) and (4.41) by replacing z_{F}, z_{m} and z_{Σ} by their conjugates and the ψ-data by χ-data. At this stage, one might set up at once the formulae for Fig.6d by using the interchange rule given above. It should be observed that this

rule actually arises from replacing the conjugate potential kernels $\overset{\Omega}{O}_{A\Sigma A'}$, $\overset{\Sigma}{O}_{ARA'}$ by $\overset{\sigma}{O}_{AKA'}$, $\overset{K}{O}_{A\sigma A'}$, respectively. For the scattering process of Fig.6b, for instance, we thus obtain the $\hat{\pi}$-datum, see Eq.(2.43),

$$\langle\langle R^-(B)L^-(N)R^+(P)R^-(\sigma)\rangle\rangle = -\frac{ie^2}{4\pi^2}\frac{\bar{z}_\sigma}{\bar{z}_m z_\sigma \bar{z}_\sigma r_{Nm} r_{P\sigma} r_{B\sigma}}$$

$$\times \hat{\pi}_{N1/2-}\psi_L^-(\overset{NC}{O};N)\hat{\pi}_{P1/2+}\bar{\psi}_R^+(\overset{\bar{M}'}{O}_P;P)\hat{\pi}_{B1/2+}\chi_R^-(\overset{\bar{C}'}{O}_B;B). \qquad (4.43)$$

Accordingly, we have the graphical representation displayed in Table 1.

Table 1.

Symbolic expressions and colored graphs for the configurations b, c and d of Fig.6.

		GRAPHS
PHASE-SHIFT	$\langle\langle R^-(B)L^-(N)R^+(P);P_A,(x)\rangle\rangle$	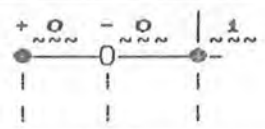
	$\langle\langle R^-(D)L^+(P)R^-(N);\mathcal{P}_A,(x)\rangle\rangle$	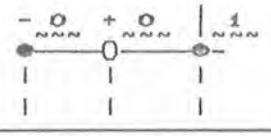
	$\langle\langle L^-(B)R^-(N)L^+(P);P_A(x)\rangle\rangle$	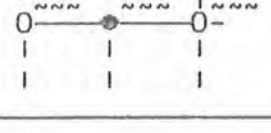
SCATTERING	$\langle\langle R^-(B)L^-(N)R^+(P)R^-(\sigma);\sigma_A,(x)\rangle\rangle$	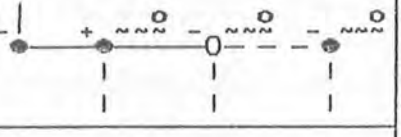
	$\langle\langle R^-(D)L^+(P)R^-(N)R^-(\Sigma);S_A,(x)\rangle\rangle$	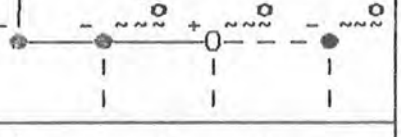
	$\langle\langle L^-(B)R^-(N)L^+(P)L^-(\sigma);S_A(x)\rangle\rangle$	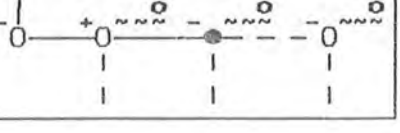

CHAPTER FIVE

TWISTORIAL DESCRIPTION OF SCATTERING PROCESSES

5.1 Introduction

This chapter mainly aims at transcribing the scattering integrals presented before into the framework of twistor theory. As was pointed out earlier, the construction of the structures exhibited here is largely based upon the prescriptions involved in the twistorial description of the processes of mass scattering of Dirac fields [16]. Therefore, all the basic formulae will be built up in a straightforward way. The twistor expressions related to the geometric properties of the null configurations are derived in connection with the construction of generalized scattering and volume differential forms (Sec.5.2). These latter expressions are relevant for contributions arising out of appropriately coupling the basic null diagrams. The adequate twistor data are defined in Sec.5.3. The basic twistor diagrammatic structures are built up in conjuntion with the transcription of the $\mathbb{RM}$-scattering integrals (Sec.5.4). At this stage, the twistor representation of the electromagnetic free-field contributions is included. It will be seen that the fundamental features of genuine twistorial integrals, namely holomorphicity, scaling invariance and handedness-twistor-valence property, all emerge automatically here. In addition, the definition of the contour over which each basic twistor integral is taken arises naturally. It must be stressed that the existence assumption underlying this construction rests only upon the nullity of the relevant

Minkowskian patterns. I shall not enter into a detailed discussion concerning a formal proof here, however. The kernel letter used for denoting a twistor will be the same as that used for labelling the spinors entering into the flag pole for the corresponding geodesic. In fact, each such spinor always appears as a π-part of a null twistor. In Sec.5.4, Penrose's diagrammatic notation is used [3,11]. This procedure will considerably facilitate setting up the twistorial blocks. All the step functions occurring in the scattering integrals will be deleted as the corresponding fields are to be evaluated at interior points (see Ref.[3]).

5.2 Formulae for Null Configurations

We saw that the denominator of the NID expression for each of the basic scattering processes explicitly involves the product of the "internal" affine parameters that occur in the corresponding RDM-pattern. In the case of Fig.5, either scattering datum actually involves the sum of two pairs of parameters in its denominator. For the structures describing the interaction between an arbitrary incoming field of one handedness and a potential density produced by a current pattern, the formation of the Dirac datum spots of the scatterer branch involves combining the basic scattering configurations in such a way that the parameter starting at the spot bearing the other handedness is always coupled with the ones that enter into the underlying NID expressions. Nevertheless, the above prescription turns out to be unsuitable for L^{o}-R^{o} and current branches which are eventually carried by the underlying structures. In this latter case, it is particularly

convenient to couple together the parameters that enter into the contributions of the currents to the scattering data involved. In fact, the null data on $\mathscr{E}_o^+$ generating these RM-patterns have to be modified in case their handedness is opposite to that of the outgoing field. One obvious reason for this modification is that the expression arising from the actual twistorial transcription of the associated Minkowskian integral has to carry only manifestly independent twistors. It appears that the total number of parameters involved in the denominator of the whole modified $\hat{\pi}$-datum turns out to be even in any case. This will be discussed further in Sec.5.4.

In order to derive the twistor expressions for products of pairs of parameters, one has first to construct the structure for a single parameter. For let the twistors $\{A_\alpha, B_\alpha, C_\alpha, D_\alpha\}$ and their pseudo-Hermitian conjugates be associated with the null geodesics that contain the pieces of the zigzag-like branch depicted in Fig.14. We thus have the incidence relations at the vertices $A^{AA'}$, $B^{AA'}$ and $C^{AA'}$

$$\bar{A}^\alpha B_\alpha = \bar{B}^\alpha C_\alpha = \bar{C}^\alpha D_\alpha = 0, \tag{5.1}$$

along with their conjugates. Evidently, we also have

$$A_{\alpha\beta} = 2(I^{\mu\nu} A_\mu B_\nu)^{-1} A_{[\alpha} B_{\beta]}, \tag{5.2a}$$

$$B_{\alpha\beta} = 2(I^{\mu\nu} B_\mu C_\nu)^{-1} B_{[\alpha} C_{\beta]}, \tag{5.2b}$$

$$C_{\alpha\beta} = 2(I^{\mu\nu} C_\mu D_\nu)^{-1} C_{[\alpha} D_{\beta]}, \tag{5.2c}$$

as the SI dual version of the (simple) twistors associated, respectively, with $A^{AA'}$, $B^{AA'}$ and $C^{AA'}$. In (5.2), $I^{\mu\nu}$ stands for the usual $\left[\begin{smallmatrix} z \\ o \end{smallmatrix}\right]$-infinity twistor [11,12]. The explicit duality relationships are written as

$$\bar{G}^{\alpha\beta} = 1/2\ \varepsilon^{\alpha\beta\gamma\delta}\ G_{\gamma\delta}, \tag{5.3}$$

where the kernel letter G stands for either A, B or C, and $\varepsilon^{\alpha\beta\gamma\delta}$

denotes the $\left[\begin{smallmatrix}4\\0\end{smallmatrix}\right]$-alternating twistor for the standard frame [12]. Thus, contracting the connected-vertex property

$$B^{AA'} - A^{AA'} = r_{AB}\, o^{BA}\, \bar{o}^{-A'}_{B}, \tag{5.4}$$

with $o^{A}_{AC}\,\bar{o}_{CA'}$, and using the null-separation relation

$$\bar{C}^{A} = iC^{AA'}\,\bar{o}_{CA'} = iB^{AA'}\,\bar{o}_{CA'}, \tag{5.5}$$

we readily obtain the expression

$$r_{AB} = i\,\frac{\bar{C}^{\mu}A_{\mu}}{(I^{\mu\nu}A_{\mu}B_{\nu})(I_{\alpha\beta}\bar{B}^{\alpha}\bar{C}^{\beta})}, \tag{5.6}$$

together with its conjugate. It is obvious that the expressions for r_{BC} can be immediately obtained from the above structure by replacing A, B and C by B, C and D, respectively. Therefore, transvecting the duality relation involving (5.2b) with A_{α} and D_{β} and invoking (5.1) together with the twistor expressions for r_{AB} and r_{BC}, yields

$$r_{AB}r_{BC} = (-1)\,\frac{\varepsilon^{\alpha\beta\gamma\delta}A_{\alpha}B_{\beta}C_{\gamma}D_{\delta}}{(I^{\lambda\tau}A_{\lambda}B_{\tau})(I^{\gamma\delta}B_{\gamma}C_{\delta})(I_{\alpha\beta}\bar{B}^{\alpha}\bar{C}^{\beta})(I^{\rho\sigma}C_{\rho}D_{\sigma})}, \tag{5.7}$$

along with the corresponding conjugate.

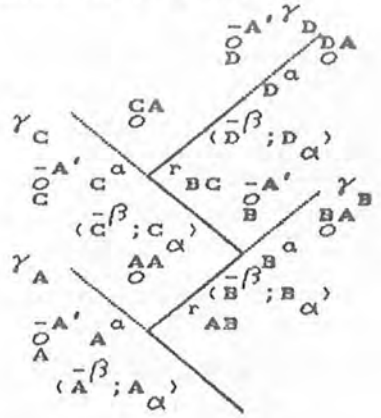

Figure 14

Null zigzag pattern for deriving the twistor expressions for affine parameters. Each edge is associated with a pair of conjugate null twistors $\bar{P}^{\alpha} = (\bar{P}^{A}, \bar{o}_{PA'})$, $P_{\alpha} = (o^{P}_{A}, P^{A'})$. *The* π*-parts of the twistors define the flag poles for the geodesics* $\{\gamma_P\}$.

To obtain the expressions for the relevant differential forms, it is convenient to consider a null structure of the type shown in Fig.15. Such a configuration appears indeed to be useful when successive scattering processes are to be effectively calculated. Each loop denotes here a scatterer pattern s_n, the whole structure having j scattering branches. The nth-branch involves the scattering of a density coming from $D_n^{AA'}$ which has arbitrarily been taken as left-handed. The starting-point $D_0^{AA'}$ and the end-point $D_{j+2}^{AA'}$ are taken to coincide with O and $x^{AA'}$, respectively, whence $D_1^{AA'} \in \mathscr{C}_O^+$. For simplicity, the affine parameter connecting $D_M^{AA'}$ and $D_{M+1}^{AA'}$ bears the label M+1, with

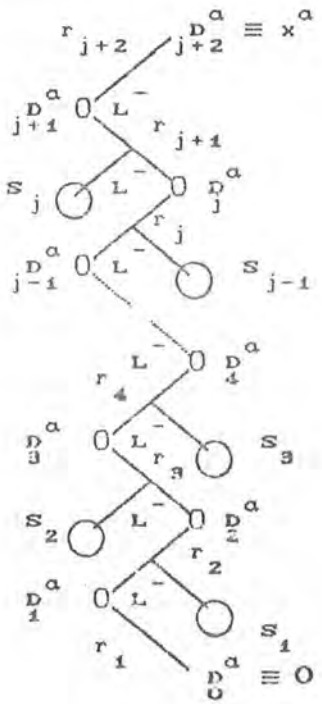

Figure 15

Structure involving successive scattering processes. The incoming field emanates from a datum-spot D_1^A lying on $\mathscr{C}_O^+$. Each scatterer s_n is denoted by a loop, the whole configuration having j scattering branches. The end-point D_{j+2}^A is identified with x^A.

M running over the values 0,1,2,3,...,j+1. When performing the calculations yielding the forms, one has to make use also of upper-index twistors, however. Thus, a null-twistor set similar to that used before is employed.

The defining expression for the generalized SI scattering form is written as [5]

$$\underset{\sim}{\mathcal{K}}^{123\ldots j+1} = \Big(\bigwedge_{K=1}^{j} \underset{\sim}{r}^{K} \wedge \underset{\sim}{\mathcal{P}}^{K}\Big) \wedge \underset{\sim}{\mathcal{K}}^{j+1}, \tag{5.8}$$

with $\underset{\sim}{r}^{K}$ being the one-form $\dfrac{dr_K}{r_K}$ at $\underset{K}{D}^{AA'}$. This generalized form can be thought of as being defined on a (3j+2)-dimensional space $\mathbb{K}^{123\ldots j+1}$ whose elements are null zigzag-patterns that possess j+2 edges [5]. Each three-form entering into the bracket part of (5.8) contributes an integral taken over a subspace whose topology is $S^1 \times S^2$. It involves the (space-like) element of two-surface area $\underset{\sim}{\mathcal{P}}^{K}$ at $\underset{K}{D}^{AA'} \in \mathcal{C}^{+}_{K-1} \cap \mathcal{C}^{-}_{K+1}$; $\underset{\sim}{\mathcal{K}}^{j+1}$ is the KAP-form at $\underset{j+1}{D}^{AA'} \in \mathcal{C}^{+}_{j} \cap \mathcal{C}^{-}_{j+2}$ which is defined by

$$\underset{\sim}{\mathcal{K}}^{j+1} = \frac{\underset{\sim}{\mathcal{P}}^{j+1}}{z_{j+1}\bar{z}_{j+1}r_{j+1}r_{j+2}}, \tag{5.9}$$

whence the whole expression (5.8) appears as a (3j+2)-differential form on $\mathbb{K}^{123\ldots j+1}$. The explicit SI defining expression for $\underset{\sim}{\mathcal{P}}^{m}$ is given by

$$\underset{\sim}{\mathcal{P}}^{m} = \frac{i}{z_m\bar{z}_m}\, o^{mA}\, \bar{o}^{-A'}_{m+1}\, dD_{mAA'} \wedge o^{m+1B}\, \bar{o}^{-B'}_{m}\, dD_{mBB'}, \quad m=1,2,3,\ldots,j+1. \tag{5.10}$$

Hence, differentiating the twistor relationship $D^{mA'} = -iD^{AA'}_{m}\, o^{m}_{A}$ and taking into account the relevant null-separation relation, upon suitable transvections with $\bar{o}_{m+1A'}$ and $\bar{o}_{mA'}$ we get

$$\underset{\sim}{\mathscr{S}}^{m} = (-i)\,\frac{\bar{D}^{\mu}_{m+1}\,dD^{m}_{\mu} \wedge \bar{D}^{\nu}_{m}\,d\,D^{m+1}_{\nu}}{(I^{\alpha\beta}D^{m}_{\alpha}\,D^{m+1}_{\beta})(I_{\lambda\tau}\bar{D}^{\lambda}_{m}\,\bar{D}^{\tau}_{m+1})}, \tag{5.11}$$

together with its conjugate. The twistor expression for $\underset{\sim}{r}^{K}$ can be derived by working out successive steps [16]. We thus have

$$\underset{\sim}{r}^{K} = (-1)\,\frac{(I_{\mu\nu K-1}\bar{D}^{\mu}_{K}\,\bar{D}^{\nu}_{K})}{(I_{\mu\nu}\bar{D}^{\mu}_{K}\,\bar{D}^{\nu}_{K+1})(_{k-1}\bar{D}^{\lambda}_{1}\,D^{K+1}_{\lambda})}\,(\bar{D}^{\tau}_{K+1}d\,D^{K+1}_{\tau} + i\sum_{n=1}^{K-1}\xi_{n}dr_{n}), \tag{5.12}$$

where ξ_{n} is the (real) scalar $(I_{\mu\nu}\bar{D}^{\mu}_{n}\,\bar{D}^{\nu}_{K+1})(I^{\lambda\tau}D^{n}_{\lambda}\,D^{K+1}_{\tau})$. Consequently, making use of the relations

$$\bar{D}^{\mu}_{j+1}d\,D^{j+2}_{\mu} = -i\bar{z}_{j+1}r_{j+2}I^{\alpha\beta}D^{j+2}_{\alpha}d\,D^{j+2}_{\beta},\ \bar{D}^{\mu}_{2}dD^{1}_{\mu} = -i\bar{z}_{1}r_{1}I^{\alpha\beta}D^{1}_{\alpha}dD^{1}_{\beta}, \tag{5.13}$$

and

$$\bar{D}^{\mu}_{K}d\,D^{K+1}_{\mu}\wedge\bar{D}^{\nu}_{K+1}d\,D^{K+1}_{\nu}\wedge\bar{D}^{\lambda}_{K+2}d\,D^{K+1}_{\lambda} = \frac{(I_{\mu\nu K+1 K+2}\bar{D}^{\mu}_{K+1}\bar{D}^{\nu}_{K+2})}{(I^{\alpha\beta}{}^{K+1 K+2}D_{\alpha}\,D_{\beta})}\,(\bar{D}^{\lambda}_{K}D^{K+2}_{\lambda})\Delta\,D^{K+1}, \tag{5.14}$$

with $\Delta\,D^{K+1} = 1/3!\,\varepsilon^{\alpha\beta\gamma\delta}D^{K+1}_{\alpha}d\,D^{K+1}_{\beta}\wedge d\,D^{K+1}_{\gamma}\wedge d\,D^{K+1}_{\delta}$, along with (5.11) and (5.12), yields the SI holomorphic structure

$$\underset{\sim}{\mathscr{K}}^{123\ldots j+1} = i^{j+1}\,\frac{I^{\alpha\beta}D^{1}_{\alpha}dD^{1}_{\beta}\wedge(\bigwedge_{n=2}^{j+1}\Delta D^{n})\wedge I^{\mu\nu}D^{j+2}_{\mu}d\,D^{j+2}_{\nu}}{\prod_{m=1}^{j+1}(I^{\lambda\tau}D^{m}_{\lambda}\,D^{m+1}_{\tau})^{2}}. \tag{5.15}$$

The explicit computations leading to the relation (5.14) are given in Ref.[4]. It should be noticed that the wedge-products involved in (5.8) actually annihilate the ξ-terms of (5.12) when the relevant pieces are fitted together. The Δ-forms occurring in (5.15) are the universal dual projective three-forms [11,12,28,32], and appear to be associated with the internal edges of the zigzag-branch. Obviously, the twistorial structure that is of relevance for scattering processes involving

right-handed outgoing fields can be immediately constructed from (5.15) by taking a complex conjugation. The relations (5.13) appear as a consequence of the fact that both O and $x^{AA'}$ are held fixed when the pertinent RM-scattering integral is actually performed. To derive the lower-index twistor expression for the product of volume forms $\{\underset{\sim}{\Omega}_m\}$ at $\{D_m^{AA'}\}$, it suffices to replace the contributions coming from (5.9) by twistor pieces associated with $\overset{j+1}{\underset{\sim}{r}} \wedge \overset{j+1}{\underset{\sim}{\mathcal{S}}}$. Thus, using also a duality relation of the type (5.3), we get the SI structure

$$\overset{j+1}{\underset{m=1}{\Lambda}} \underset{\sim}{\Omega}_m = \left(\frac{i}{2}\right)^{j+1} \frac{I^{\alpha\beta} D^1_\alpha dD^1_\beta \wedge \left(\overset{j+1}{\underset{n=2}{\Lambda}} \Delta D^n\right) \wedge \varepsilon^{\mu\nu\lambda\tau} D^{j+1}_\mu D^{j+2}_\nu D^{j+2}_\lambda \wedge dD^{j+2}_\tau}{\left(I^{\rho\sigma} D^{j+1}_\rho D^{j+2}_\sigma\right)^3 \overset{j}{\underset{h=1}{\Pi}} \left(I^{\lambda\tau} D^h_\lambda D^{h+1}_\tau\right)^2}. \qquad (5.16)$$

It is evident that the structure (5.16) does not correspond to any scattering form. However, it is particularly useful for building up the twistorial structures associated with the total contributions coming from current spots. The explicit expression (5.15) constitutes a generalization of the scattering forms that involve zigzags carrying only two edges [16,17]. It should be noted that the integration of (5.15) and (5.16) does not play any important role here. These forms are defined on product spaces of appropriate closed subsets of the Riemann spheres associated with all the vertices of the zigzag configuration of Fig.15. The prescription for constructing these spaces will be given in Sec.5.4 when the basic twistorial scattering integrals are introduced. It will become apparent that the singularities of the integrands have to take part in the construction of the relevant contours.

5.3 Twistor Null Initial Data

In accordance with the definitions of Sec.2.3, the pattern of the null data on $\mathscr{E}_o^+$ generating all the elementary contributions is the same as that of data for spinning massless free fields. This fact enables one to make use of the twistor data given in Ref.[17] when carrying out the explicit translation of the Minkowskian scattering integrals. In the case of left-handed fields of spin s<0, the expression for these twistor data at some $U^{AA'} \in \mathscr{E}_o^+$ that is past-null separated from another relevant interior point $V^{AA'}$ is written as

$$(I^{\mu\nu}U_\mu V_\nu)^{-2s+1}\Lambda_L(U_\alpha,V_\alpha), \tag{5.17}$$

where $\Lambda_L(U_\alpha,V_\alpha)$ is a holomorphic twistor function possessing the following homogeneity-symmetry properties

$$U_\beta \frac{\partial}{\partial U_\beta}\Lambda_L(U_\alpha,V_\alpha) = -\Lambda_L(U_\alpha,V_\alpha), \tag{5.18a}$$

$$V_\beta \frac{\partial}{\partial V_\beta}\Lambda_L(U_\alpha,V_\alpha) = (2s-1)\Lambda_L(U_\alpha,V_\alpha), \tag{5.18b}$$

and

$$U_\beta \frac{\partial}{\partial V_\beta}\Lambda_L(U_\alpha,V_\alpha) = 0. \tag{5.18c}$$

This twistor function is defined on the product of two subsets, $\mathscr{D}_o^*$ and $\mathscr{D}_V^*$, of the Riemann spheres, $\mathscr{R}_o^*$ and $\mathscr{R}_V^*$, associated with O and $V^{AA'}$, respectively. In principle, the former (resp. latter) factor consists only of projective null twistors $\{U_\alpha\}$ (resp. $\{V_\alpha\}$) lying in $\mathbb{PN}^*$. Thus, (5.17) appears as the {-2s,0;0,0}-twistor NID on $\mathscr{D}_o^*\times\mathscr{D}_V^*$. Of course, the values of s which are of relevance here are -1/2 and -1. It must be observed that the holomorphicity of (5.17) actually entails analicity to the elementary RM-data on $\mathscr{E}_o^+$ [28]. As regards the KAP-integrals for the electromagnetic free contributions, the S^2-topology involved turns out to be split into the product of two S^1's, one lying in $\mathscr{D}_o^*$ and the

other in $\mathcal{D}_v^*$, the point $V^{AA'}$ being thus identified with $x^{AA'}$. The contour lying in $\mathcal{D}_v^*$ is usually required to separate the relevant singularities into two disconnected closed subsets [3]. It can not therefore be shrunk to a point without crossing any singularity.

In order to construct the corresponding $\hat{\pi}$-data, it is useful to employ the following twistor expression [17]

$$\underset{Us-}{\hat{\pi}} = \frac{(-1)^{-2s+1}}{(I^{\mu\nu}U_\mu V_\nu)^{-2s}} \overset{V}{o}_A \frac{\partial}{\partial \overset{V}{o}_A}, \tag{5.19}$$

which is taken to act only upon the twistor-function kernel of (5.17). Hence, the {0,2s;0,0}-datum is expressed by

$$(-1)^{-2s+1}(I^{\mu\nu}U_\mu V_\nu)\, \overset{V}{o}_A \frac{\partial}{\partial \overset{V}{o}_A} \Lambda_L(U_\alpha, V_\alpha). \tag{5.20}$$

The twistor transcription procedures involve coupling this latter datum with the one-form $I^{\mu\nu}U_\mu dU_\nu$, whence it appears to be convenient to use the following relation at $U^{AA'}$ (see Ref.[17]):

$$\overset{V}{o}_A I^{\mu\nu}U_\mu dU_\nu = (I^{\mu\nu}U_\mu V_\nu)d\overset{U}{o}_A + \underset{\sim}{\nu}\, \overset{U}{o}_A, \tag{5.21}$$

where $\underset{\sim}{\nu}$ is a certain one-form on $\mathcal{C}_o^+$ of the type {1,1;0,0}. Therefore, the pertinent holomorphic twistor-datum one-form turns out to be given by

$$\underset{\sim}{\mathcal{T}}_L(U_\alpha, V_\alpha) = (-1)^{-2s+1}(I^{\mu\nu}U_\mu V_\nu)^2 \underset{\sim}{\Lambda}_L(U_\alpha, V_\alpha), \tag{5.22}$$

with $\underset{\sim}{\Lambda}_L(U_\alpha, V_\alpha) = \frac{\partial}{\partial V_\tau} \Lambda_L(U_\alpha, V_\alpha)dU_\tau$. It is obvious that the $\underset{\sim}{\nu}$-term of (5.21) does not appear in (5.22) because of the property (5.18c). We thus have the "combined" homogeneity-symmetry property

$$\underset{\sim}{\Lambda}_L(\mu U_\alpha, \lambda U_\alpha + \tau V_\alpha) = \tau^{2s-2}\underset{\sim}{\Lambda}_L(U_\alpha, V_\alpha), \tag{5.23}$$

where $\lambda \in \mathbb{C}$ and μ, τ belong both to $\mathbb{C} - \{0\}$. All the twistor-datum expressions for right-handed fields can be constructed from those defined above by replacing U_α and V_α by upper-index twistors, the role played by $\mathbb{PN}^*$ being accordingly taken over by that played by $\mathbb{PN}$.

5.4 Twistorial Scattering Integrals and Twistor Diagrams

On the basis of the formulae built up in the previous sections, I shall now carry out the translation of the basic RM-structures of chapter 4 in a direct way. As was observed before, the twistorial KAP-integral expressions for the electromagnetic free contributions constitute a particular version of those provided earlier [17]. These electromagnetic integrals can be written down by invoking Eqs.(5.15) and (5.22). Ignoring non-essential overall signs, we thus obtain the formal SI expression

$$\langle\langle L^{o}(M);\phi_{AB}(x)\rangle\rangle = \frac{1}{2\pi i}\oint_{\gamma_o\times\gamma_x} o^{x}_{A}\, o^{x}_{B}\, \underset{\sim}{\phi}_{L}{}^{o}(M_\alpha,X_\alpha)\wedge I^{\mu\nu}X_\mu dX_\nu, \qquad (5.24)$$

along with its conjugate. We have the simple topological structure

$$\mathcal{D}^{*}_{o} \supset \gamma_o \cong S^1 \cong \gamma_x \subset \mathcal{D}^{*}_{x}. \qquad (5.25)$$

The left-handed diagrammatic equality is exhibited in Fig.16. "Outgoing" dashed lines denote spinors appearing explicitly in (5.24). Such a line bears a number which refers to the contribution of the spinors to the homogeneity of the integrand. The meaning of the dashed and dotted lines starting at points of the loop will be explained later (see Fig.17). It is worth mentioning that the structure of the X-vertex can be modified by using a method given by Penrose [12], whereby the

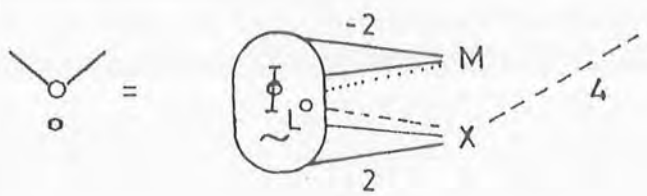

Figure 16

Equality between the tree and the twistor diagram associated with the left-handed electromagnetic free-field contribution.

* This contour structure was discussed in detail in the papers [16,17,33]. For completeness, further points have been made here on the opposite page.

integral of a projective one-form may be re-expressed as the integral of a projective three-form. This method was particularly adapted to the case of the generalized KAP-integrals [33], the modification giving rise then to a spotted-end-vertex structure. It will be used later in this section to simplify the scattering twistor diagrams.

The construction of the twistorial version of left-handed scattering integrals is based upon the formulae (5.7), (5.15), (5.16) and (5.22). For an arbitrary contribution, the corresponding null configuration involves a zigzag pattern of the type exhibited in Fig.15. The integration of the twistor D^{n}_{α} associated with the internal edge r_n, see (5.15), is taken over a closed three-real-dimensional contour which lies on the product $\mathcal{D}^{*}_{n-1}\times\mathcal{D}^{*}_{n}$ of two subsets of the Riemann spheres $\mathcal{R}^{*}_{n-1}$ and $\mathcal{R}^{*}_{n}$ that represent the vertices $_{n}D^{AA'}_{1}$ and $D^{AA'}_{n}$, respectively. This contour involves an S^1-factor which is associated with the integration along the generators of $\mathcal{S}^{+}_{n-2}$. At this stage, both $_{n-1}D^{AA'}$ and $D^{AA'}_{n}$ move in such a way that the contour is continuously deformed without meeting any singularity. Furthermore, the twistor integration process breaks down the S^2-elements of surface area at $_{n-1}D^{AA'}$ and $D^{AA'}_{n}$. The contour then picks up one S^1-factor from each of these S^2-structures, the remaining factors appearing as contributions to the integrations associated with the adjacent edges. Hence, the topology of the contour is really $S^1\times S^1\times S^1$. The integration of the (projective) one-forms which involve the twistors associated with the external edges of the zigzag pattern is performed over the remaining S^1-contours that come from the S^2-pieces of the RM-contributions emanating from the vertices $D^{AA'}_{1}$ and $_{j+1}D^{AA'}$. These latter contours lie

in the subspaces $\mathcal{D}^*_{o\ldots i}$ and $\mathcal{D}^*_{j+2}$ which consist of the dual projective twistors $\{D_\alpha\}$ and $\{D_\alpha\}$, respectively. It is evident that, when the translation of the integral associated with the entire null configuration is carried out, one has to consider all the subsets $\{\mathcal{D}^*_{o\sigma}\}$ of $\mathcal{R}^*_o$ which contain those twistors $\{G_\alpha\}$ meeting at O. The prescriptions for performing the integrations that involve generalized volume forms of the type (5.16) are similar to those given above, but the integration of the two-form associated with r_{j+2} is now taken over a two-real-dimensional contour contained in $\mathcal{D}^*_{j+1}\times\mathcal{D}^*_{j+2}$ whose topology is $S^1\times S^1$. In fact, one of these S^1-factors comes from the splitting of the S^2-structure at $D^{AA'}_{j+1}$ whereas the other is associated with the integration along the generators of $\mathcal{C}^+_j$. It should be stressed that, when the twistor integrands are actually introduced, the product spaces have to be suitably enlarged so as to accommodate the relevant singularities. The integration along the generators of $\mathcal{C}^+_o$ entails an enlargement of the subspace $\mathcal{D}^*_2$, but leaves $\mathcal{D}^*_o$ unaffected. It turns out that, in the case of "higher-order" fields, the product space on which the twistor NID are specified does not appear to be exactly the same as that for the case of massless free contributions. Obviously, the product spaces which are of relevance for right-handed fields appear all as subsets of Riemann spheres corresponding to lines lying in $\mathbb{PN}$.

To see how the transcription prescriptions work, one can initially suppose that the incoming densities are produced by data centred at points lying on $\mathcal{C}^+_o$. For the $\hat{\pi}$-datum (4.15), we have the structure

$$\frac{z_m}{\bar{z}_m z_S r_{Mm} r_{DS}} = \frac{\square\!\square\,(\square\!\square)^2\,\square\!\square}{\square\!\square\!\square\!\square\!\square\!\square\!\square\!\square} \,, \qquad (5.26)$$

provided that

$$\square\!\square\!\square\!\square\!\square\!\square\!\square\!\square = \square\!\square\!\square\!\square\!\square - \square\!\square\!\square\!\square\!\square \,. \qquad (5.27)$$

Working out the combined double $\mathscr{E}$-twistor piece, yields the expression

$$\square\!\square\!\square\!\square\!\square\!\square\!\square\!\square = 4 \;\frac{\square\!\square}{\square\!\square}\;\square\;\square\!\square\!\square\!\square\!\square\!\square\;\frac{\square\!\square}{\square\!\square}$$

$$= \square\!\square\;\square\!\square\;\square\!\square\;\square\!\square\;\square\!\square\; r_{Mm} r_{DS} \,, \qquad (5.28)$$

which leads at once to (5.27). Hence, up to a constant overall factor, the (SI) twistorial integral associated with (4.16) reads

$$\langle\langle L^{-}(D) L^{o}(M) L^{-}(S); \mathscr{P}_A(x)\rangle\rangle$$

$$= \frac{e}{2\pi}\,\frac{1}{2\pi i} \oint_{\Gamma_{DSMKX}} \overset{x}{\circ}_A \; \underset{\sim}{\Psi} L^{-}(D_\alpha, S_\alpha) \wedge \Delta S \wedge \underset{\sim}{\phi} L^{o}(M_\alpha, K_\alpha) \wedge \underset{\sim}{\mathscr{V}}(M_\alpha, K_\alpha) \wedge \square\!\square\; dx$$

$$\times \frac{(\square\!\square)^2}{\square\!\square\!\square\!\square\!\square\!\square\!\square\!\square\!\square\!\square} \,, \qquad (5.29)$$

where the Ψ-form implicitly carries the factor $(\square\!\square)^2$ which comes from the scattering datum, and $\underset{\sim}{\mathscr{V}}(M_\alpha, K_\alpha)$ stands for the two-form involved in the one-vertex version of (5.16). The symbol appearing beneath the integral sign denotes the contour involved in the whole integration. For the D-integration, we have the contour

$$S^1 \cong \Gamma_D \subset \mathcal{D}^*_{OD} \times \mathcal{D}^*_D \times \mathcal{D}^*_S \times \mathcal{D}^*_X, \qquad (5.30)$$

while the contour for the S-integration is defined by

$$S^1 \times S^1 \times S^1 \cong \Gamma_S \subset \mathcal{D}^*_O \times \mathcal{D}^*_M \times \mathcal{D}^*_m \times \mathcal{D}^*_D \times \mathcal{D}^*_S \times \mathcal{D}^*_X, \;\; \mathcal{D}^*_O = \mathcal{D}^*_{OM} \times \mathcal{D}^*_{OD}. \qquad (5.31)$$

The integrations of M_α and K_α are performed over contours Γ_M and Γ_K lying both in $\mathcal{D}^*_{OM}\times\mathcal{D}^*_M\times\mathcal{D}^*_m\times\mathcal{D}^*_D\times\mathcal{D}^*_S$. We have

$$S^1\cong\Gamma_M\subset\mathcal{D}^*_{OM}\times\mathcal{D}^*_M\times\mathcal{D}^*_m\times\mathcal{D}^*_D\times\mathcal{D}^*_S\supset\Gamma_K\cong S^1\times S^1. \tag{5.32}$$

For the X-integration, the contour is given by

$$S^1\cong\Gamma_X\subset\mathcal{D}^*_{OD}\times\mathcal{D}^*_D\times\mathcal{D}^*_S\times\mathcal{D}^*_X. \tag{5.33}$$

It is worth remarking that the ε-structure carried by the denominator of the integrand of (5.29) naturally separates the subsets $\mathcal{D}^*_{OM}$ and $\mathcal{D}^*_{OD}$ of $\mathcal{R}^*_o$. The corresponding diagrammatic representation is depicted in Fig.17. One important feature of the twistor diagram is the coupling of the branches associated with the incoming field and scatterer. The squared inner product carried by the numerator, in effect, plays the role of a connecting block. It is clear that such inner product is set up at the "middle" vertex $m^{AA'}$ of the (underlying) null configuration shown in Fig.5a. The $\mathcal{V}$-form is represented by a loop, the dotted line joining the vertex K indicating that the structure involves the two-form $dK_\alpha\wedge dK_\beta$. Similarly, the combined ε-piece appears as a loop bearing a letter and five homogeneity lines.

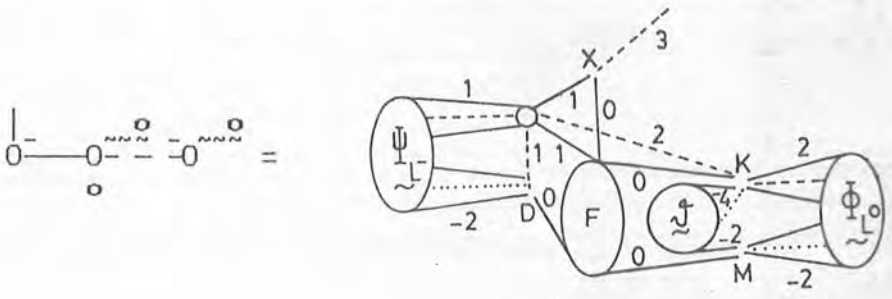

Figure 17

Equality between the tree and the twistor diagram for the scattering integral (4.16). The Dirac spot of Fig.5a is taken to lie on $\mathcal{E}^+_o$.

The dotted and dashed lines emanating from the Maxwell and Dirac loops mean that each of the datum one-forms carries a one-form of the type dU_α and a derivative operator of the type $\partial/\partial V_\alpha$, respectively (see (5.22)). The "outgoing" dashed line bears a meaning which is the same as that of Fig.16.

The structure of the expression (5.29) enables one to construct at once the twistor integral for the outgoing field of Fig.15 in the case where the scatterer loops are all identified with L^o-branches. Each of the electromagnetic datum spots, in effect, contributes a form $\oint_L \mathfrak{o}(M_\alpha^n, K_\alpha^n) \wedge \underset{\sim}{\mathcal{Y}}(M_\alpha^n, K_\alpha^n)$ to the numerator of the integrand, the coupling of the $\hat{\pi}$-datum that produces the incoming Dirac field with the internal zigzag branch being the standard one [16,17]. In particular, this latter coupled structure explicitly involves the differential form $\bigwedge_{m=2}^{j+1} \Delta S^m$ in its numerator and the product of $\prod_{m=1}^{j} (I^{\alpha\beta} D_\alpha^m D_\beta^{m+1})$ with $(I^{\mu\nu} D_\mu^{j+1} D_\nu^{j+2})^2$ in its denominator. The resulting contribution coming from the successive-scattering data appears as the product of pieces which involve the connecting inner products in their numerators and the double $\mathcal{E}$-twistor blocks in their denominators. It is evident that a trivial extension of the formulae (5.30)-(5.33) yields the definition of the relevant contour.

According to what was observed before, one has in general to modify the elementary data that generate some of the current spots before applying the transcription techniques to the RM-scattering integrals associated with Fig.6. Indeed, there are situations wherein the null patterns giving rise to the formation of these spots are produced by NID on $\mathcal{E}_o^+$, which need not be modified. Such configurations

actually involve the combination of mass-scattering branches [5,16,23,34] with electromagnetic patterns, and will not be exhibited here. The usual modification procedure [15] consists simply in using the following relation at some $U^{AA'} \in \mathcal{C}_o^+$, see (5.17),

$$V^{A'} = i(I^{\mu\nu}U_\mu V_\nu)r_{OU}\,\bar{o}_U^{A'}, \qquad (5.34)$$

together with its conjugate. Thus, the information carried by the π-parts of the twistors $\{U_\alpha, \bar{U}^\beta\}$, which are indeed the spinors that enter into the definition of the elementary NID on $\mathcal{C}_o^+$, is suitably transferred to the ω-parts of $\{\bar{V}^\beta, V_\alpha\}$. It follows that null data bearing one handedness turns out to be specified by twistor-function kernels involving twistors whose π-parts carry the other handedness. These modified twistor functions appear as reversed-homogeneity holomorphic functions on the same product space as that for the standard data (5.17), the coupling of the corresponding $\hat{\pi}$-data with the relevant differential forms being accomplished by using (5.21). The modified datum one-forms are of the type (5.22), but their homogeneity degrees turn out to be the same as those of twistor data for massless free fields [5,12,17]. When applied to a datum involving a field of spin s, the modification device (5.34) gives rise to $2|s|$ affine parameters which are actually carried by the denominator of the resulting datum. For incoming fields emanating from data on $\mathcal{C}_o^+$, for instance, this leads to a prescription for building up products involving adjacent parameters carried by modified uncharged data which gives rise to pieces proportional to factors of the form $\varepsilon^{\alpha\beta\gamma\delta}A_\alpha B_\beta C_\gamma D_\delta$. It should be clear that these factors carry the information about pairs of parameters that come from modified Dirac and electromagnetic data

involved in different branches. To construct an explicit scattering integral involving a typical twistorial pattern in the denominator of its integrand, it suffices to work out the transcription prescriptions for the RM-expression associated with any one of the configurations of Fig.6, supposing once again that all the Dirac spots start at points of $\mathcal{E}_o^+$. For the expression (4.41), say, we use the coupling

$$\frac{\hat{\pi}_{P\,1/2+}\,\bar{\Psi}_R^+(\bar{o}_P^{A'};P)}{z_m r_{Pm}}\;\frac{P\;dP}{(P\;K)^3}\wedge\frac{P\;K\;dK\wedge dK}{}$$

$$= i\,\frac{N\;P}{N\;R\;P\;K}\,\bar{\Psi}_R^+(P_\alpha,K_\alpha)\wedge P\;K\;dK\wedge dK, \qquad (5.35)$$

to obtain the SI integral

$$\langle\langle L^-(D)R^+(P)L^-(N)L^-(\Sigma);\Sigma_A(x)\rangle\rangle$$

$$= \frac{e^2}{2\pi}\frac{1}{2\pi i}\oint_{\Gamma_{NRPKDSX}} o_A^X\,\Psi_L^-(D_\alpha,S_\alpha)\wedge\Delta S\wedge\Psi_L^-(N_\alpha,R_\alpha)\wedge\mathcal{Y}(N_\alpha,R_\alpha)\wedge\bar{\Psi}_R^+(P_\alpha,K_\alpha)$$

$$\wedge\,\mathcal{Y}(P_\alpha,K_\alpha)\wedge X\;dX\;\frac{N\;P\;R\;S}{(D\;S\;S\;X)^2\;N\;R\;P\;K\;N\;R\;S\;D\;S\;X}, \qquad (5.36)$$

where $\Psi_L^-(D_\alpha,S_\alpha)$ carries implicitly the factor $(I^{\mu\nu}D_\mu S_\nu)^2$ as before. The definition of the contour involved in the integration is essentially the same as the one given earlier, see (5.29), but the product spaces for the integration of N_α and R_α have to be suitably enlarged because of the presence of the $\mathcal{E}$-piece coming from the modification of the datum at $P^{AA'}$. Of course, the relevant subspace $\mathcal{D}_o^*$ appears now as the product $\mathcal{D}_{ON}^*\times\mathcal{D}_{OP}^*\times\mathcal{D}_{OD}^*$. It is of some interest to introduce an auxiliary (null) twistor A^β satisfying

$$\frac{1}{(2\pi i)^3}\oint_{\Gamma_A}\frac{\Delta A}{N\ R\ P\ K}=\frac{(-1)}{N\ R\ P\ K}. \qquad (5.37)$$

This twistor can be thought of as being associated with the generators of the null cone $\mathcal{C}_Y$ of a fixed point $Y^{AA'}$. It is represented in $\mathbb{PN}^*$ by a projective plane $\mathcal{A}$, the (dual) projective line $\mathcal{Y}^*$ corresponding to $Y^{AA'}$ being chosen such that $\mathcal{Y}^* \cap \mathcal{X}^* = \emptyset$, with $\mathcal{X}^*$ standing for the dual projective version of $x^{AA'}$. Thus, $Y^{AA'}$ is *not* taken to be null separated from $x^{AA'}$. When the integral (5.37) is explicitly performed, the planes $\{\mathcal{A}\}$ sweep out a closed subset $\mathcal{S}^*_A$ of $\mathcal{Y}^*$, which consists of equivalence classes $[\lambda\bar{A}_\alpha]$ of proportional dual twistors, $\lambda \in \mathbb{C} - \{0\}$. Moreover, $\mathcal{S}^*_A$ is isomorphic to a subset $\mathcal{D}_A$ of the Riemann sphere associated with the $\mathbb{PN}$-version of $Y^{AA'}$. The singularities occur when the generators of $\mathcal{C}_Y$ meet the geodesics $\{\gamma_N,\gamma_R,\gamma_P,\gamma_K\}$. In each case, the intersection takes place at a point $M^{AA'}$ which is null separated from $Y^{AA'}$ whence the dual projective line $\mathcal{M}^*$ associated with $M^{AA'}$ meets both $\mathcal{Y}^*$ and $\mathcal{A}$ at some $\{\bar{A}_\alpha\}$. Evidently, a corresponding situation also takes place in $\mathbb{PN}$. Thus, the contour Γ_A appears as a three-real-dimensional closed contour lying in $\mathcal{D}_A \times \mathcal{D}^*_{ON} \times \mathcal{D}^*_{OF} \times \mathcal{D}^*_N \times \mathcal{D}^*_F \times \mathcal{D}^*_P \times \mathcal{D}^*_m$ whose topology can be taken as the product of S^1's provided that the singularities of the integrand of (5.37) are all simple poles. It must be observed that the above prescription rests crucially upon the requirement that the integrations of all the twistors involved have to be carried out independently of one another when (5.37) is effectively coupled together with (5.36). This procedure entails introducing an auxiliary (black) twistor vertex in the diagram representing (5.36). The resulting structure is shown in Fig.18.

Each of the twistor-function loops carried by the diagrams of Figs. 17 and 18 can be replaced by a three-spotted-twistor-vertex structure. The basic procedure consists essentially in combining the Penrose method to which I referred before [12,33] with a very useful lemma due to Hughston [22] whereby one may "stick" together the pieces that enter into each combined double ε-twistor block by performing a simple integration. In the case of the integral (5.29), for instance, the relevant (projective) statements are expressed as

$$\frac{1}{2\pi i}\oint_{\gamma_Z}\frac{Z\,dZ}{M\,K\,S\;\;D\,S\,X}=\frac{1}{M\,K\,S\;\;D\,S\,X}$$

$$=\frac{1}{(2\pi i)^3}\oint_{\Gamma_Z}\frac{\Delta Z}{G\,H\,M\,K\,S\;\;D\,S\,X}\,. \qquad (5.38)$$

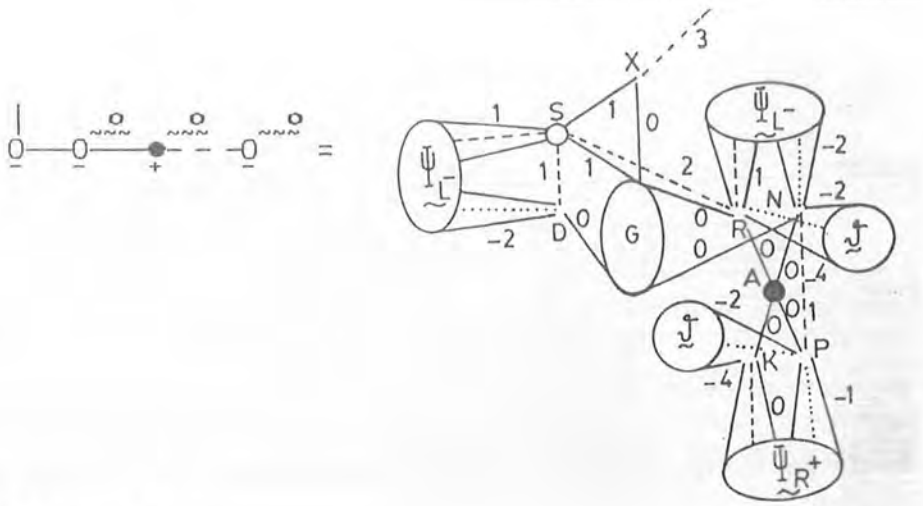

Figure 18

Diagrammatic equality for the configuration of Fig.6a. The twistor integrand involves a typical structure in its denominator. The ε-piece arising from the modification of the datum at $P^{AA'}$ is taken up by a suitable auxiliary vertex.

To visualize the situation involved in the one-dimensional integration, it is convenient to consider the following null twistors

$$\underset{M\,K\,S}{\sqcup\!\sqcup\!\sqcup} \equiv \underset{A}{|} = -ir_{Mm} \underset{M\,K\,K\,S}{\sqcup\!\sqcup\!\sqcup} \; \underset{\bar{K}}{|}\,, \tag{5.39a}$$

and

$$\underset{D\,S\,X}{\sqcup\!\sqcup\!\sqcup} \equiv \underset{B}{|} = ir_{DS} \underset{D\,S\,S\,X}{\sqcup\!\sqcup\!\sqcup} \; \underset{\bar{S}}{|}\,, \tag{5.39b}$$

which are represented in $\mathbb{PN}^*$ by two projective planes, $\mathcal{A}$ and $\mathcal{B}$, respectively. The former plane is defined by the dual twistors $\{M_\alpha\}$, $\{K_\alpha\}$ and $\{S_\alpha\}$, whereas the latter is specified by $\{D_\alpha\}$, $\{S_\alpha\}$ and $\{X_\alpha\}$. Their intersection is the dual projective line $\mathcal{L}^*$ that passes through $\{K_\alpha\}$ and $\{S_\alpha\}$. Of course, the line that joins $\{M_\alpha\}$, $\{K_\alpha\}$ lies in $\mathcal{A}$, while those joining $\{D_\alpha\}$, $\{S_\alpha\}$ and $\{X_\alpha\}$, $\{S_\alpha\}$ are contained in $\mathcal{B}$. It is clear that the $\mathbb{RM}$-point associated with $\mathcal{L}^*$ is $m^{AA'}$ provided that

$$\underset{M\,K\,S}{\sqcup\!\sqcup\!\sqcup}\underset{\bar{D}\,\bar{S}\,\bar{X}}{\sqcup\!\sqcup\!\sqcup} = 0 = \underset{D\,S\,X}{\sqcup\!\sqcup\!\sqcup}\underset{\bar{M}\,\bar{K}\,\bar{S}}{\sqcup\!\sqcup\!\sqcup}\,, \text{ at } m^{AA'}. \tag{5.40}$$

At this stage, the Z^β-twistors can be looked upon as the generators of the null cone of some point $W^{AA'}$ which is not taken to be null separated from $x^{AA'}$. The singularities arise when the π-part of Z^β becomes proportional to those of A^β and B^β, the projective plane corresponding to some $\{Z^\beta\}$ thus becoming coincident with each of $\mathcal{A}$ and $\mathcal{B}$. Accordingly, the contour γ_Z appears as an S^1-contour lying in the product space $\mathcal{D}_Z \times \mathcal{D}^*_{OM} \times \mathcal{D}^*_{OD} \times \mathcal{D}^*_M \times \mathcal{D}^*_m \times \mathcal{D}^*_D \times \mathcal{D}^*_S \times \mathcal{D}^*_X$, with $\mathcal{D}_Z$ being a subset of the Riemann sphere associated with the $\mathbb{PN}$-version $\mathcal{W}$ of $W^{AA'}$, which is isomorphic to a subset $\mathcal{Z}\mathcal{W} \subset \mathcal{W}$ that consists only of $\{Z^\beta\}$-twistors. The auxiliary twistors G_α and H_α involved in the three-dimensional integration are taken to be null (dual) twistors through a suitable fixed point P^a, this suitability being obviously that $\mathcal{P}^* \cap \mathcal{X}^* = \emptyset = \mathcal{P}^* \cap \mathcal{W}^*$,

with $P^a \longmapsto \mathcal{P}^* \subset \mathbb{PN}^*$. Once again, either of the latter singularities occurswhen the geodesics associated with the Z^β-twistors meet those corresponding to G_α and H_α. Now, the product space in which the relevant contour lies also involves the factor $\mathcal{D}^*_{PG}\times\mathcal{D}^*_{PH}$, with the subscript P playing a role similar to that played by O. In accordance with the prescription given in Ref.[33], this contour is defined so as to bear the topology $\Gamma_Z \cong S^1\times S^1\times S^1$. Therefore, invoking the auxiliary-vertex prescription given earlier, see (5.37) above, we can re-express (5.38) as

$$\frac{1}{(2\pi i)^9}\oint_{\mathcal{C}_{ZRT}} \prod^{G\ H} \frac{\Delta Z\wedge\Delta R\wedge\Delta T}{G\ H\ M\ K\ S\ \ \ \ \ \ D\ S\ X \;\Big|\; Z\ Z\ R\ R\ R\ R\ Z\ Z\ T\ T\ T\ T} = \frac{1}{M\ K\ S\ \ \ D\ S\ X \;\big|\; M\ K\ S\ \ \ D\ S\ X}\ , \quad (5.41)$$

where $\mathcal{C}_{ZRT}$ stands for the product of three suitable contours bearing the topology $S^1\times S^1\times S^1$. The corresponding diagrammatic structure is depicted in Fig.19. Notice that the infinity-twistor inner products occurring in the denominator of the integrand of (5.41) have been represented by lines joining vertices of the same type. Thus, we can re-depict the twistor diagram of Fig.17 as shown in Fig.20. Notice, also, that the homogeneity-line structure of the Dirac-datum bubble has been suitably modified.

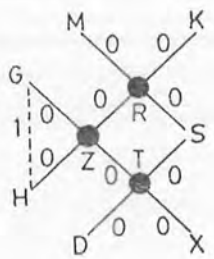

Figure 19

Twistor-diagram pattern for the five-variable functions that enter into the twistorial scattering integrals.

The construction of the structures of the integrand of any left-handed scattering integral can actually be carried out by coupling blocks which are of the same type as those entering into the explicit integrals exhibited here. One important feature of these structures is the fact that the inner products carried by their denominators constitute the same structure as the one specifying the singularities of mass-scattering integrals [23,34]. This result might have been expected since arbitrary $\mathbb{RM}$-configurations involve "internal" zigzag branches. In particular, the "dual" integrals associated with the diagrams of Fig.6 can be readily obtained from each other by applying the conjugation and interchange rules of Sec.4.3. When right-handed fields are effectively allowed for, the roles played by $\mathbb{PN}^*$ and $\mathbb{PN}$ are once again interchanged. We are therefore led to a natural correspondence between null structures and twistor diagrams.

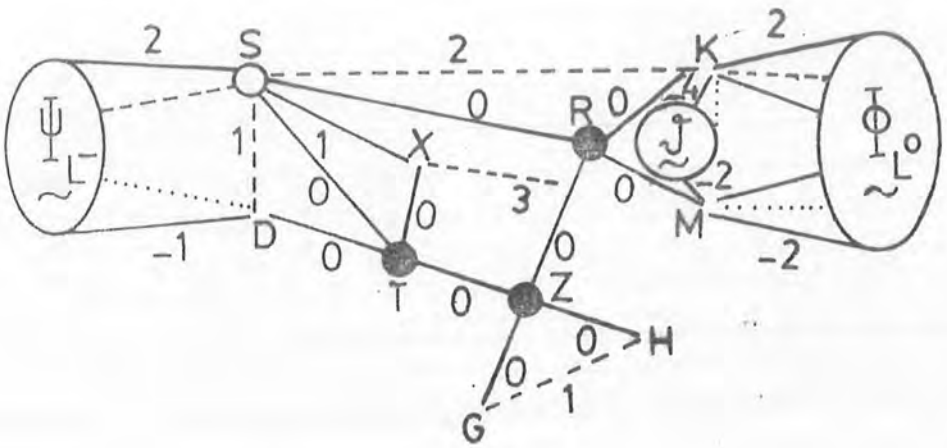

Figure 20

Modified twistor diagram for the scattering integral associated with Fig.17.

CHAPTER SIX

CONCLUSIONS AND OUTLOOK

One remarkable feature of the IRM-expressions presented here, which has arisen as a consequence of the particular choice of NID for all the elementary contributions, is the formal simplicity of the potential and field integrals. The introduction of null data for potentials on $\mathcal{I}_o^+$ would entail the generation of electromagnetic fields which would, in turn, produce elementary Dirac current contributions. The procedure for working out the corresponding FDE would therefore be reversed, but the new integral expressions would not provide any further insight into the whole picture. It was seen that the procedure involving a suitable replacement of the potential vector kernels gives rise automatically to adequate NID expressions for the processes. However, such a procedure did not yield any explicit expressions for the scattering densities. The requirements amounting to the vanishing of the scattering data on the future null cones of the spotted vertices that occur in the scatterer branches, were indeed made in order to balance the "degrees" of the distributions involved in the FDE. An important feature of these data is the fact that the contributions due to the incoming densities are naturally separable from those due to the scatterers. It is believed that this property would play a significant role in a quantum description of the scattering processes. In this connection, it would be convenient to employ the usual definition of the charge-helicity conjugation which actually preserves the handedness

of the Dirac fields. The helicity of the electromagnetic-field subgraphs occurring in the scattering diagrams would, therefore, be specified by the sign of the charge borne by appropriate current spots. Nevertheless, both the masslessness of the Maxwell fields and the divergencelessness of the potentials have to be retained, regardless of whether the conjugate Dirac fields are effectively taken to propagate towards the past. Of course, the structure of the statements involving the directional derivatives of the phase-shift functions leads immediately to expressions which allow one to calculate explicitly any phase-shift integral contribution. The constants arising from the integration of the relevant differential equations have to be specified so as to avoid the vanishing of the densities on the future null cones of the spots that generate the incoming fields. In the case of (4.10), for instance, the integration constant appears to be proportional to $1/r_{mK}$. When the contractions yielding the directional derivative relations are made, the pieces of the defining expressions that contribute to the scattering data are "annihilated". Thus, it may be said that the role played by these datum pieces is to make up the data so as to "neutralize" the vanishing of the $\hat{\pi}$-expressions which actually arise from the combination of the contributions due only to the derivatives of $\overset{D}{\Delta}_o(x)$ with the right-hand sides of the FDE.

It is of some interest to note that the graphs that enter into the mass-scattering expansions recovering the Dirac fields [5] can also be associated with colored trees of the type defined in Sec.2.5. The only internal lines carried by these trees are solid lines. At this stage, the structure represented by each such solid line consists of

two inner products with one affine parameter. The inner products are set up at the IRM-points which correspond to the vertices connected by the line, but the middle vertex occurring in any adjacent-edge branch contributes just one inner product to a higher-order integrand. Their specification is attained by using the white-black interchange rule. They always carry spinors bearing opposite helicities whence the line actually connects two vertices carrying different colors. The parameter is the one that connects the spots associated with the vertices. For a left-handed field of order N, the tree possesses N colored vertices carrying wavy lines together with one vertex which actually bears the external spinor line. All the wavy lines carry the number 0. The vertex associated with the datum spot on $\mathscr{C}_o^+$ is taken to be white or black according as N is even or odd. In the even-order (resp. odd-order) case, the graph thus carries $\frac{N}{2}+1$ (resp. $\frac{N+1}{2}$) white vertices and $\frac{N}{2}$ (resp. $\frac{N+1}{2}$) black vertices. For the right-handed contribution of the same order, the colored-vertex configuration appears the other way round. Thus, the number of internal lines occurring in any graph equals the order of the corresponding field in the case of either handedness. The expansion for the left-handed field, for example, turns out then to be given by

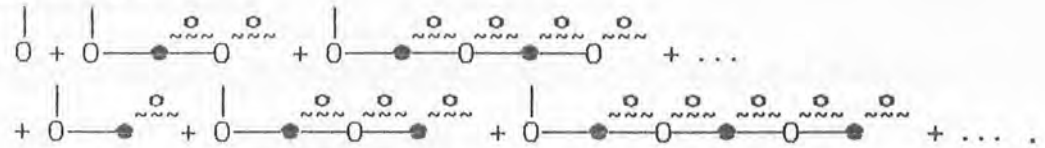

In fact, the graphical label device is particularly useful for calculating contributions that involve the coupling of several basic null configurations.

In principle, the Δ_1-functions that enter into the phase-

shift and electromagnetic-field integral expressions make the twistor transcription of the relevant patterns awkward. Nevertheless, this undesirable circumstance can be circumvented by carrying out the integration $\int f(x)\overset{M}{\Delta}_1(x)\Omega_{\sim M} = \int f(0)\mathcal{K}_{\sim M}$, which effectively removes the wavy line from the corresponding vertex and restricts the values of some appropriate function to those specified on $\mathcal{C}^{+}_{M}$. It turns out that vertices carrying external dashed lines without wavy lines have ultimately to be taken into consideration. The structures occurring in the twistor diagrams that correspond to the latter field integrals are of the same type as those depicted in Figs.17 and 18. As regards the integrals involved in the construction of the twistor structures associated with the five-variable twistor functions, it should be stressed that the integration of each of the triples of auxiliary spotted vertices brings the (corresponding) former structure back again. It is convenient to re-define appropriately the product spaces for the basic integrations in case these have to be performed first. The prescriptions for building up the relevant projective pictures can be readily constructed by using the work of Sec.5.4 along with the methods involved in the modification of the end-vertex structures of the diagrams that represent mass-scattering integrals [34]. This fact together with the features of the scattering diagrams of chapters 4 and 5 is what exhibits the usefulness of the thesis, and goes hand-in-hand with the original motivation for carrying out the entire work presented here. In respect of this situation, the hope is that the twistorial transcription of NID expressions can provide a clue to explain the hitherto unknown twistor mechanism of breaking of conformal invariance.

APPENDIX

In this appendix, the exacteness relations for the Maxwell-Dirac system are derived. All the main results were exhibited earlier by Penrose [3]. The field equations of Sec.2.2 will be used so many times here that I will not refer to them explicitly. It will suffice to work out the basic statements for the potential and left-handed fields. The corresponding equations for the right-handed fields can be at once constructed from the others by first interchanging unprimed and primed indices and then replacing the kernel letters that denote the Dirac fields appropriately.

To start with, consider the simple identity

$$\mathcal{D}_{B}^{B'}\psi_{C}(x) = \mathcal{D}_{(B}^{B'}\psi_{C)}(x) - \frac{1}{2}\mu\varepsilon_{BC}\chi^{B'}(x). \tag{A1}$$

For the second covariant derivative, we have the relation

$$\begin{aligned}\mathcal{D}_{A}^{A'}\mathcal{D}_{B}^{B'}\psi_{C}(x) &= \mathcal{D}_{(A}^{(A'}\mathcal{D}_{B}^{B')}\psi_{C)}(x) + \frac{1}{2}\varepsilon^{A'B'}\mathcal{D}_{M'(A}\mathcal{D}_{B}^{M'}\psi_{C)}(x)\\ &- \frac{1}{3}\varepsilon_{AB}\left[\mathcal{D}^{M(A'}\mathcal{D}_{(C}^{B')}\psi_{M)}(x) + \frac{1}{2}\varepsilon^{A'B'}\mathcal{D}_{M'}^{M}\mathcal{D}_{(C}^{M'}\psi_{M)}(x)\right]\\ &- \frac{1}{3}\varepsilon_{AC}\left[\mathcal{D}^{M(A'}\mathcal{D}_{(B}^{B')}\psi_{M)}(x) + \frac{1}{2}\varepsilon^{A'B'}\mathcal{D}_{M'}^{M}\mathcal{D}_{(B}^{M'}\psi_{M)}(x)\right]\\ &- \frac{1}{2}\varepsilon_{BC}\left[\mathcal{D}_{A}^{(A'}\mathcal{D}^{B')M}\psi_{M}(x) + \frac{1}{2}\varepsilon^{A'B'}\mathcal{D}_{AM'}\mathcal{D}^{MM'}\psi_{M}(x)\right].\end{aligned} \tag{A2}$$

The first term of (A2) can be simplified by using the equation [3,26]

$$\Box_{(AB}\psi_{C)}(x) = -ie\phi_{(AB}(x)\psi_{C)}(x), \tag{A3}$$

with $\Box_{AB}=\mathcal{D}_{A'(A}\mathcal{D}_{B)}^{A'}$. In effect, we have

$$\begin{aligned}\mathcal{D}_{M'(A}\mathcal{D}_{B}^{M'}\psi_{C)}(x) &= \mathcal{D}_{M'((A}\mathcal{D}_{B)}^{M'}\psi_{C)}(x) = -ie\phi_{(AB}(x)\psi_{C)}(x)\\ &= -ie\left[\phi_{A(B}(x)\psi_{C)}(x) + \frac{1}{3}\varepsilon_{A(B}\phi_{C)}^{M}(x)\psi_{M}(x)\right].\end{aligned} \tag{A4}$$

Using the conjugate of $\Box_{AB}$, after some manipulations we arrive at the

following expression for the first piece of the second term

$$\mathcal{D}^{M(A'}\mathcal{D}^{B')}_{(C}\psi_{M)}(x) = [\, ie\bar{\phi}^{A'B'}(x)\psi_C(x) + \frac{1}{2}\mu\mathcal{D}^{(A'}_{C}\chi^{B')}(x)] \,, \quad (A5)$$

whereas the kernel of the second piece reads (see (2.20))

$$\mathcal{D}^{M}_{M'}\mathcal{D}^{M'}_{(C}\psi_{M)}(x) = -\frac{1}{4}[\,3\,\blacksquare\,\psi_C(x) + 2ie\phi^{M}_{C}(x)\psi_M(x)]$$
$$= \frac{1}{2}[\,3\,\mu^2\psi_C(x) - 4ie\phi^{M}_{C}(x)\psi_M(x)] \,, \quad (A6)$$

provided that $(\blacksquare + 2\mu^2)\psi_C(x) = 2ie\phi^{M}_{C}(x)\psi_M(x)$. The third term can be readily obtained from (A5) and (A6) by replacing C by B, and the fourth is given simply by

$$\mathcal{D}^{(A'}_{A}\mathcal{D}^{B')M}\psi_M(x) + \frac{1}{2}\varepsilon^{A'B'}\mathcal{D}_{AM'}\mathcal{D}^{MM'}\psi_M(x)$$
$$= \mu\mathcal{D}^{(A'}_{A}\chi^{B')}(x) - \frac{\mu^2}{2}\varepsilon^{A'B'}\psi_A(x). \quad (A7)$$

Thus, combining the relations (A2)-(A7), yields

$$\mathcal{D}^{A'}_{A}\mathcal{D}^{B'}_{B}\psi_C(x) = \mathcal{D}^{(A'}_{(A}\mathcal{D}^{B')}_{B}\psi_{C)}(x) - \frac{2ie}{3}\varepsilon_{A(B}\psi_{C)}(x)\bar{\phi}^{A'B'}(x)$$
$$- \mu\,[\frac{1}{3}\varepsilon_{A(B}\mathcal{D}^{(A'}_{C)}\chi^{B')}(x) + \frac{1}{2}\varepsilon_{BC}\mathcal{D}^{(A'}_{A}\chi^{B')}(x)]$$
$$+ \varepsilon^{A'B'}[\frac{ie}{2}(\varepsilon_{A(B}\phi^{M}_{C)}(x)\psi_M(x) - \phi_{A(B}(x)\psi_{C)}(x))$$
$$+ \frac{\mu^2}{2}(\frac{1}{2}\varepsilon_{BC}\psi_A(x) - \varepsilon_{A(B}\psi_{C)}(x))] \,. \quad (A8)$$

In (A8), the term involving products between the left-handed Maxwell and Dirac fields equals $-ie\varepsilon^{A'B'}[\,\phi_{A(B}(x)\psi_{C)}(x) - 1/2\phi_{BC}(x)\psi_A(x)]$, while the μ^2-piece reads $-\mu^2/2\,\varepsilon^{A'B'}\varepsilon_{AB}\psi_C(x)$. The computation of the μ-term is more elaborate. To keep track of the relevant indices, it is convenient to introduce the block ABC for denoting the ordered (unprimed) indices carried by $\varepsilon_{AB}\mathcal{D}^{(A'}_{C}\chi^{B')}(x)$. We thus have the symmetry property

$$ABC = 2C[BA] = -BAC, \quad (A9)$$

whence the μ-piece carried by (A8) turns out to be given by

$$- 1/3\ A(BC) - 1/2\ BCA = - 1/3\ C[BA] - 1/3\ B[CA] - 1/2\ BCA$$

$$= - 1/3\ C[BA] + 1/3\ C[AB] + 2/3\ CBA$$

$$= 1/3\ CAB + 1/3\ CBA = 2/3\ C(AB). \qquad (A10)$$

Hence, replacing these latter results into (A8), leads to the exactness statements involving the left-handed Dirac fields.

The computations for the Maxwell fields are carried out as follows

$$\nabla_{A}^{A'}\phi_{BC}(x) = \nabla_{(A}^{A'}\phi_{BC)}(x) - 2/3\ \varepsilon_{A(B}\nabla^{A'M}\phi_{C)M}(x)$$

$$= \nabla_{(A}^{A'}\phi_{BC)}(x) - 4\pi/3\ \varepsilon_{A(B}j_{C)}^{A'}(x). \qquad (A11)$$

The higher derivatives take a similar form since the skew-symmetric part $\nabla^{A'[A}j_{A'}^{B]}(x)$ and its conjugate both vanish identically (see Eq.(2.21)). For the potential, we have

$$\nabla_{A}^{A'}\Phi_{B}^{B'}(x) = \nabla_{(A}^{(A'}\Phi_{B)}^{B')}(x) + 1/2\ \varepsilon^{A'B'}\phi_{AB}(x)$$

$$+ 1/2\ \varepsilon_{AB}\bar{\phi}^{A'B'}(x) + 1/4\ \varepsilon_{AB}\varepsilon^{A'B'}(\nabla_{C}\Phi^{C}(x)), \qquad (A12)$$

whence the exacteness of the entire set (2.1) is achieved whenever the Lorentz condition (2.5) is adopted. The manifest $SL(2,\mathbb{C})$-covariance of the above statements ensures the invariance of the system.

REFERENCES

[1] R.Penrose, *Conformal Approach to Infinity*, in Relativity, Groups and Topology: The 1963 Les Houches Lectures, eds. B.S.DeWitt and C.M.DeWitt (Gordon and Breach, New York, 1964).

[2] R.Penrose, Gen. Rel. Grav., 12(1980)225-64.

[3] R.Penrose and W.Rindler, *Spinors and Spacetime*, Vol.1 (Cambridge University Press, 1984).

[4] J.G.Cardoso, M.Sc. Thesis (University of Oxford, 1988).

[5] J.G.Cardoso, Int.Jour.Theor.Phys., 12(1991)1565-1588.

[6] J.G.Cardoso, Jour.Math.Phys., 33(1992)3-6.

[7] P.A.M.Dirac, Proc.Ry.Soc.London, A155(1936)447-59.

[8] W.L.Bade and H.Jehle, Rev.Mod.Phys., 25(1953)714-28.

[9] R.Penrose, Rep.Math.Phys., 12(1977)65.

[10] J.G.Cardoso, *Complexified Theory of Positive-Frequency Dirac Fields* (QAU, Islamabad, 1992).

[11] R.Penrose and M.A.H.MacCallum, Phys.Rep., 6C(1972)241.

[12] R.Penrose, *Twistor Theory: Its Aims and Achievements*, in Quantum Gravity: An Oxford Symposium, eds.C.J.Isham, R.Penrose and D.W. Sciama (Oxford University Press, 1975).

[13] A.Qadir, Phys.Rep., 39(1978)131.

[14] A.Qadir, Ph.D. Thesis (London, 1971).

[15] A.P.Hodges, Proc.Roy.Soc.Lond., A386(1983)185; Proc.Roy.Soc. Lond., A397(1985)341; Proc.Roy.Soc.Lond., A397(1985)375.

[16] J.G.Cardoso, *Twistorial Description of the Processes of Mass Scattering of Dirac Fields* (QAU, Islamabad, 1992).

[17] J.G.Cardoso, Int.Jour.Theor.Phys., 4(1991)447-62.

[18] R.Penrose, *Twistors and Particles*, in Quantum Theory and the Structures of Time and Space, ed. L.Castell, M.Drieschner and C.F. von Weiszacker (Verlag, München, 1975).

[19] R.Penrose and R.Ward, *Twistors for Flat and Curved Spacetime*, in General Relativity and Gravitation, One Hundred After the Birth of Albert Einstein, ed. A.Held (Plenum, New York, 1980).

[20] R.Penrose and W.Rindler, *Spinors and Spacetime*, Vol.2 (Cambridge University Press, 1986).

[21] R.Penrose, *On the Twistor Descriptions of Massless Fields*, in Complex Manifold Techniques in Theoretical Physics, eds. D.E.Lerner and P.D.Sommers (Pitman Advanced Publishing Program, 1979).

[22] L.P.Hughston, Lecture Notes in Physics, 97, (Springer-Verlag, Berlin, Heidelberg, New York, 1979).

[23] J.G.Cardoso, *Twistor-Diagram Representation of Mass-Scattering Integrals for Dirac Fields* (QAU, Islamabad, 1992).

[24] Z.Perjes and G.Sparling, *The Twistor Structure of Hadrons*, in Advances in twistor Theory, ed. L.P.Hughston and R.S.Ward (Pitman, San Francisco,1979).

[25] A.P.Hodges and S.Huggett, Surveys in High Energy Physics **1** (1980)333.

[26] J.G.Cardoso, *Two-Spinor Formulation of the Theory of Positive-Frequency Maxwell-Dirac Fields* (QAU, Islamabad, 1992).

[27] J.G.Cardoso, *Theory of Positive-Frequency Photons*, in Proceedings of the Workshop on Relativity, Astrophysics and Cosmology, ed. A.Qadir (QAU, Islamabad, 1992).

[28] R.Penrose, Int.Jour.Theor.Phys., **1**(1968)61-99.

[29] R.Geroch, A.Held and R.Penrose, Jour.Math.Phys., **14**(1973)874.

[30] F.G.Friedlander, *The Wave Equation on a Curved Spacetime*, Cambridge Monographs on Mathematical Physics 2 (Cambridge University Press, 1976).

[31] F.G.Friedlander, *Introduction to the Theory of Distributions* (Cambridge University Press, 1982).

[32] A.P.Hodges, Physica **114A**(1982)157.

[33] J.G.Cardoso, *New Twistor Diagrams for Massless free Fields of Arbitrary Spin*, Int.Jour.Mod.Phys (to appear).

[34] J.G.Cardoso, *Twistor-Diagram Equalities for Generalized Mass-Scattering Integrals for Dirac Fields* (QAU, Islamabad, 1992).

[35] J.G. Cardoso and Asghar Qadir, "*Explicit Evaluation of Classical Twistor Diagrams*" (to be submitted).

[36] J.G. Cardoso, "*A Diagrammatic Description of the Processes of Mass Scattering of Dirac Fields*" (to be submitted).

International Journal of Theoretical Physics, Vol. 30, No. 12, 1991

Generalized Mass-Scattering Integrals for Dirac Fields and Their Graphical Representation

J. G. Cardoso[1]

Received December 27, 1990

Penrose suggested that Dirac fields could be constructed from an infinite number of elementary distributional fields scattering off each other, with the mass of the entire fields playing the role of a coupling constant. Following this suggestion, we present a complete null description of the mass-scattering processes. The general pattern of the null initial data for successive processes is explicitly exhibited. The entire fields are given by four series of terms, each being a manifestly finite scaling-invariant integral which is taken over a compact space of appropriate mass-scattering zigzags. A set of simple rules which enable one to evaluate any term of the series in a graphical way is given. These rules give rise to a colored-graph representation of the scattering integrals.

1. INTRODUCTION

Penrose's null initial data (NID) techniques constitute a powerful instrument for describing the dynamics of sets of interacting spinor fields in real Minkowski space $\mathbb{RM}$ (Penrose, 1980; Penrose and Rindler, 1984). In this framework, the key concept is that of an invariant exact set, which guarantees a consistent description of the field dynamics. Likewise, the initial data for all the relevant processes are specified at nonsingular points of null hypersurfaces in $\mathbb{RM}$. The evaluation of the entire fields is then carried out by using either integral devices or appropriate power series expansions.

Penrose suggested (Penrose and Rindler, 1984) that, regarding the Dirac fields as the elements of an invariant exact set of interacting spinor fields on $\mathbb{RM}$, one could use these techniques to build up a solution of the source-free Dirac equation. In accordance with this procedure, the Van der Waarden form of the field equation should be employed such that the mass of the entire fields would appear as a coupling constant. The entire Dirac fields

[1]Department of Mathematics, Quaid-i-Azam University, Islamabad, Pakistan.

would then be given as a linear superposition involving an infinite number of elementary distributional fields, which propagate for a while along null geodesics of $\mathbb{RM}$, and repeatedly scatter off each other at points lying in the interior of the future cone of an origin of $\mathbb{RM}$.

In this paper, we develop Penrose's suggestion further to describe completely the mass scattering of Dirac fields in $\mathbb{RM}$. All the densities associated with the elementary contributions satisfy Dirac-like (proper Lorentz-invariant) distributional field density equations on the interior of the future cone of the origin (Section 2). The initial data generating the elementary fields are specified at points of the future null cone of the origin. Thus, the successive mass-scattering processes take place at suitable vertices of appropriate null zigzags that start at the origin and terminate at a fixed point of the interior of the future cone of the origin. These vertices are indeed the points at which the NID for the scattering processes are explicitly evaluated. Each element of the infinite Dirac set appears then to be given as a scaling-invariant (SI) Kirchhoff-like integral (Cardoso, 1990*a*) which is taken over a suitable space of such null graphs (Section 3). Hence, as far as the scattering processes are concerned, the propagation of all elementary fields is viewed as taking place entirely along the edges of these graphs. A representation of the field integrals in terms of colored graphs associated with mass-scattering zigzags leads us to four graphical expansions for the entire fields (Section 4).

Throughout this work all the fields are looked upon as classical, and there will be no attempt at this stage to regard them as quantized fields. We shall make use of some basic properties of distributional fields on $\mathbb{RM}$ (Penrose and Rindler, 1984).

2. FIELD DENSITY EQUATIONS

The main aim of this section is to present the distributional field density equations (DFDE). We endow the null graphs, which appear to play an important role here, with appropriate sets of spin bases. These bases enter into the definition of the relevant NID sets.

2.1. Forward Mass-Scattering Null Zigzags

Let V_0^+ denote the interior of the future cone of an origin O of $\mathbb{RM}$. Let, also, $\mathscr{C}_0^+$ be the future null cone of O. A forward null geodesic zigzag ζ_N is a simple graph (see, for example, Busacker and Saaty, 1965) whose vertex-set is the set

$$V(\zeta_N)=\{{}^{0}x^{AA'}, {}^{1}x^{AA'}, {}^{2}x^{AA'}, \ldots, {}^{N}x^{AA'}\} \tag{2.1}$$

of $N+1$ vertices all belonging to $\mathbb{RM}$, with $N\geq 2$. The vertex ${}^{n-1}x^{AA'}$ lies on the (future) forward null cone C_n^+ of ${}^{n}x^{AA'}$, $n=0, 1, 2, \ldots, N-1$. The edge-set of ζ_N is the set

$$E(\zeta_N)=\{{}^{1}r, {}^{2}r, {}^{3}r, \ldots, {}^{N}r\} \tag{2.2}$$

of N suitable affine parameters, where each ${}^{n-1}r$ lies on the (null geodesic) generator γ_{n-1} of C_n^+ that passes through ${}^{n}x^{AA'}$ and ${}^{n-1}x^{AA'}$. The elements ${}^{0}x^{AA'}$ and ${}^{N}x^{AA'}$ of (2.1) are the starting-vertex and end-vertex of $V(\zeta_N)$, respectively.

We next introduce the set of N pairs of forward spin bases

$$\begin{aligned}\mathrm{FSBS}=\{&\{\{{}^{0}o^{A}, {}^{1}o^{A}\}, \{\bar{o}_0^{A'}, \bar{o}_1^{A'}\}\}, \{\{{}^{1}o^{A}, {}^{2}o^{A}\}, \{\bar{o}_1^{A'}, \bar{o}_2^{A'}\}\},\\ &\ldots \{\{{}^{N-1}o^{A}, {}^{N}o^{A}\}, \{\bar{o}_{N-1}^{A'}, \bar{o}_N^{A'}\}\}\}\end{aligned} \tag{2.3}$$

where

$$\{\{{}^{n}o^{A}, {}^{n-1}o^{A}\}, \{\bar{o}_n^{A'}, \bar{o}_{n+1}^{A'}\}\}$$

is set up at the vertex ${}^{n}x^{AA'}\in V(\zeta_N)$, n running over the same values as before. This set is here called a forward spin-basis set. The pair

$$\{\{{}^{0}o^{A}, {}^{1}o^{A}\}, \{\bar{o}_0^{A'}, \bar{o}_1^{A'}\}\}$$

has been introduced even though it does not play any role herein. However, it is relevant when one carries out the twistorial transcription of the mass-scattering formulas (Cardoso, 1988). In (2.3), the spinors ${}^{n-1}o^{A}$, $\bar{o}_{n+1}^{A'}$ are chosen to be covariantly constant along γ_{n+1}. The real null vectors

$$\{{}^{n}o^{A}\bar{o}_n^{A'}, {}^{n-1}o^{A}\bar{o}_{n-1}^{A'}\} \tag{2.4}$$

point in (forward) future null directions through ${}^{n}x^{AA'}$, and the conjugate spin-inner products at ${}^{n}x^{AA'}$,

$$\xi_n={}^{n}o^{A}\,{}^{n+1}o_{A}, \qquad \bar{\xi}_n=\bar{o}_n^{A'}\bar{o}_{n+1A'} \tag{2.5}$$

are held fixed. Let ζ_N be equipped with an FSBS. In this case, if the starting-vertex of ζ_N is the vertex of $\mathscr{C}_0^+$ and if the elements ${}^{2}x^{AA'}, {}^{3}x^{AA'}, \ldots, {}^{N}x^{AA'}$ of $V(\zeta_N)$ all belong to V_0^+, ζ_N is said to be a mass-scattering null zigzag (MSNZZ).

We now take the element ${}^{N-1}x^{AA'}$ of the vertex-set of an MSNZZ, and transport the spinors ${}^{N}o^{A}$, $\bar{o}_{N-1}^{A'}$ (forwardly) parallelly along the generator γ_{N-1} of C_{N-2}^+. An ${}^{N-1}y^{AA'}\in V_0^+$ that is future-null-separated from an ${}^{N-1}R^{AA'}\in C_{N-2}^+$ which is, in turn, future-null-separated from ${}^{N-1}x^{AA'}$ is defined,

with respect to ${}^{N-1}x^{AA'}$, by

$$ {}^{N-1}y^{AA'} = {}^{N-1}q\, {}^{N-1}o^{A}\, \bar{o}^{A'}_{N-1} + {}^{N}u\, {}^{N}o^{A}\, \bar{o}^{A'}_{N} \tag{2.6} $$

In this relation, ${}^{N-1}q$ and ${}^{N}u$ are appropriate affine parameters, ${}^{N-1}q$ lying on γ_{N-1} and ${}^{N}u$ lying on the null geodesic that passes through ${}^{N-1}R^{AA'}$ and ${}^{N-1}y^{AA'}$ (see Figure 1). Recalling that the inner products ${}^{N-1}\xi$ and $\underset{N-1}{\xi}$ are fixed, and letting ${}^{N-1}y^{AA'}$ vary suitably, after a short calculation, we obtain

$$ {}^{N-1}\nabla_{AA'}\, {}^{N}o^{B} = (-1/{}^{N-1}\xi\, \underset{N-1}{\xi}\, {}^{N}u)\, {}^{N}o_{A}\, \bar{o}_{N-1}{}^{A'}\, {}^{N-1}o^{B} \tag{2.7} $$

and

$$ {}^{N-1}\nabla_{AA'}\, {}^{N}u = (1/{}^{N-1}\xi\, \underset{N-1}{\xi})\, {}^{N-1}o_{A}\, \bar{o}_{N-1}{}^{A} \tag{2.8} $$

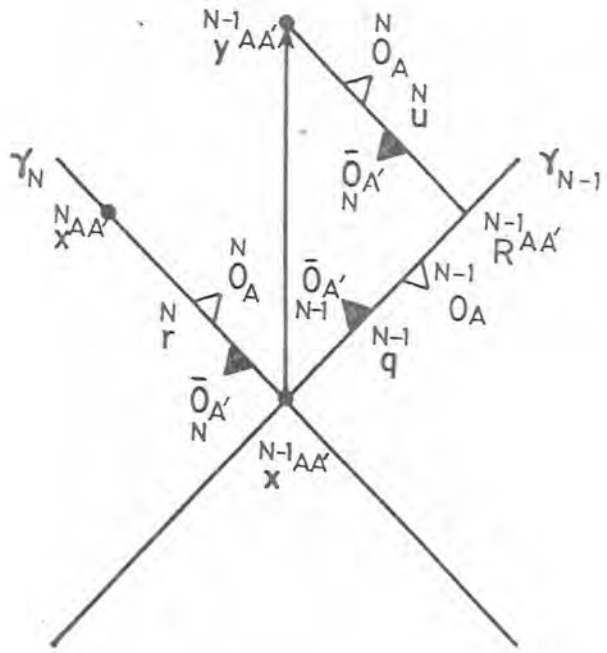

Fig. 1. A point ${}^{N-1}y^{AA'} \in V_0^+$ is defined with respect to the element ${}^{N-1}x^{AA'}$ of the vertex-set of an MSZZ.

where ${}^{N-1}\nabla_{AA'} = \partial/\partial\, {}^{N-1}y^{AA'}$. Notice that the spinors ${}^{N-1}o^{A}$, $\bar{o}_{N-1}{}^{A'}$ and the vertices ${}^{0}x^{AA'}, {}^{1}x^{AA'}, \ldots, {}^{N-1}x^{AA'}$ have been held fixed at this stage. The complex conjugate of (2.7) is

$$ {}^{N-1}\nabla_{AA'}\, \bar{o}^{B}_{N} = (-1/{}^{N-1}\xi\, \underset{N-1}{\xi}\, {}^{N}u)\, {}^{N-1}o_{A}\, \bar{o}_{N}{}^{A}\, \bar{o}_{N-1}{}^{B} \tag{2.9} $$

We assume that an appropriate MSNZZ will be involved in the definition of each of the quantities which are to be considered in what follows. The letters ζ, λ, and η will be sometimes used to refer it to these quantities.

2.2. Infinite Dirac Sets

In the absence of electromagnetism, the two-component spinor form of the Dirac equation on $\mathbb{R}^4$ is written as (Penrose and Rindler, 1984)

$$ \nabla^{AA'}\psi_{A}(x) = \mu\chi^{A'}(x), \qquad \nabla_{AA'}\chi^{A'}(x) = -\mu\psi_{A}(x) \tag{2.10} $$

where $\mu = (2)^{-1/2}\hbar^{-1}m$, m being the mass of the fields and $2\pi\hbar$ the usual Planck constant. Hence the Dirac fields form the invariant exact set of interacting spinor fields (Penrose, 1980)

$$ \mathrm{DS} = \{\psi_{A}(x),\ \chi^{A'}(x)\} \tag{2.11} $$

the constant μ appearing in (2.10) playing the role of a coupling constant.

The exactness of (2.11) allows us to split it into the infinite invariant exact set on V_0^+

$$ \mathrm{IDS} = \{\overset{0}{\psi}_{A}(x),\ \overset{0}{\chi}{}^{A'}(x),\ \overset{1}{\psi}_{A}(x),\ \overset{1}{\chi}{}^{A'}(x),\ \overset{2}{\psi}_{A}(x),\ \overset{2}{\chi}{}^{A'}(x), \ldots\} \tag{2.12} $$

whose elements yield a solution of (2.10) whenever we put

$$ \psi_{A}(x) = \sum_{K=0}^{\infty} \overset{K}{\psi}_{A}(x), \qquad \chi^{A'}(x) = \sum_{K=0}^{\infty} \overset{K}{\chi}{}^{A'}(x) \tag{2.13} $$

In (2.12), $x^{AA'} \in V_0^+$ is effectively identified with the end-vertices

$$ \overset{2K+2}{\underset{\lambda}{x}}{}^{AA'}, \ \overset{2K+3}{\underset{\eta}{x}}{}^{AA'} $$

of MSNZZs λ_{2K+2}, η_{2K+3} such that we can reexpress it as

$$ \mathrm{IDS} = \{\overset{0}{\psi}_{A}(\overset{2}{\underset{\lambda}{x}}),\ \overset{0}{\chi}{}^{A'}(\overset{2}{\underset{\lambda}{x}}),\ \overset{1}{\psi}_{A}(\overset{3}{\underset{\eta}{x}}),\ \overset{1}{\chi}{}^{A'}(\overset{3}{\underset{\eta}{x}}),\ \overset{2}{\psi}_{A}(\overset{4}{\underset{\lambda}{x}}),\ \overset{2}{\chi}{}^{A'}(\overset{4}{\underset{\lambda}{x}}), \ldots\} \tag{2.14} $$

We thus have

$$\overset{2K}{\psi}_A(x)=\overset{2K}{\psi}_A(\overset{2K-2}{\underset{\lambda}{x}}), \qquad \underset{2K}{\chi}{}^{A'}(x)=\underset{2K}{\chi}{}^{A'}(\overset{2K-2}{\underset{\lambda}{x}}) \tag{2.15a}$$

$$\overset{2K-1}{\psi}{}^{A'}(x)=\overset{2K-1}{\psi}{}^{A'}(\overset{2K-3}{\underset{\eta}{x}}), \qquad \underset{2K-1}{\chi}{}^{A'}(x)=\underset{2K-1}{\chi}{}^{A'}(\overset{2K-3}{\underset{\eta}{x}}) \tag{2.15b}$$

Let ζ_N stand for either λ_{2K-2} or η_{2K-3}. We now associate SI massive distributional field densities with the elements

$$\overset{N-1}{\psi}{}_A(\overset{N-1}{\underset{\zeta}{x}}) \quad \text{and} \quad \underset{N-1}{\chi}{}^{A'}(\overset{N-1}{\underset{\zeta}{x}})$$

of (2.14), satisfying the DFDE on I_0^-

$$\overset{N-1}{\underset{\zeta}{\nabla}}{}^{AA'}\overset{N-1}{\Psi}{}_A(\overset{N-1}{\underset{\zeta}{y}})=\mu\,\underset{N-2}{X}{}^{A'}(\overset{N-1}{\underset{\zeta}{y}}), \qquad \overset{N-1}{\underset{\zeta}{\nabla}}{}_{AA'}\underset{N-1}{X}{}^{A}(\overset{N-1}{\underset{\zeta}{y}})=-\mu\,\overset{N-2}{\Psi}{}_A(\overset{N-1}{\underset{\zeta}{y}}) \tag{2.16}$$

The fields

$$\overset{0}{\psi}_A(\overset{2}{\underset{\zeta}{x}}) \quad \text{and} \quad \underset{0}{\chi}{}^{A'}(\overset{2}{\underset{\zeta}{x}})$$

are the massless free elements of (2.14) whose SI densities satisfy the DFDE

$$\overset{1}{\underset{\zeta}{\nabla}}{}^{AA'}\overset{0}{\Psi}_A(\overset{1}{\underset{\zeta}{y}})=0, \qquad \overset{1}{\underset{\zeta}{\nabla}}{}_{AA'}\underset{0}{X}{}^{A'}(\overset{1}{\underset{\zeta}{y}})=0 \tag{2.17}$$

The precise meaning of these field densities will be made clear in Section 3. It is evident that the $\underset{\zeta}{y}$'s appearing in (2.16) and (2.17) are of the same form as (2.6).

2.3. Symbolic Expressions for Null Initial Data for Successive Mass-Scattering Processes

The choice of $\mathscr{C}_0^+$ as the NID hypersurface for all the fields in (2.14) enables us to define the NID set (Penrose, 1980; Penrose and Rindler, 1984)

$$\text{NIDS}=\{\overset{0}{\psi}(\overset{1}{o}{}^A;\overset{1}{x}),\ \underset{0}{\chi}(\overset{1}{\bar{o}}{}^{A'};\overset{1}{x}),\ 0,\ 0,\ \dots\} \tag{2.18}$$

Its nonvanishing elements are the complex scalar functions on $\mathscr{C}_0^+$

$$\overset{0}{\psi}(\overset{1}{o}{}^A;\overset{1}{x})=\overset{1}{o}{}^A\overset{0}{\psi}_A(\overset{1}{x}), \qquad \underset{0}{\chi}(\overset{1}{\bar{o}}{}^{A'};\overset{1}{x})=\overset{1}{\bar{o}}{}^{A'}\underset{O}{\chi}{}^{B'}(\overset{1}{x})\varepsilon_{B'A'} \tag{2.19}$$

which are specified at the element $\overset{1}{x}{}^{AA'}$ of the vertex-sets of MSNZZs. These NID actually generate the elementary fields of (2.14), and will therefore appear in the explicit expressions for the NID for successive mass-scattering processes (see Section 3.2).

We define the NID hypersurface for the $(N-1)$th mass-scattering process as being the future null cone C_{N-1}^+ of $\overset{N-1}{x}{}^{AA'}\in V(\zeta_{N-1})$. It is clear that this process involves the mass scattering of the massive field densities

$$\overset{N-1}{\Psi}{}_A(\overset{N-1}{y}), \qquad \underset{N-1}{X}{}^{A'}(\overset{N-1}{y})$$

The NID set for it is

$$\text{MSNIDS}=\{\overset{N-1}{\psi}(\overset{N}{o}{}^A;\overset{N}{x}),\ \underset{N-1}{\chi}(\overset{N}{\bar{o}}{}^{A'};\overset{N}{x})\} \tag{2.20}$$

where

$$\overset{N-1}{\psi}(\overset{N}{o}{}^A;\overset{N}{x})=\overset{N}{o}{}^A\overset{N-1}{\Psi}{}_A(\overset{N}{x}), \qquad \underset{N-1}{\chi}(\overset{N}{\bar{o}}{}^{A'};\overset{N}{x})=\overset{N}{\bar{o}}{}^A\underset{N-1}{X}{}^{B'}(\overset{N}{x})\varepsilon_{B'A} \tag{2.21}$$

are complex scalar functions on C_{N-1}^+ at $\overset{N}{x}{}^{AA'}\in V(\zeta_{N-1})$. For successive mass-scattering processes, we thus have the infinite NID set

$$\text{IMSNIDS}=\{\overset{1}{\psi}(\overset{2}{o}{}^A;\overset{2}{x}),\ \underset{1}{\chi}(\overset{2}{\bar{o}}{}^{A'};\overset{2}{x}),\ \overset{2}{\psi}(\overset{3}{o}{}^A;\overset{3}{x}),\ \underset{2}{\chi}(\overset{3}{\bar{o}}{}^{A'};\overset{3}{x}),\ \dots\} \tag{2.22}$$

In order to rewrite the DFDE in a symbolic form, we now introduce the conjugate spin scalar operators at $\overset{N}{x}{}^{AA'}$

$$\hat{\pi}_{N}^{1/2-}=(\overset{N}{r}/\overset{N}{\xi})\{\overset{N}{\mathbb{D}}-2^{N-1}\overset{N}{\rho}{}^{-1}(\overset{N}{x})\}=(\overset{N}{r}/\overset{N}{\xi})\overset{N}{\mathrm{p}}_{\mathrm{L}} \tag{2.23}$$

$$\hat{\pi}_{N}^{1/2+}=(\overset{N}{r}/\overset{N}{\bar{\xi}})\{\overset{N}{\mathbb{D}}-2\underset{N-1}{R}(\overset{N}{x})\}=(\overset{N}{r}/\overset{N}{\bar{\xi}})\overset{N}{\mathrm{p}}_{\mathrm{R}} \tag{2.24}$$

In these expressions, $\overset{N}{r}\in E(\zeta_{N+1})$ and $\overset{N}{\mathbb{D}}$ is the differentiation operator in the direction of γ_N at $\overset{N}{x}{}^{AA'}$. The functions $\overset{N-1}{\rho}{}^{-1}(\overset{N}{x})$ and $\underset{N-1}{R}(\overset{N}{x})$ are real and measure the convergence of the generators of C_{N-1}^+ at $\overset{N}{x}{}^{AA'}$ (Penrose, 1980). Their defining expression is

$$\overset{N-1}{\rho}{}^{-1}(\overset{N}{x})=(\overset{N}{\xi})^{-1}\overset{N}{o}{}_A\overset{N+1}{o}{}^C\overset{N}{\bar{o}}{}^{C'}(\partial/\partial\overset{N}{x}{}^{CC'})\overset{N}{o}{}^A=\underset{N-1}{R}(\overset{N}{x}) \tag{2.25}$$

The operators $\overset{N}{\mathrm{p}}_{\mathrm{L}}$ and $\overset{N}{\mathrm{p}}_{\mathrm{R}}$ are the usual real forms of the compacted spin-coefficient derivative operator at $\overset{N}{x}{}^{AA'}$ (Penrose and Rindler, 1984). In fact, for the general case of spin s, the $\hat{\pi}$ operators are given in Cardoso (1990*a*). Letting (2.23) and (2.24) act appropriately on the elements of (2.20), we get for the $(N-1)$th process

$$\hat{\pi}\text{-MSNIDS}=\{\hat{\pi}_{\overset{N}{}}^{1/2-}\overset{N-1}{\psi}(\overset{N}{o}{}^A;\overset{N}{x}),\ \hat{\pi}_{\overset{N}{}}^{1/2+}\underset{N-1}{\chi}(\overset{N}{\bar{o}}{}^{A'};\overset{N}{x})\} \tag{2.26}$$

The general pattern of the $\hat{\pi}$-NID for successive mass-scattering processes now becomes clear. We have the infinite $\hat{\pi}$-NID set

$$\hat{\pi}\text{-IMSNIDS} = \{\overset{1}{\hat{\pi}}_{1/2-}\overset{1}{\psi}(\overset{2}{o}{}^{A}; \overset{2}{x}),\ \overset{2}{\hat{\pi}}_{1/2-}\overset{1}{\chi}(\overset{2}{\bar{o}}{}^{A'}; \overset{2}{x}),\ \overset{3}{\hat{\pi}}_{1/2-}\overset{2}{\psi}(\overset{3}{o}{}^{A}; \overset{3}{x}),\ \overset{3}{\hat{\pi}}_{1/2-}\overset{2}{\chi}(\overset{3}{\bar{o}}{}^{A'}; \overset{3}{x}), \ldots\} \tag{2.27}$$

We shall see later (Section 3.2) that the explicit expressions for all the elements of (2.27) can be given in terms of the elements of the following NID set:

$$\hat{\pi}\text{-NIDS} = \{\overset{1}{\hat{\pi}}_{1/2-}\overset{0}{\psi}(\overset{1}{o}{}^{A}; \overset{1}{x}),\ \overset{1}{\hat{\pi}}_{1/2-}\overset{0}{\chi}(\overset{1}{\bar{o}}{}^{A'}; \overset{1}{x})\} \tag{2.28}$$

where the $\hat{\pi}$ operators are now defined on $\mathscr{C}_0^-$ at $\overset{1}{x}{}^{AA'}$. A diagrammatic representation of the functions appearing as the elements of (2.26) is shown in Figure 2. The $\hat{\pi}$-null datum involving $\overset{N-1}{\psi}(\underset{N-1}{\chi})$ has been represented by a white (black) datum spot. These datum spots bear the letters L and R, which stand for left and right, respectively. Such a diagrammatic representation shall be used also in Section 3. We will effectively make use of the corresponding terminology in Section 4.

As mentioned before, each of the elements of (2.14) propagates for a while along the edges of the relevant MSNZZs. Thus, by splitting

$$\overset{N-2}{\psi}{}_{A}(\overset{N}{x}) \quad \text{and} \quad \underset{N-2}{\chi}{}^{A'}(\overset{N}{x})$$

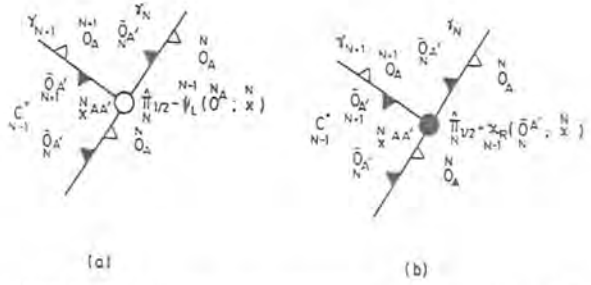

Fig. 2. The $\hat{\pi}$-NID for the $(N-1)$th mass-scattering process are represented by datum spots centered at the element $\overset{N}{x}{}^{AA'}$ of the vertex set of an MSNZZ. (a) The ψ datum is denoted by a white datum spot; (b) the χ datum is denoted by a black datum spot.

at $\overset{N-1}{y}{}^{AA'}$, we obtain

$$\overset{N-2}{\Psi}{}_{A}(\overset{N-1}{y}) = \frac{1}{2\pi}\overset{N}{o}{}_{A}\overset{N-1}{\Delta}{}_{1}(\overset{N-1}{y})\,\underset{N-1}{\hat{\pi}}{}_{1/2-}\overset{N-2}{\psi}(\overset{N-1}{o}{}^{M}; \overset{N-1}{x}) \tag{2.29}$$

and

$$\underset{N-2}{X}{}^{A'}(\overset{N-1}{y}) = \frac{1}{2\pi}\overset{N}{\bar{o}}{}^{A'}\overset{N-1}{\Delta}{}_{1}(\overset{N-1}{y})\,\underset{N-1}{\hat{\pi}}{}_{1/2-}\underset{N-2}{\chi}(\underset{N-1}{\bar{o}}{}^{M}; \overset{N-1}{x}) \tag{2.30}$$

where $\overset{N-1}{\Delta}{}_{1}(\overset{N-1}{y})$ is (Penrose and Rindler, 1984) a proper Lorentz scalar distributional field (PLSDF) on V_0^- (with the origin displaced to $\overset{N-1}{x}{}^{AA'}$) whose support is C^-_{N-1}. Therefore the massive DFDE (2.16) are rewritten as

$$\overset{N-1}{\nabla}{}^{AA'}\overset{N-1}{\Psi}{}_{A}(\overset{N-1}{y}) = (\mu/2\pi)\overset{N}{\bar{o}}{}^{A'}\overset{N-1}{\Delta}{}_{1}(\overset{N-1}{y})\,\underset{N-1}{\hat{\pi}}{}_{1/2-}\underset{N-2}{\chi}(\underset{N-1}{\bar{o}}{}^{M}; \overset{N-1}{x}) \tag{2.31}$$

$$\overset{N-1}{\nabla}{}_{AA'}\underset{N-1}{X}{}^{A'}(\overset{N-1}{y}) = (-\mu/2\pi)\overset{N}{o}{}_{A}\overset{N-1}{\Delta}{}_{1}(\overset{N-1}{y})\,\underset{N-1}{\hat{\pi}}{}_{1/2-}\overset{N-2}{\psi}(\overset{N-1}{o}{}^{M}; \overset{N-1}{x}) \tag{2.32}$$

Notice that these DFDE are invariant under both Lorentz transformations and arbitrary scalings.

3. MASS-SCATTERING INTEGRALS

To obtain the explicit mass-scattering integral formulas, we need first to solve the DFDE exhibited in Section 2.3. We shall be led to explicit NID for the mass-scattering processes. Each of the elementary fields of (2.14) emerges as an SI mass-scattering integral which is taken over an appropriate space of MSNZZs. The entire Dirac fields appear to be given in terms of four series as each of the expressions (2.13) is split up into two series. We will here use the diagrammatic representation of Section 2.3 whereby the $\hat{\pi}$-NID involved in the scattering processes are represented by white and black datum spots bearing L's and R's.

3.1. Solutions of the DFDE

The solutions of the massless free DFDE (2.17) can be obtained at once by putting $N=2$ in (2.29) and (2.30). We thus have

$$\overset{0}{\Psi}{}_{A}(\overset{1}{y}) = (1/2\pi)\overset{2}{o}{}_{A}\overset{1}{\Delta}{}_{1}(\overset{1}{y})\,\overset{1}{\hat{\pi}}{}_{1/2-}\overset{0}{\psi}(\overset{1}{o}{}^{M}; \overset{1}{x}) \tag{3.1}$$

and

$$\underset{0}{X}{}^{A'}(\overset{1}{y}) = (1/2\pi)\overset{2}{\bar{o}}{}^{A'}\overset{1}{\Delta}{}_{1}(\overset{1}{y})\,\overset{1}{\hat{\pi}}{}_{1/2+}\underset{0}{\chi}(\overset{1}{\bar{o}}{}^{M}; \overset{1}{x}) \tag{3.2}$$

These are the expressions arising from the usual splitting of the Kirchhoff-D'Adhemar–Penrose (KAP) integrals in the case of spin $\pm 1/2$ (Penrose and Rindler, 1984; Cardoso, 1990*b*). To the massive DFD equation (2.31), we seek a distributional solution of the form

$$ {}^{N-1}\Psi_{A}({}^{N-1}y) = {}^{N-1}\alpha_{A}({}^{N-1}y)\,{}^{N-1}\Delta_{j}({}^{N-1}y)\,{}_{N-1}\hat{\pi}_{1/2+}\,{}_{N-2}\chi({}_{N-1}\bar{o}^{M'};\,{}^{N-1}x) \tag{3.3} $$

where ${}^{N-1}\alpha_{A}({}^{N-1}y)$ is a spinor to be determined, and ${}^{N-1}\Delta_{j}({}^{N-1}y)$ is a PLSDF defined with respect to ${}^{N-1}x^{AA'}$. By differentiating out (3.3), using (2.7), (2.8), and the SI distributional relation on V_0^+,

$$ {}^{N-1}\nabla_{AA'}\,{}^{N-1}\Delta_{j}({}^{N-1}y) = {}^{N}u\,{}^{N}o_{A}\,\bar{o}_{N\,A'}\,{}^{N-1}\Delta_{j+1}({}^{N-1}y) - (j/{}^{N-1}z - {}_{N-1}\bar{\xi}\,{}^{N}u)\,{}^{N}o^{1}{}_{A}\,\bar{o}_{N-1\,A'}\,{}^{N-1}\Delta_{j}({}^{N-1}y) \tag{3.4} $$

we conclude that $j=0$, and

$$ {}^{N-1}\alpha_{A}({}^{N-1}y) = -[(\mu/2\pi)/{}^{N-1}z\,{}^{N}u]\,{}^{N}o^{1}{}_{A} \tag{3.5} $$

It follows that our SI solution is

$$ {}^{N-1}\Psi_{A}({}^{N-1}y) = -[(\mu/2\pi)/{}^{N-1}z\,{}^{N}u]\,{}^{N-1}o^{1}{}_{A}\,{}^{N-1}\Delta_{0}({}^{N-1}y)\,{}_{N-1}\hat{\pi}_{1/2+}\,{}_{N-2}\chi({}_{N-1}\bar{o}^{M'};\,{}^{N-1}x) \tag{3.6} $$

${}^{N-1}\Delta_{0}({}^{N-1}y)$ being (Penrose and Rindler, 1984) a proper Lorentz-invariant step function on V_0^+ defined with respect to ${}^{N-1}x^{AA'}$. A similar procedure leads to

$$ {}_{N-1}X^{A'}({}^{N-1}y) = -[(\mu/2\pi)/{}_{N-1}\bar{\xi}\,{}^{N}u]\,{}_{N-1}\bar{o}^{1}{}_{A'}\,{}^{N-1}\Delta_{0}({}^{N-1}y)\,{}_{N-1}\hat{\pi}_{1/2-}\,{}^{N-2}\Psi({}^{N-1}o^{M};\,{}^{N-1}x) \tag{3.7} $$

as the SI solution of (3.2). Since we are concerned here only with forward MSNZZs, we shall henceforth take ${}^{N-1}\Delta_{0}({}^{N-1}y)=1$.

3.2. Explicit NID Expressions for Successive Mass-Scattering Processes

The SI solutions (3.6) and (3.7) give rise to certain symbolic relations involving the elements of (2.27). These relations are easily established by making use of the defining expressions (2.21), (2.23), and (2.24). We thus have

$$ {}^{N-1}_{N}\hat{\pi}_{1/2-}\,{}^{N-1}\Psi({}^{N}o^{A};\,{}^{N}x) = [(\mu/2\pi)/{}^{NN}z\,r]\,{}_{N-1}\hat{\pi}_{1/2+}\,{}_{N-2}\chi({}_{N-1}\bar{o}^{A'};\,{}^{N-1}x) \tag{3.8} $$

and

$$ {}^{N}_{N}\hat{\pi}_{1/2+}\,{}_{N}\chi(\bar{o}^{A'};\,{}^{N}x) = [(\mu/2\pi)/{}^{N}_{N}\bar{\xi}\,r]\,{}_{N-1}\hat{\pi}_{1/2-}\,{}^{N-2}\Psi({}^{N-1}o^{A};\,{}^{N-1}x) \tag{3.9} $$

Let us now start with ${}^{0}_{1}\hat{\pi}_{1/2-}\psi({}^{1}o^{A};\,{}^{1}x)$ on $\mathscr{C}_0^+$ at ${}^{1}x^{AA'}\in V(\lambda_{2K+2})$, where $K\in\mathbb{N}\cup\{0\}$, $\mathbb{N}$ being the set of natural numbers. Using (3.8) and (3.9), we obtain the following expression for the NI datum for the ($2K$th-process) mass scattering of the SI field density ${}^{2K}\Psi_{A}({}^{2K}y)$ on C_{2K}^+ at ${}^{2K+1}x^{AA'}\in V(\lambda_{2K+2})$:

$$ {}^{2K}_{2K+1}\hat{\pi}_{1/2-}\psi({}^{2K+1}o^{A};\,{}^{2K+1}x) = (\mu/2\pi)^{2K}\,{}^{0}_{1}\hat{\pi}_{1/2-}\psi({}^{1}o^{A};\,{}^{1}x)\Big/\left[\left(\prod_{n=1}^{K}{}^{2n-1}z\right)\left(\prod_{m=1}^{K}{}_{2m}\bar{\xi}\right)\left(\prod_{j=1}^{2K}{}^{j+1}r\right)\right] \tag{3.10} $$

where the explicitly involved affine parameters belong to $E(\lambda_{2K+2})$ whenever K takes on the values 1, 2, 3, ... Similarly, starting with

$$ {}^{1}_{1}\hat{\pi}_{1/2+}\,{}^{0}_{0}\chi(\bar{o}^{A'};\,{}^{1}x) \quad \text{on} \quad \mathscr{C}_0^+ \quad \text{at} \quad {}^{1}x^{AA'}\in V(\eta_{2K+3}) $$

we obtain

$$ {}^{2K+1}_{2K+2}\hat{\pi}_{1/2-}\,{}^{2K+1}\Psi({}^{2K+2}o^{A};\,{}^{2K+2}x) = (\mu/2\pi)^{2K+1}\,{}^{1}_{1}\hat{\pi}_{1/2+}\,{}^{0}_{0}\chi(\bar{o}^{A'};\,{}^{1}x)\Big/\left[\left(\prod_{m=1}^{K+1}{}^{2m}z\right)\left(\prod_{n=1}^{K}{}_{2n+1}\bar{\xi}\right)\left(\prod_{j=1}^{2K+1}{}^{j+1}r\right)\right] \tag{3.11} $$

which is the expression for the NI datum for the [$(2K+1)$th-process] mass scattering of the (SI)

$$ {}^{2K+1}\Psi_{A}({}^{2K+1}y) \quad \text{on} \quad C_{2K+1}^+ \quad \text{at} \quad {}^{2K+2}x^{AA'}\in V(\eta_{2K+3}) $$

It is clear that the affine parameters involved in (3.11) all belong to $E(\eta_{2K+3})$.

The results for the mass-scattering processes involving the SI densities

$$ {}_{2K}X^{A'}({}^{2K}y) \quad \text{and} \quad {}_{2K+1}X^{A'}({}^{2K+1}y) $$

can be obtained from the previous ones as follows. We first make the replacements

$$\hat{\pi}_{2K+1}{}^{1/2-}{}_{2K}\chi\left({}^{2K+1}_{\circ}o^{A};\,{}^{2K+1}x\right)\to\hat{\pi}_{2K+1}{}^{1/2+}{}_{2K}\chi\left({}^{\bar{\circ}}_{2K+1}{}^{A'};\,{}^{2K+1}x\right)$$

$$\hat{\pi}_{2K+2}{}^{1/2-}{}_{2K+1}\psi\left({}^{2K+2}_{\circ}o^{A};\,{}^{2K+2}x\right)\to\hat{\pi}_{2K+2}{}^{1/2+}{}_{2K+1}\chi\left({}^{\bar{\circ}}_{2K+2}{}^{A'};\,{}^{2K+2}x\right)$$

Next we apply the interchange rule

$$\hat{\pi}_{1}{}^{1/2-}{}_{0}\psi\left({}^{1}_{\circ}o^{A};\,{}^{1}x\right)\leftrightarrow\hat{\pi}_{1}{}^{1/2+}{}_{0}\chi\left({}^{\bar{\circ}}_{1}{}^{A'};\,{}^{1}x\right)$$

Finally we take the complex conjugates of the explicitly involved inner products. We thus get

$$\hat{\pi}_{2K+1}{}^{1/2+}{}_{2K}\chi\left({}^{\bar{\circ}}_{2K+1}{}^{A'};\,{}^{2K+1}x\right)$$

$$=(\mu/2\pi)^{2K}\hat{\pi}_{1}{}^{1/2+}{}_{0}\chi\left({}^{\bar{\circ}}_{1}{}^{A'};\,{}^{1}x\right)\Bigg/\left[\left(\prod_{m=1}^{K}{}^{2m}z\right)\left(\prod_{n=1}^{K}{}_{2n+1}\bar{z}\right)\left(\prod_{j=1}^{2K}{}^{j+1}r\right)\right]\qquad(3.12)$$

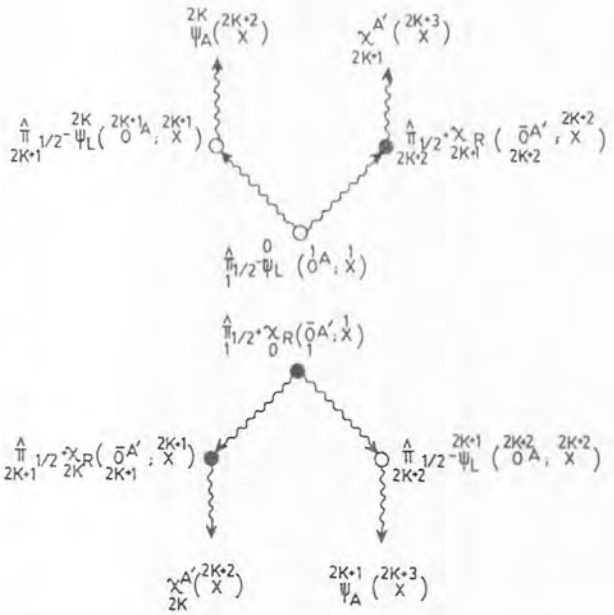

Fig. 3. Scheme showing the generation of the NID for the mass-scattering processes involving the SI distributional field densities in V_0^+.

on C_{2K}^{+} at ${}^{2K+1}x^{AA'}\in V(\lambda_{2K+2})$, and

$$\hat{\pi}_{2K+2}{}^{1/2+}{}_{2K+1}\chi\left({}^{\bar{\circ}}_{2K+2}{}^{A'};\,{}^{2K+2}x\right)$$

$$=(\mu/2\pi)^{2K+1}\hat{\pi}_{1}{}^{1/2-}{}_{0}\psi\left({}^{1}_{\circ}o^{A};\,{}^{1}x\right)\Bigg/\left[\left(\prod_{n=1}^{K}{}^{2n+1}z\right)\left(\prod_{m=1}^{K+1}{}_{2m}\bar{z}\right)\left(\prod_{j=1}^{2K+1}{}^{j+1}r\right)\right]$$

on C_{2K+1}^{+} at ${}^{2K+2}x^{AA'}\in V(\eta_{2K+3})$. A schematic representation of the above procedure is shown in Figure 3.

It is now evident that the elements of (2.28) are the NID for the "zeroth-mass-scattering process." These are the NID that enter into a modified SI version of the KAP field integrals in the case of spin $\pm 1/2$ (Cardoso, 1990*a*). The explicit p-NID for successive mass-scattering processes are given in Cardoso (1988).

3.3. The Entire Dirac Fields

For writing down the SI mass-scattering integrals for the elements of the infinite Dirac set (2.14), we need to define a mass-scattering $(3j-1)$-differential form, $j\in\mathbb{N}$. Such a form is an SI $(3j-1)$-volume form ${}^{123\ldots j}\underset{\sim}{K}$ on the compact space ${}^{123\ldots j}\mathbb{K}$ of MSNZZs whose edge-sets possess $j+1$ edges. The relevant defining expression is

$${}^{123\ldots j}\underset{\sim}{K}=\left(\bigwedge_{m=1}^{j-1}{}^{m}\underset{\sim}{r}\wedge{}^{m}\underset{\sim}{S}\right)\wedge{}^{j}\underset{\sim}{K}\qquad(3.14)$$

where ${}^{m}\underset{\sim}{r}$ is the SI one-form $d{}^{m}r/{}^{m}r$ at the element ${}^{m}x^{AA'}$ of the vertex-set of some $\zeta_{j+1}\in{}^{123\ldots j}\mathbb{K}$, with ${}^{m}r\in E(\zeta_{j+1})$; ${}^{m}\underset{\sim}{S}$ is the SI two-form of surface area provided by the (spacelike) intersection of the (past) backward null cone C_{m+1}^{-} of ${}^{m+1}x^{AA'}\in V(\zeta_{j+1})$ with the (future) forward null cone C_{m-1}^{+} of ${}^{m-1}x^{AA'}\in V(\zeta_{j+1})$, and ${}^{j}\underset{\sim}{K}$ is an SI two-form on the (two-dimensional) space of pairs of adjacent edges ${}^{j}r$ and ${}^{j+1}r$ of $E(\zeta_{j+1})$ incident at ${}^{j}x^{AA'}\in V(\zeta_{j+1})$, which is given by

$${}^{j}\underset{\sim}{K}={}^{j}\underset{\sim}{S}/({}^{j}z\,{}^{j}\bar{z}\,{}^{j}r\,{}^{j+1}r)\qquad(3.15)$$

We are now in a position to introduce the SI mass-scattering formulas. We have

$$\overset{2K}{\psi}_A(\overset{2K-2}{x}) = \frac{\mu^{2K}}{(2\pi)^{2K-1}} \int_{\underset{\mathbb{K}}{123\ldots 2K-1}} \overset{2K-2}{O}_A \times \frac{\hat{\pi}_{\underset{1}{1}\,1/2-} \overset{0}{\psi}(\overset{1}{o}^M; \overset{1}{x})\, \underset{\underset{}{}}{\overset{123\ldots 2K-1}{\underset{}{K}}}}{\left(\prod_{n=1}^{K} \overset{2n-1}{z}\right)\left(\prod_{m=1}^{K} \overset{2m}{z}\right)\left(\prod_{p=1}^{2K} \overset{p+1}{r}\right)} \tag{3.16}$$

$$\overset{2K+1}{\psi}_A(\overset{2K-3}{x}) = \frac{\mu^{2K-1}}{(2\pi)^{2K-2}} \int_{\underset{\mathbb{K}}{123\ldots 2K-2}} \overset{2K-3}{O}_A \times \frac{\hat{\pi}_{\underset{1}{1}\,1/2-} \overset{0}{\chi}(\overset{1}{\bar{o}}^{M'}; \overset{1}{x})\, \underset{\underset{}{}}{\overset{123\ldots 2K+2}{\underset{}{K}}}}{\left(\prod_{m=1}^{K-1} \overset{2m}{z}\right)\left(\prod_{n=1}^{K} \overset{2n+1}{z}\right)\left(\prod_{p=1}^{2K-1} \overset{p+1}{r}\right)} \tag{3.17}$$

for the unprimed elements of (2.14), and

$$\overset{A'}{\chi}_{2K}(\overset{2K+2}{x}) = \frac{\mu^{2K}}{(2\pi)^{2K+1}} \int_{\underset{\mathbb{K}}{123\ldots 2K+1}} \overset{\bar{o}}{}_{2K+2}^{A'} \times \frac{\hat{\pi}_{\underset{1}{1}\,1/2+} \overset{0}{\chi}(\overset{1}{\bar{o}}^{M'}; \overset{1}{x})\, \underset{\underset{}{}}{\overset{123\ldots 2K+1}{\underset{}{K}}}}{\left(\prod_{m=1}^{K} \overset{2m}{z}\right)\left(\prod_{n=1}^{K} \overset{2n-1}{z}\right)\left(\prod_{p=1}^{2K} \overset{p+1}{r}\right)} \tag{3.18}$$

$$\overset{A'}{\chi}_{2K+1}(\overset{2K+3}{x}) = \frac{\mu^{2K+1}}{(2\pi)^{2K+2}} \int_{\underset{\mathbb{K}}{123\ldots 2K+2}} \overset{\bar{o}}{}_{2K+3}^{A'} \times \frac{\hat{\pi}_{\underset{1}{1}\,1/2-} \overset{0}{\psi}(\overset{1}{o}^M; \overset{1}{x})\, \underset{\underset{}{}}{\overset{123\ldots 2K+2}{\underset{}{K}}}}{\left(\prod_{n=1}^{K} \overset{2n+1}{z}\right)\left(\prod_{m=1}^{K+1} \overset{2m}{z}\right)\left(\prod_{p=1}^{2K+1} \overset{p+1}{r}\right)} \tag{3.19}$$

for the primed elements. Each of the above mass-scattering integrals takes into account all the contributions coming from the spotted vertices of the appropriate MSNZZs (see Figure 2). Additionally, it is evident that these integrals carry explicitly the NID expressions given previously. These

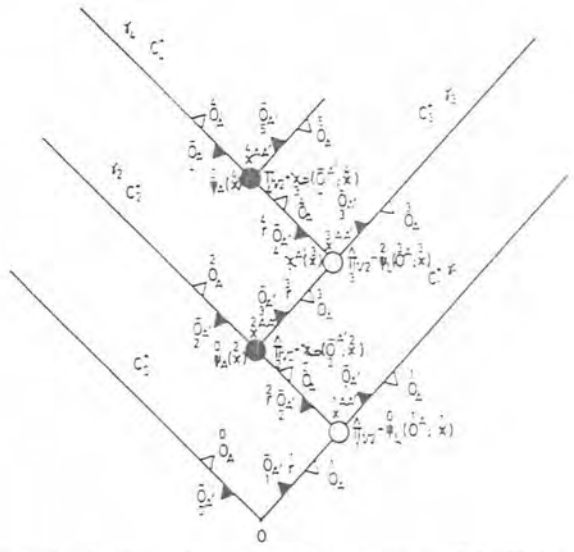

Fig. 4. Diagram showing successive mass-scattering processes of the SI distributional field densities on $V_{\bar{0}}$. The NID for the processes are generated by $\hat{\pi}_{\underset{1}{1}\,1/2-} \overset{0}{\psi}(\overset{1}{o}^A; \overset{1}{x})$ on $\mathscr{C}_{\bar{0}}$.

features are illustrated in Figs. 4 and 5. Particularly, the integral expressions for the massless free elementary fields are written out explicitly as

$$\overset{0}{\psi}_A(\overset{2}{x}) = \frac{1}{2\pi} \int_{\underset{\mathbb{K}}{1}} \overset{2}{o}_A \hat{\pi}_{\underset{1}{1}\,1/2-} \overset{0}{\psi}(\overset{1}{o}^M; \overset{1}{x})\, \overset{1}{\underset{}{K}} \tag{3.20}$$

and

$$\overset{A'}{\chi}_0(\overset{2}{x}) = \frac{1}{2\pi} \int_{\underset{\mathbb{K}}{1}} \overset{\bar{o}}{}_2^{A'} \hat{\pi}_{\underset{1}{1}\,1/2+} \overset{0}{\chi}(\overset{1}{\bar{o}}^{M'}; \overset{1}{x})\, \overset{1}{\underset{}{K}} \tag{3.21}$$

These are the SI version of the KAP field integrals for the case of spin $\pm 1/2$. The SI expressions for the general case of spin s are given in Cardoso (1990*a*).

Simple formal mass-scattering integral expressions can be achieved by defining suitable SI field densities on C^+_{2K} and C^+_{2K+1}, such that (see Figure 6)

$$\overset{2K}{\psi}_A(\overset{2K+2}{x}) = \frac{1}{2\pi} \int_{\underset{\mathbb{K}}{123\ldots 2K+1}} \overset{2K}{\Psi}_A(\overset{2K+1}{x})\, \underset{\underset{}{}}{\overset{123\ldots 2K+1}{\underset{}{K}}} \tag{3.22}$$

$$\overset{2K+1}{\psi}_A(\overset{2K+3}{x}) = \frac{1}{2\pi} \int_{\underset{\mathbb{K}}{123\ldots 2K+2}} \overset{2K+1}{\Psi}_A(\overset{2K+2}{x})\, \underset{\underset{}{}}{\overset{123\ldots 2K+2}{\underset{}{K}}} \tag{3.23}$$

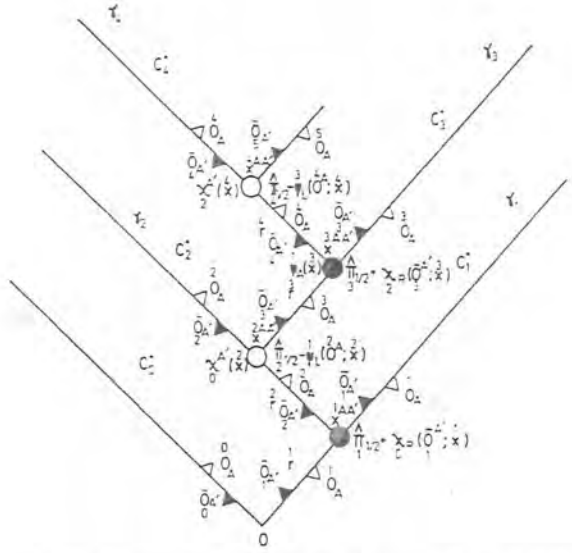

Fig. 5. Diagram showing successive mass-scattering processes of the SI distributional field densities on V_0^+. The NID for the processes are generated by $\hat{\pi}_{1/2-}\chi_0(\tilde{o}_1^{A'};\overset{1}{x})$ on $\mathscr{C}_0^-$.

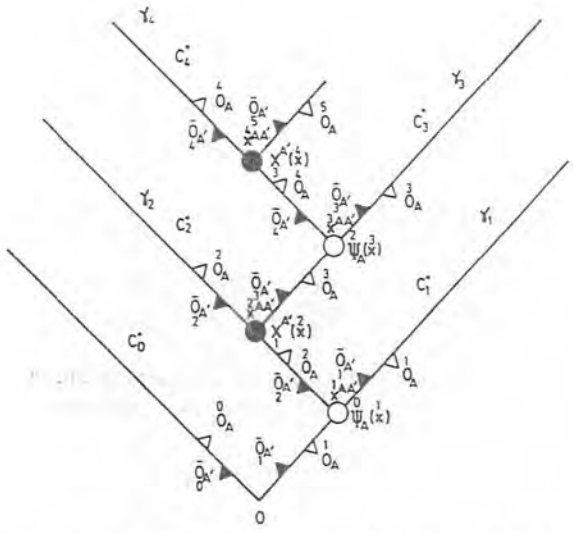

Fig. 6. The SI field densities on V_0^+ generated by $\hat{\pi}_{1/2-}\overset{0}{\psi}(\overset{1}{o}^{A};\overset{1}{x})$ on $\mathscr{C}_0^+$. These densities define simple formal mass-scattering integrals for the elementary fields $\psi_A(x)$ and $\underset{2K-1}{\chi}{}^{A'}(x)$.

and

$$\underset{2K}{\chi}{}^{A'}(\overset{2K-2}{x}) = \frac{1}{2\pi}\int_{\overset{123\ldots 2K+1}{K}} \underset{2K}{X}{}^{A'}(\overset{2K-1}{x})^{\overset{123\ldots 2K-1}{K}} \tag{3.24}$$

$$\underset{2K-1}{\chi}{}^{A'}(\overset{2K-3}{x}) = \frac{1}{2\pi}\int_{\overset{123\ldots 2K-2}{K}} \underset{2K-1}{X}{}^{A'}(\overset{2K-2}{x})^{\overset{123\ldots 2K-2}{K}} \tag{3.25}$$

Hence the entire fields (2.13) are reexpressed as

$$\psi_A(x) = \sum_{K=0}^{\infty} \overset{2K}{\psi}_A(\overset{2K-2}{\underset{\xi}{x}}) + \sum_{K=0}^{\infty} \overset{2K-1}{\psi}_A(\overset{2K+3}{\underset{\eta}{x}}) \tag{3.26}$$

$$\chi^{A'}(x) = \sum_{K=0}^{\infty} \underset{2K}{\chi}{}^{A'}(\overset{2K-2}{\underset{\xi}{x}}) + \sum_{K=0}^{\infty} \underset{2K-1}{\chi}{}^{A'}(\overset{2K-3}{\underset{\eta}{x}}) \tag{3.27}$$

A schematic diagram showing this recovery is given in Figure 7.

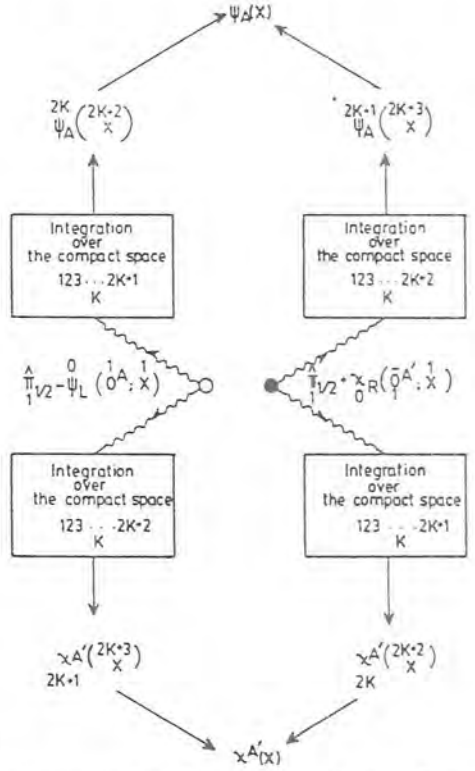

Fig. 7. Schematic representation of the recovery of the entire Dirac field set on V_0^+.

The diagrams illustrating our mass-scattering scheme, which have been exhibited above, can enable one to draw all the other relevant scattering diagrams. It is worth remarking, in particular, that the diagrams shown in Figures 4 and 5 can be obtained from one another by interchanging the datum spots appropriately (see Section 4).

4. GRAPHICAL DESCRIPTION OF THE MASS-SCATTERING PROCESSES

Basically, we shall now show how the information carried by the generalized mass-scattering integral expressions exhibited in the foregoing section can be extracted from certain simple graphs. Such graphs will henceforth be designated as mass-scattering graphs (MSGs). The unprimed and primed elementary fields shall be called left-handed and right-handed fields, respectively. For the sake of convenience, we will relabel the elements of the edge-sets of the scattering diagrams which appear to be of relevance to us.

4.1. Mass-Scattering Graphs

An MSG is a (simple) connected oriented colored graph σ_{N-2} $(N\geq 0)$ (Busacker and Saaty, 1965; Nakanishi, 1971) whose vertex-set

$$V(\sigma_{N+2})=\{\overset{0}{v}, \overset{1}{v}, \overset{2}{v}, \overset{3}{v}, \ldots, \overset{N-2}{v}\} \tag{4.1}$$

contains $N+3$ elements such that $\overset{n+1}{v}$ is "forwardly" separated from $\overset{n}{v}$, $n=0, 1, 2, \ldots, N+1$. Indeed, this "forwardness" is what defines the orientation of σ_{N+2}. The edge-set of σ_{N+2} is the set

$$E(\sigma_{N+2})=\{\overset{1}{a}, \overset{2}{a}, \overset{3}{a}, \ldots, \overset{N-2}{a}\} \tag{4.2}$$

of $N+2$ edges, where $\overset{n+1}{a}$ connects the vertices $\overset{n}{v}$ and $\overset{n+1}{v}$. We now introduce a suitable one-to-one correspondence between the (vertex-sets) edge-sets of MSNZZs and the (vertex-sets) edge-sets of MSGs. We have

$$\vartheta: \quad V(\zeta_{N+2})\to V(\sigma_{N+2}) \tag{4.3a}$$

$$\varepsilon: \quad E(\zeta_{N+2})\to E(\sigma_{N+2}) \tag{4.3b}$$

which establish the relationship between $(\overset{h}{x}{}^{AA'})\overset{n+1}{r}$ and $(\overset{h}{v})\overset{n+1}{a}$, $h=0, 1, 2, \ldots, N+2$. Both the starting-vertex $(\overset{0}{v})$ and the end-vertex $(\overset{N+2}{v})$ of σ_{N+2} carry no color, while each of the "internal" vertices carries either the color white or the color black. It becomes evident that the number of colored

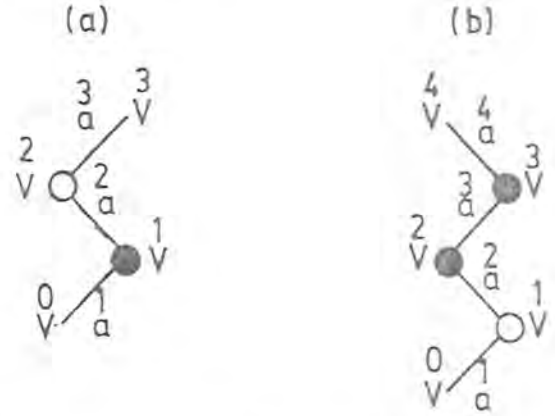

Fig. 8. Two zigzag-like patterns: (a) An MSG; (b) a zigzag which is not an MSG.

vertices of σ_{N-2} is equal to $N+1$. For $N>0$, any internal edge of $E(\sigma_{N+2})$ joins only vertices carrying different colors. Each white (black) vertex is associated with the appropriate NI datum for the scattering of a left-handed (right-handed) field. For example, we can have a graph as shown in Figure 8a, but not as shown in Figure 8b.

Notice that what appears to be of importance at this stage is the colored-vertex configuration together with the number of involved edges. For convenience, only zigzag-like MSGs are considered here. From now on we shall for simplicity drop the v's and a's from the scattering graphs.

4.2. Graphical Representation of the Mass-Scattering Integrals

Consider the left-handed outgoing field $\overset{N}{\psi}_A(x)$, which is involved in the Nth mass-scattering process. This process is graphically described by a σ_{N+2}. The vertex $\overset{1}{v}$ of this graph carries a white or black color, depending upon whether $N+2$ is even or odd. For example,

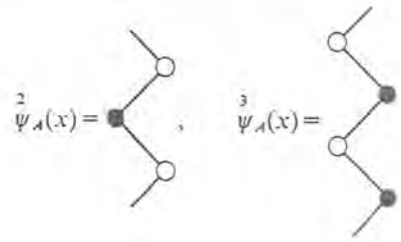

(4.4)

The case $N=0$ corresponds now to the "zeroth process," which involves the massless-free elementary contribution. We thus have

$$\overset{0}{\psi}_{A}(x)= \tag{4.5}$$

For $N>0$ the $\hat{\pi}$-NI datum for the process involves explicitly the product of N affine parameters and N appropriate spin-inner products in the denominator of the integrand of the relevant mass-scattering integral. The involved parameters are set as

$$\mathrm{LAP}_N=\{\overset{2}{r}, \overset{3}{r}, \ldots, \overset{N+1}{r}\}\subset E(\zeta_{N-2}) \tag{4.6}$$

while the involved inner products are given by

$$\mathrm{ELIP}_N=\{\overset{2}{\xi}, \overset{3}{z}, \overset{4}{\xi}, \overset{5}{z}, \ldots, \overset{N}{\xi}, \overset{N+1}{z}\} \tag{4.7a}$$

in the even-order case, and by

$$\mathrm{OLIP}_N=\{\overset{2}{z}, \overset{3}{\xi}, \overset{4}{z}, \overset{5}{\xi}, \ldots, \overset{N}{z}, \overset{N+1}{\xi}\} \tag{4.7b}$$

in the odd-order case. We observe that the elements of (4.6) correspond to the internal edges of σ_{N+2}. For (4.7a), the inner product $\overset{1}{z}$ is (suitably) implicitly carried by $(\mu/2\pi)^N \overset{1}{\hat{\pi}}_{1/2-} \overset{0}{\psi}(\overset{1}{o}^{A}; \overset{1}{x})$, while for (4.7b) the $\hat{\pi}$-NI datum $(\mu/2\pi)^N \overset{1}{\hat{\pi}}_{1/2+} \overset{0}{\chi}(\overset{1}{\bar{o}}^{A'}; \overset{1}{x})$ already involves $\overset{1}{\xi}$ adequately. Actually, each spin-inner product entering into the relevant mass-scattering integral is defined at a vertex of MSNZZs which corresponds to a colored vertex of MSGs. This inner product is barred or unbarred according as the corresponding colored vertex is black or white. It follows that, in the even-order (odd-order) case, $V(\sigma_{N+2})$ possesses $N/2+1$ [resp. $(N+1)/2$] white vertices and $N/2$ [resp. $(N+1)/2$] black vertices. In either case, the numerator of the integrand of the scattering integral involves the "outgoing" spinor $\overset{N+2}{o}_{A}$ together with a $(3N+2)$-differential form $\overset{123\ldots N+1}{K}$ on $\overset{123\ldots N+1}{\mathbb{K}}$, multiplied by the appropriate $\hat{\pi}$-NI datum at $\overset{1}{x}^{AA'}$. For example, for the graphs

(4.4), we have

$$=\left(\frac{\mu}{2\pi}\right)^2 \frac{1}{2\pi}\int_{\overset{123}{\mathbb{K}}} \overset{4}{o}_{A}\, \frac{\overset{\pi}{1}_{1\ 2-}\overset{0}{\psi}(\overset{1}{o}^{A}; \overset{1}{x})}{(\overset{3}{\xi}\overset{3}{z})(\overset{23}{r}\overset{23}{r})}\, \overset{123}{K} \tag{4.8}$$

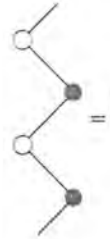

$$=\left(\frac{\mu}{2\pi}\right)^3 \frac{1}{2\pi}\int_{\overset{1234}{\mathbb{K}}} \overset{5}{o}_{A}\, \frac{\overset{\pi}{1}_{1\ 2-}\overset{0}{\chi}(\overset{1}{\bar{o}}^{A'}; \overset{1}{x})}{(\overset{2}{z}\overset{4}{\xi}\overset{3}{z})(\overset{234}{r}\overset{234}{r}\overset{234}{r})}\, \overset{1234}{K} \tag{4.9}$$

The MSG that describes the scattering of the right-handed elementary $\overset{N}{\chi}^{A'}(x)$ can be obtained from the one for $\overset{N}{\psi}_{A}(x)$ by interchanging white and black vertices. Thus, the colored-vertex configuration of the corresponding graph appears the other way about, its edge-structure being associated with (see Figures 4 and 5)

$$\mathrm{RAP}_N=\mathrm{LAP}_N \tag{4.10}$$

It follows that, in the massive case, the relevant inner products arising here are obtained from the elements of (4.7a) and (4.7b) by taking a complex conjugation. The rules for this case are essentially the same as the ones given before, but the scattering integral now involves the "outgoing" spinor $\overset{N+2}{\bar{o}}^{A'}$. We are thus led to the colored-vertex structures

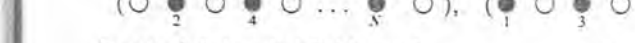

$$\tag{4.11}$$

for the left-handed fields, and

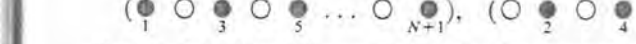

$$\tag{4.12}$$

for the right-handed ones. Evidently, the numbers carried by these structures refer to the labels of the colored vertices of the scattering graphs that represent the pertinent elementary fields. In particular, it should be noticed that the interchange rule of Section 3.2 has been automatically incorporated into this graphical scheme.

According to the above rules, the entire Dirac fields are recovered graphically as

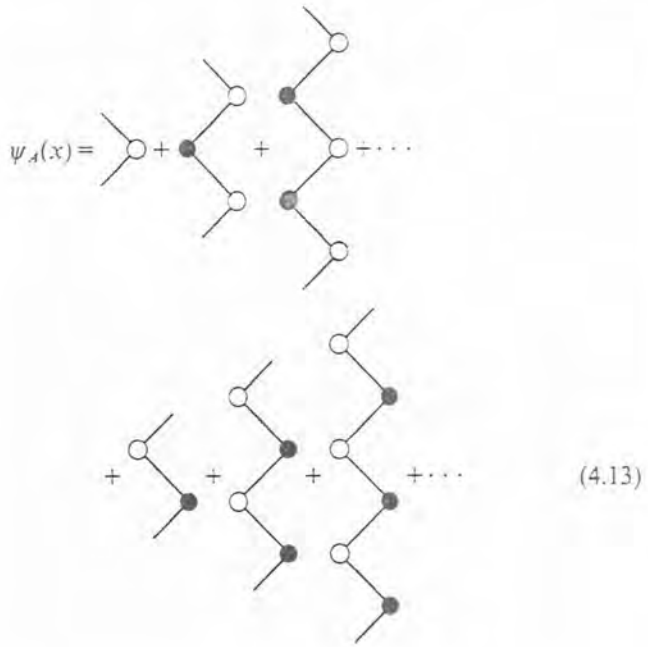

(4.13)

and

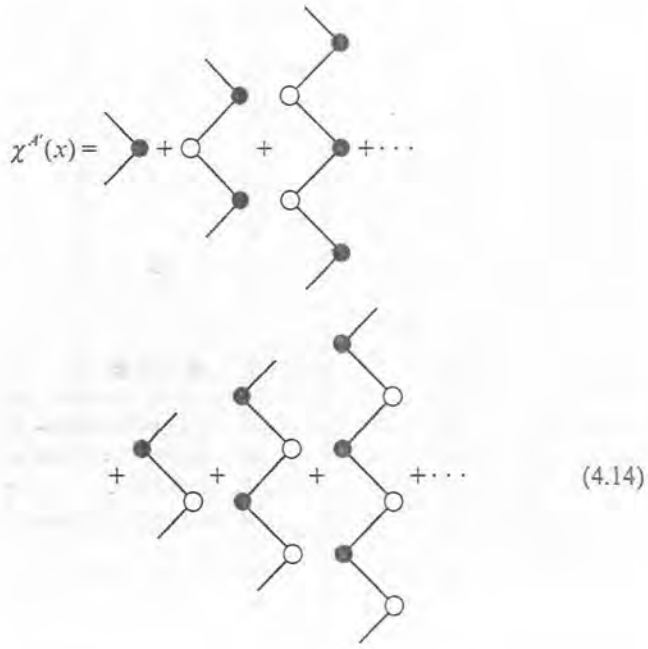

(4.14)

5. CONCLUDING REMARKS AND OUTLOOK

We presented a complete null description of the mass scattering of Dirac fields in $\mathbb{RM}$. One of the most important features of our scheme rests upon the fact that the information on the NID for mass-scattering processes is totally contained in suitably contracted derivatives of spinors entering into FSBSs. Here, the $\hat{\pi}$-spin scalar operators are regarded as being more natural than the p-operators, insofar as the former are involved in the expressions for the SI field densities. These densities are specified at points lying on forward null cones of appropriate elements of vertex-sets of MSNZZs. It should be emphasized that the particularly simple form of the scattering integrals carrying explicitly such densities is due to the choice of $\mathscr{C}_0^-$ as the NID hypersurface for all the elementary fields. At every order, the number defining the order of either field whose SI mass-scattering integral involves the $(3j-1)$-form $\overset{123\ldots j}{K}$ is equal to $j-1$. The point at which the field is evaluated is the end-vertex of some MSNZZ that possesses $j+1$ edges.

A noteworthy feature of the solutions of our DFDE is the fact that they involve a neutrino field at any order. The usual splitting of the KAP integral expressions for massless free fields thus arose once again here. In fact, as regards the PLSDFs, the mass-scattering integral for a massive contribution of order $j-1$ involves only the product of step-functions $\prod_{n=1}^{j-1} \overset{n}{\Delta}_0(\overset{n}{y})$, which is defined with respect to suitable vertices of the relevant MSNZZs. This was taken equal to 1 here, since our zigzags are forward null graphs in $\mathbb{RM}$. Nevertheless, as the DFDE of Section 2 stand thereupon, the corresponding higher-order contributions can be looked upon as massive pieces which are propagated in V_0^+ by the field equations. Indeed, what arises when the elementary contributions are broken down into distributional fields involving $\Delta_1(x)$ is that they behave themselves as massless pieces which propagate along the edges of MSNZZs. Under these circumstances, in effect, they appear to play the role of sources for the contributions associated with the densities that are involved in the left-hand sides of the DFDE. With respect to the former interpretation, it can be stated that what propagates along the null geodesics containing the edges of the scattering diagrams is the information carried by the elementary fields.

We have assumed from the outset that the series (2.13) giving the entire elements of the Dirac pair are convergent on V_0^+. This situation will probably be discussed elsewhere. The regular behavior of the NID (2.18) at the vertex of $\mathscr{C}_0^+$ is extensively discussed in Penrose and Rindler (1984), and effectively taken into account here. Actually, it provided us with a manifestly finite mass-scattering integral for each of the elementary fields. It may well be said that the relevance of the graphical description given in Section 4 stems from the fact that, once a set of rules for the scattering graphs is

at our disposal, we can obtain at once the integral expression for any elementary contribution of either handedness without performing any explicit calculation.

The generalized mass-scattering formulas exhibited in this paper fit neatly with the twistor formalism (see, for instance, Cardoso, 1990*c*). In connection with this fact, it seems to be worthwhile to set up a framework, within the NID approach, which might enable us to deal with quantized fields. It is believed that this procedure would bring new insights into the theory of twistors.

ACKNOWLEDGMENTS

I am deeply indebted to Prof. Roger Penrose for introducing me to the NID techniques. I am grateful to Dr. Asghar Qadir for useful suggestions. I wish to acknowledge the World Laboratory for supporting this work financially.

REFERENCES

Busacker, R. G., and Saaty, T. L. (1965). *Finite Graphs and Networks: An Introduction with Applications*, McGraw-Hill, New York.

Cardoso, J. G. (1988). M. Sc. thesis, University of Oxford.

Cardoso, J. G. (1990*a*). New twistorial integral formulae for massless free fields of arbitrary spin, Preprint, Quaid-i-Azam University.

Cardoso, J. G. (1990*b*). Bessel function expressions for Dirac fields, Preprint, Quaid-i-Azam University.

Cardoso, J. G. (1990c). Twistorial transcription of the mass-scattering of Dirac fields, Preprint, Quaid-i-Azam University.

Nakanishi, N. (1971). *Graph Theory and Feynman Integrals*, Gordon and Breach, New York.

Newman, E. T., and Penrose, R. (1968). *Proceedings of the Royal Society of London A*, **305**, 175.

Penrose, R. (1963). In *Relativity, Groups and Topology: The 1963 Les Houches Lectures*, B. S. DeWitt and C. M. DeWitt, eds., New York.

Penrose, R. (1980). *General Relativity and Gravitation*, **12**, 225.

Penrose, R., and Rindler, W. (1984). *Spinors and Space-Time*, Vol. 1, Cambridge University Press, Cambridge.

TWISTORIAL DESCRIPTION OF THE PROCESSES OF MASS SCATTERING OF DIRAC FIELDS

J.G. Cardoso

Department of Mathematics, Quaid-i-Azam University,
Islamabad, Pakistan.

ABSTRACT

A set of twistorial formulae for the null graphs that describe the mass scattering of Dirac fields in real Minkowski space is explicitly derived. Making particular use of two holomorphic expressions for the generalized mass-scattering differential forms we transcribe directly the scattering integrals into the framework of twistor theory.

1. INTRODUCTION

In an earlier work [1], null initial data (NID) techniques [2,3] were used to describe completely the processes of mass scattering of Dirac fields in real Minkowski space $\mathbb{RM}$. In accordance with the relevant prescriptions, the pair of Dirac fields is split up into an infinite number of elementary contributions whose scaling invariant (SI) densities satisfy Dirac-like field density equations on the interior $\mathbb{V}_o^+$ of the future cone of an origin O of $\mathbb{RM}$. These elementary fields actually propagate for a while as if they were massless, but scatter off each other at suitable points of $\mathbb{V}_o^+$. Likewise the NID for the scattering processes are explicitly evaluated at appropriate vertices of mass-scattering null zigzags (MSNZZ's) that start at O and terminate at a fixed point lying in $\mathbb{V}_o^+$. Such scattering data appear indeed to be generated by those which are specified on the future null cone C_o^+ of O. It was shown that the null graphs carry edge-vertex structures which contain all the information about the processes. Each element of the Dirac-field pair turned out, then, to be entirely recovered by two infinite series of terms which were expressed as manifestly finite SI scattering integrals taken over abstract spaces of adequate MSNZZ's.

This paper is mainly concerned with transcribing the mass-scattering integrals into the framework of twistor theory. We present a set of twistorial formulae for MSNZZ's which are directly obtained from the definition and properties of the graphs (Sec.2). Each holomorphic twistor NI datum is defined on a product space which involves two subspaces of the Riemann spheres that are associated with certain

projective lines (Sec.3). We exhibit two conjugate twistorial expressions which represent SI volume-forms defined on the abstract space of MSNZZ's carrying an arbitrary number of edges. Either of these differential forms involves twistors of the same valence, and is defined on a product space of subsets of Riemann spheres associated with appropriate vertices of MSNZZ's (Sec.4). All the twistorial field integrals arising here involve SI holomorphic projective structures. The definition of the contours over which the integrals for contributions of any order are taken, is explicitly given (Sec.5). For the sake of completeness, we shall briefly review the basic prescriptions for building up the RM-scattering integrals.

One of the main motivations lying behind our procedures is the fact that we might eventually gain new insights into the theory of twistors upon transcribing explicit field integrals arising from the use of NID techniques. Indeed our holomorphic scattering differential forms are here thought of as bearing a certain deal of universality. It is thus believed that this work could be of some relevance to the twistor programme [4-6]. The unprimed and primed fields with which we deal here will be referred to as left-handed and right-handed fields, respectively. However, there will be no attempt at this stage to look upon them as quantum fields.

2. TWISTORIAL FORMULAE FOR MASS-SCATTERING NULL ZIGZAGS

An MSNZZ is [1] a simple connected oriented colored graph ζ_N in $\mathbb{RM}$, with $N \geq 2$, whose vertex-set is

$$V(\zeta_N) = \{ {}^{0}x^{AA'}, {}^{1}x^{AA'}, {}^{2}x^{AA'}, \ldots, {}^{N}x^{AA'} \}, \tag{2.1}$$

where ${}^{b+1}x^{AA'}$ is future-null separated from ${}^{b}x^{AA'}$, b running over the values 0,1,2,...,N-1. In fact, it is this forwardness what defines the orientation of ζ_N. By definition, the vertex ${}^{0}x^{AA'}$ is identified with O whence ${}^{1}x^{AA'} \in C_O^+$. All the vertices ${}^{2}x^{AA'}, {}^{3}x^{AA'}, \ldots, {}^{N}x^{AA'}$ belong to $\mathbb{V}_O^+$, ${}^{N}x^{AA'}$ being identified with the (fixed) point at which all the elementary fields are effectively evaluated. The edge-set of ζ_N is defined by

$$E(\zeta_N) = \{ {}^{1}r, {}^{2}r, {}^{3}r, \ldots, {}^{N}r \}, \tag{2.2}$$

where each ${}^{m}r$ is a suitable affine parameter on the generator γ_m of the future null cone C_{m-1}^+ of ${}^{m-1}x^{AA'}$ that passes through ${}^{m}x^{AA'}$. It actually connects the vertices ${}^{m-1}x^{AA'}$ and ${}^{m}x^{AA'}$. For $N > 2$, any one of the (N - 2) internal edges connects two vertices of different colors. Both the starting-vertex (O) and the end-vertex (${}^{N}x^{AA'}$) of ζ_N carry no color, while each of the vertices connected by internal edges carries either the white color or the black color, the allowable forward configurations accordingly being <white-black> and <black-white>. Each white (black) vertex represents the mass scattering of a left-handed (right-handed) field. Indeed the (colored) vertex ${}^{N-1}x^{AA'}$ is the point at which the scattering process giving rise to an outgoing field of order N - 2 takes place. Evidently, the number of colored vertices of

$V(\zeta_N)$ is equal to N - 1 in any case. The cases for which N = 2 correspond to the "zeroth-mass-scattering processes". For odd-order elementary contributions, the associated graphs carry the same number of white and black vertices which is, in effect, equal to $\frac{N-1}{2}$. It follows that the vertex $\overset{1}{x}^{AA'}$ of each of these graphs bears the white color or the black color according as the corresponding outgoing field is right- or left-handed. In the case of even-order (massive) left-handed fields, the number of white (resp. black) vertices equals $\frac{N}{2}$ (resp. $\frac{N}{2} - 1$). For (higher) even-order right-handed contributions, these numbers turn out to be interchanged. Hence, in the latter even-order case, each relevant vertex $\overset{1}{x}^{AA'}$ is white or black depending upon whether the outgoing field is left- or right-handed. It should be noticed that this prescription still works in the case of the massless free contributions. It will become clear later (see Sec.5) that each colored vertex is indeed associated with the integral of a suitable differential form. Any elementary field thus appears to be unambiguously represented by an MSNZZ. Accordingly, we have the colored-vertex structures

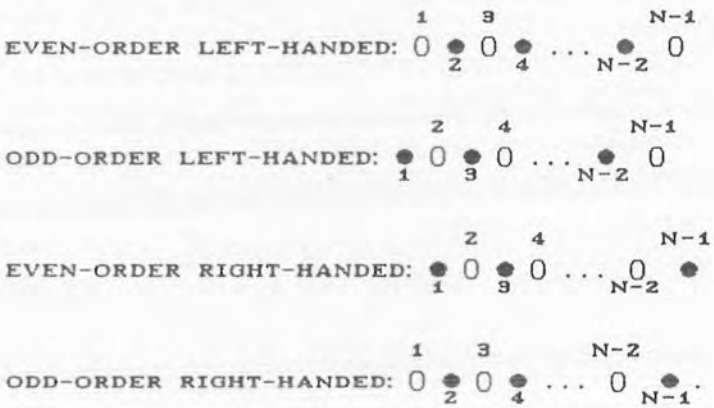

We shall return to the description of the scattering processes in Sec.5 upon recalling the rules for building up the explicit field integrals. Our discussion together with the above-given prescriptions will allow one to achieve at once the graphical recovery of the complete fields as exhibited in Ref.1.

We equip each MSNZZ whose edge-set possesses N elements with a forward spin-basis set consisting of pairs of spin bases

$$\{\{o^{bA}, o^{b+1A}\}, \{o^{-A'}_{b}, o^{-A'}_{b+1}\}\}, \tag{2.3a}$$

which are suitably set up at the vertex $x^{bAA'}$, with the conjugate spin-inner products

$$z^{b} = o^{bA}\, o^{b+1}_{A}, \quad \bar{z}^{}_{b} = o^{-A'}_{b}\, o^{-}_{b+1A'} \tag{2.3b}$$

not being necessarily held fixed, b running over the same values as before (see (2.1)). This procedure actually enables one to carry out [1] the explicit evaluation of the graph that represents any elementary contribution. The suitability to which we have somehow referred above is particularly related to the fact that the flagpoles $\{o^{b+1}_{A}\, o^{-}_{b+1A'}\}$ are taken to be covariantly constant along the (null) geodesics $\{\gamma_{b+1}\}$, in addition to being future-pointing real null vectors. We shall see that the inner products at O are relevant only to odd-order fields. The abstract (compactified) space of such MSNZZ's is defined by

$$\mathbb{K}^{123\ldots N-1} \cong (S^1 \times S^2) \times (S^1 \times S^2) \times \ldots \times (S^1 \times S^2) \times S^2, \tag{2.4}$$

where S^1 and S^2 stand for the usual one- and two-spheres. The number of $(S^1 \times S^2)$-factors occurring in the topological product (2.4) is equal to

the number, N - 2, of internal edges of the relevant graphs. For N >2, these factors actually specify the topology that appears to be relevant to the integration of SI three-differential forms set up at the (colored) vertices $x^{1AA'}, x^{2AA'}, \ldots, x^{N-2AA'}$ of an element of (2.4), whereas the "end-factor" S^2 is correspondingly associated with the integration of a Kirchoff-D'Adhemar-Penrose (KAP) two-form [1,3] at $x^{N-1AA'}$ (see also Sec.5 below). Clearly, $\dim \overset{123\ldots N-1}{\mathbb{K}} = 3N - 4$. In particular, for N = 2 we have

$$\overset{1}{\mathbb{K}} \cong S^2, \tag{2.5}$$

which is the relevant statement for the case of the "zeroth-order scattering processes".

To translate the geometric properties of MSNZZ's directly into twistor terms, we take some $\zeta_{j+1} \in \overset{123\ldots j}{\mathbb{K}}$, $j \in \mathbb{N}$, with $\mathbb{N}$ denoting the set of natural numbers. Introduce the set of conjugate null twistors

$$T(\zeta_{j+1}) = \{\overset{0}{W}_\alpha, \overset{0}{Z}^\beta, \overset{1}{W}_\alpha, \overset{1}{Z}^\beta, \ldots, \overset{j+1}{W}_\alpha, \overset{j+1}{Z}^\beta\}, \tag{2.6}$$

where

$$\overset{m}{W}_\alpha = (\overset{m}{o}_A, -ix^{mAA'}\overset{m}{o}_A) = (\overset{m}{o}_A, \overset{m}{W}^{A'}), \tag{2.7a}$$

$$\overset{m}{Z}^\beta = (ix^{mAA'}\bar{o}_{mA'}, \bar{o}_{mA'}) = (\overset{m}{Z}^A, \bar{o}_{mA'}), \tag{2.7b}$$

pass through $x^{mAA'} \in V(\zeta_{j+1})$, with m = 0,1,2,...,j+1. The spinors involved in (2.7) enter into the definition of the forward spin-basis set for ζ_{j+1} whence each twistor pair $\{\overset{m}{W}_\alpha, \overset{m}{Z}^\beta\}$ can be associated with the geodesic γ_m whenever m takes on the values 1,2,3,...,j+1. The

elements of the pair $\{\overset{o}{W}_{\alpha}, \overset{\beta}{Z}_{o}\}$ are held fixed, and play an auxiliary role when the transcription of the odd-order contributions is explicitly carried out. It is obvious that the above twistors satisfy the following incidence relations at $\overset{n}{x}^{AA'}$

$$\overset{\mu}{Z}_{n}\ \overset{n+1}{W}_{\mu} = 0 = \overset{\mu}{Z}_{n+1}\ \overset{n}{W}_{\mu},\ n = 0,1,2,\ldots,j. \qquad (2.8)$$

The set (2.6) is here called the twistor set for ζ_{j+1}. Thus, the (real) vertex $\overset{n}{x}^{AA'}$ is defined by [4]

$$\overset{n}{x}^{AA'} = \frac{(-i)}{\overset{n}{z}}\ (\overset{n+1}{o}^{A}\ \overset{n}{W}^{A'} - \overset{n}{o}^{A}\ \overset{n+1}{W}^{A'}) = \frac{i}{\overset{-}{z}_{n}}\ (\overset{A}{Z}_{n}\ \overset{-A'}{o}_{n+1} - \overset{A}{Z}_{n+1}\ \overset{-A'}{o}_{n}), \qquad (2.9)$$

where the z-factors are indeed the spin-inner products at $\overset{n}{x}^{AA'}$. A manifestly SI twistorial version of (2.9) is

$$\overset{n}{X}_{\alpha\beta} = 2(I^{\mu\nu}\overset{n}{W}_{\mu}\ \overset{n+1}{W}_{\nu})^{-1}\ \overset{n}{W}_{[\alpha}\ \overset{n+1}{W}_{\beta]}, \qquad (2.10)$$

or, alternatively,

$$\overset{\alpha\beta}{X}_{n} = 2(I_{\mu\nu}\ \overset{\mu}{Z}_{n}\ \overset{\nu}{Z}_{n+1})^{-1}\ \overset{[\alpha}{Z}_{n}\ \overset{\beta]}{Z}_{n+1}, \qquad (2.11)$$

with $I^{\mu\nu}$ and $I_{\mu\nu}$ being the usual infinity twistors [6], and the square brackets denoting skew-symmetrization.

Let us consider the connected-vertex relation

$$\overset{h}{x}^{AA'} - \overset{h-1}{x}^{AA'} = \overset{h}{r}\ \overset{h}{o}^{A}\ \overset{-A'}{\rho_{h}},\ h = 1,2,3,\ldots,j, \qquad (2.12)$$

where $\overset{h}{r} \in E(\zeta_{j+1})$. Transvecting (2.12) with $\overset{h-1}{o}_{A}\ \overset{-}{o}_{h+1A'}$ and using (2.7) together with the null-separation property

$$Z^{A}_{h+1} = i\,X^{h+1AA'}\,\bar{o}_{h+1A'} = iX^{hAA'}\,\bar{o}_{h+1A'}\,, \tag{2.13}$$

we readily obtain the relation

$$r^{h} = i\,\frac{Z^{\lambda}_{h+1}\;W^{h-1}_{\lambda}}{(I^{\alpha\beta}\,W^{h-1}_{\alpha}\;W^{h}_{\beta})(I_{\mu\nu}\;Z^{\mu}_{h}\;Z^{\nu}_{h+1})}\,. \tag{2.14}$$

Obviously the complex conjugate of (2.14) is

$$r^{h} = (-i)\,\frac{Z^{\lambda}_{h-1}\;W^{h+1}_{\lambda}}{(I^{\alpha\beta}\;W^{h}_{\alpha}\;W^{h+1}_{\beta})(I_{\mu\nu}\;Z^{\mu}_{h-1}\;Z^{\nu}_{h})}\,. \tag{2.15}$$

We now contract the usual duality relation [4] between $X^{k}_{\alpha\beta}$ and $X^{\lambda\tau}_{k}$ with $W^{k-1}_{\alpha}\;W^{k+2}_{\beta}$, k = 1,2,3,...,j-1, to obtain

$$(Z^{\alpha}_{k}\;W^{k+2}_{\alpha})(Z^{\beta}_{k+1}\;W^{k-1}_{\beta}) = (-1)\,\frac{(I_{\rho\sigma}\;Z^{\rho}_{k}\;Z^{\sigma}_{k+1})}{(I^{\mu\nu}W^{k}_{\mu}\;W^{k+1}_{\nu})}\,\varepsilon^{\alpha\beta\gamma\delta}\;W^{k-1}_{\alpha}\;W^{k}_{\beta}\;W^{k+1}_{\gamma}\;W^{k+2}_{\delta}\,, \tag{2.16}$$

where the relations (2.8) have been taken into account. Hence, combining (2.14) and (2.15) with (2.16) yields the structure

$$r^{k}\;r^{k+1} = (-1)\,\frac{\varepsilon^{\alpha\beta\gamma\delta}\;W^{k-1}_{\alpha}\;W^{k}_{\beta}\;W^{k+1}_{\gamma}\;W^{k+2}_{\delta}}{(I^{\alpha\beta}W^{k-1}_{\alpha}\;W^{k}_{\beta})(I^{\gamma\delta}\;W^{k}_{\gamma}\;W^{k+1}_{\delta})(I_{\rho\sigma}\;Z^{\rho}_{k}\;Z^{\sigma}_{k+1})(I^{\lambda\tau}W^{k+1}_{\lambda}\;W^{k+2}_{\tau})}\,, \tag{2.17}$$

whose complex conjugate is written as

$$
{}^{k}_{r}\,{}^{k+1}_{r} = (-1)\,\frac{\varepsilon_{\alpha\beta\gamma\delta}\;{}^{\alpha}_{k-1}Z\;{}^{\beta}_{k}Z\;{}^{\gamma}_{k+1}Z\;{}^{\delta}_{k+2}Z}{(I_{\alpha\beta}\;{}^{\alpha}_{k-1}Z\;{}^{\beta}_{k}Z)(I_{\gamma\delta}\;{}^{\gamma}_{k}Z\;{}^{\delta}_{k+1}Z)(I^{\rho\sigma}\;{}^{k}_{\rho}W\;{}^{k+1}_{\sigma}W)(I_{\lambda\tau}\;{}^{\lambda}_{k+1}Z\;{}^{\tau}_{k+2}Z)}\,. \tag{2.18}
$$

In (2.17) and (2.18), the ε-twistors are indeed the alternating twistors for the standard frames [4]. For k=1 the above expressions carry the twistors ${}^{o}_{\alpha}W$, ${}^{\beta}_{o}Z$, and will actually appear as auxiliary structures in the twistorial integrals for odd-order fields (see Sec.5). Now holding fixed both the starting-vertex and the end-vertex of ζ_{j+1}, we derive the relations

$$
{}^{\lambda}_{j}Z\;d\,{}^{j+1}_{\lambda}W = i(I_{\mu\nu}\;{}^{\mu}_{j}Z\;{}^{\nu}_{j+1}Z)\,{}^{j+1}_{r}(I^{\rho\sigma}\;{}^{j+1}_{\rho}W\;d\,{}^{j+1}_{\sigma}W), \tag{2.19}
$$

and

$$
{}^{\lambda}_{z}Z\;d{}^{1}_{\lambda}W = i(I_{\mu\nu}\;{}^{\mu}_{1}Z\;{}^{\nu}_{z}Z)\,{}^{1}_{r}(I^{\rho\sigma}\;{}^{1}_{\rho}W\;d{}^{1}_{\sigma}W), \tag{2.20}
$$

along with their complex conjugates.

We must emphasize that the above formulae have been derived independently of whether the graph taken as prototype represents an even- or an odd-order field of a given handedness. Nevertheless, it should be particularly pointed out that the type of the twistor inner products carried by the denominators of (2.17) and (2.18) is intimately related to the color of the vertices at which these inner products are defined. For k > 1, there are six colored vertices that are connected by the edges entering into the structures, the forward configurations being <white-black-white> and <black-white-black>. Actually these

configurations are appropriate for higher even-order fields, with the former (latter) being relevant when ζ_{j+1} represents a left- (right-) handed field. In either case, the element $\overset{k}{x}^{AA'}$ of $V(\zeta_{j+1})$ evidently appears as a middle vertex, the internal edges of $E(\zeta_{j+1})$ being the only affine parameters allowed for. Thus the corresponding denominator carries the (conjugate) inner products at $\overset{k}{x}^{AA'}$ along with the ones which are set up at the other two vertices of the relevant configuration. These two inner products actually carry W_α- or Z^β-twistors depending upon whether the vertices at which they are defined bear the white color or the black color. When k = 1, the edge $\overset{1}{r}$ comes into play, and the (uncolored) origin accordingly contributes a suitable inner product to each of the expressions. This is indeed the case wherein ζ_{j+1} represents an odd- order field of either handedness. Of course, similar considerations are also applicable to (2.14) and (2.15). We will make one further point concerning this latter situation in Sec.5.

We end this section by considering the SI two-form of surface area $\overset{h}{\mathcal{S}}$ of the (space-like) intersection of the future null cone C^+_{h-1} of $\overset{h-1}{x}^{AA'}$ with the past null cone C^-_{h+1} of $\overset{h+1}{x}^{AA'}$, with h running over the same values as in (2.12). In fact, these two-forms are always set up at the colored vertices of $V(\zeta_{j+1})$, the relevant defining expression being

$$\overset{h}{\mathcal{S}} = \frac{i}{\overset{h}{Z}\,\overset{-}{\overset{h}{Z}}}\, \overset{h}{o}_A\, \overset{-}{\overset{h+1}{o}}_{A'}\, d\overset{h}{x}^{AA'} \wedge \overset{h+1}{o}_B\, \overset{-}{\overset{h}{o}}_{B'}\, d\overset{h}{x}^{BB'} . \qquad (2.21)$$

Differentiating (2.7a) and making adequate contractions, we obtain the structure

$$\underset{\sim}{\mathcal{S}}^{h} = (-i)\,\frac{{}_{h+1}Z^{\lambda}_{h}\,dW_{\lambda}\wedge {}_{h}Z^{\tau}\,d\,W_{\tau}}{(I^{\alpha\beta}W_{\alpha}\,W_{\beta})(I_{\mu\nu}{}_{h}Z^{\mu}\,{}_{h+1}Z^{\nu})}. \qquad (2.22)$$

Clearly its complex conjugate is

$$\underset{\sim}{\mathcal{S}}^{h} = i\,\frac{W_{\lambda}\,d{}_{h}Z^{\lambda}\wedge W_{\tau}\,d\,{}_{h+1}Z^{\tau}}{(I^{\alpha\beta}W_{\alpha}\,W_{\beta})(I_{\mu\nu}{}_{h}Z^{\mu}\,{}_{h+1}Z^{\nu})}. \qquad (2.23)$$

3. TWISTOR NULL INITIAL DATA

The formal simplicity of the mass-scattering formulae exhibited in Ref.1 rests upon the choice of $\mathcal{C}_{o}^{+}$ as the NID hypersurface for all the elementary fields (see also Sec.5). This fact enables us to use a definition of the relevant twistor NID which is similar to that given earlier by Cardoso in connection with the problem of deriving twistor integrals for massless free fields [8]. In the left-handed case, we thus have

$$(I^{\mu\nu}W_{\mu}W_{\nu})^{2}\,\Psi_{L}(W_{\alpha},W_{\alpha}), \qquad (3.1)$$

as the twistor {1,0;0,0}-NI datum. This complex scalar function is defined on the product space $\mathcal{D}_{oz}^{*}$ of two subspaces $\mathcal{D}_{o}^{*}$ and $\mathcal{D}_{z}^{*}$ of the Riemann spheres $\mathcal{R}_{o}^{*}$ and $\mathcal{R}_{z}^{*}$ that represent the dual projective lines [9] associated with O and $x^{zAA'}$, respectively (see (4.10)). The actual evaluation of the massive contributions involves particularly integrations along the generators of appropriate null cones [10]. Such integrations actually produce an enlargement of the subspace $\mathcal{D}_{z}^{*}$, but

leave $\mathcal{D}_o^*$ unaffected. It follows that $\mathcal{D}_{oz}^*$ in these cases is not precisely the same as that associated with the evaluation of the massless contributions. In any case, the twistor-function kernel carried by (3.1) is a holomorphic function in both W_α^1 and W_α^2, homogeneous of degrees -1 in W_α^1 and -2 in W_α^2, and has a suitable singularity set. It also possesses the symmetry property

$$W_\lambda^1 \frac{\partial}{\partial W_\lambda^2} \Psi_L^o(W_\alpha^1, W_\alpha^2) = 0. \qquad (3.2)$$

Similarly, the holomorphic {0,0;0,1}-NI datum generating right-handed fields is defined on the product space $\mathcal{D}_{oz} = \mathcal{D}_o \times \mathcal{D}_z$ as

$$(I_{\mu\nu} Z_1^\mu Z_2^\nu)^2 \, X_{oR}(Z_1^\beta, Z_2^\beta). \qquad (3.3)$$

It should be clear that the relevant projective lines lie now in the (unstarred) null portion $\mathbb{PN}$ of projective twistor space.

At this stage, it is convenient to introduce the twistor $\hat{\pi}$-NID. These NID involve certain spin operators [8] defined at $x^{AA'} \in C_o^+$ which, in the case of spin $\pm$ 1/2, are given by

$$\hat{\pi}_{1/2-}^1 \Psi_L^o(W_\alpha^1, W_\alpha^2) = (I^{\mu\nu} W_\mu^1 W_\nu^2)^{-1} \, o_A^2 \frac{\partial}{\partial o_A^2} \Psi_L^o(W_\alpha^1, W_\alpha^2), \qquad (3.4)$$

$$\hat{\pi}_{1/2+}^1 X_{oR}(Z_1^\beta, Z_2^\beta) = (I_{\mu\nu} Z_1^\mu Z_2^\nu)^{-1} \, \bar{o}_{2A'} \frac{\partial}{\partial \bar{o}_{2A'}} X_{oR}(Z_1^\beta, Z_2^\beta). \qquad (3.5)$$

Actually the $\hat{\pi}$-operators are defined so as to act only on the twistor-function kernels of (3.1) and (3.3). When multiplied by $(I^{\mu\nu} W_\mu^1 W_\nu^2)^2$, the datum (3.4) gives rise to the holomorphic twistor

{0,-1;0,0}-NI datum on $\mathcal{D}^{*}_{oz}$, while (3.5) similarly turns out to be the holomorphic twistor {0,0;-1,0}-NI datum on $\mathcal{D}_{oz}$, the appropriate inner-product factor for the latter datum being evidently $(I_{\mu\nu}Z_1^{\mu}Z_2^{\nu})^2$.

4. HOLOMORPHIC MASS-SCATTERING DIFFERENTIAL FORMS

We shall next be concerned with deriving two holomorphic expressions for the scattering differential forms that enter explicitly into the RM-field integrals [1,10] (see also Sec.5). As was mentioned before, each of these structures carries twistors of the same type. What happens here is, in effect, that for one handedness the spin-inner products involving spinors of the other handedness are all canceled when the intermediate stages of the transcription process are effectively worked out. The pertinent Minkowskian pattern carries SI differential forms which are defined only at colored vertices of MSNZZ's. Whenever the scattering integrals are actually performed, these forms thus provide the contributions emanating from all the relevant vertices. We will carry through the procedure for deriving the structure that involves W_{α}- twistors without specifying explicitly the colored-vertex structure of the graphs involved. The corresponding structure carrying Z^{β}- twistors will then be obtained by taking a complex conjugation.

For the MSNZZ involved in (2.6), we have the defining expression

$$\underset{\sim}{\mathcal{K}}^{123\ldots j} = (\bigwedge_{k=1}^{j-1}(\underset{\sim}{r}^{k} \wedge \underset{\sim}{\mathcal{S}}^{k}))\wedge \underset{\sim}{\mathcal{K}}^{j}, \qquad (4.1)$$

which is indeed an SI (3j-1)-volume form on $\mathbb{K}^{123\ldots j}$. This volume-form involves the one-form $\underset{\sim}{r}^{k} = \frac{d\underset{\sim}{r}^{k}}{r^{k}}$ at $x^{kAA'} \in V(\zeta_{j+1})$ along with the $\underset{\sim}{\mathcal{P}}^{h}$- forms considered before (see (2.22) and (2.23)). In fact, $\underset{\sim}{\mathcal{P}}^{j}$ enters into it through the SI two-form at $x^{jAA'}$

$$\underset{\sim}{\mathcal{K}}^{j} = \frac{\underset{\sim}{\mathcal{P}}^{j}}{z_{j}^{-}\underset{\sim}{r}^{j}\underset{\sim}{r}^{j+1}}, \tag{4.2}$$

where $\underset{\sim}{r}^{j}$ and $\underset{\sim}{r}^{j+1}$ belong both to $E(\zeta_{j+1})$. Now, working out successive steps, we arrive at the following SI expression at $x^{kAA'}$

$$\underset{\sim}{r}^{k} = (-1)\frac{(I_{\mu\nu k-1}Z^{\mu}_{1}\,Z^{\nu}_{k})}{(I_{\mu\nu}\,Z^{\mu}_{k}\,Z^{\nu}_{k+1})(Z^{\lambda}_{k-1}\,W^{k+1}_{\lambda})}\,(Z^{\tau}_{k+1}\,d\,W^{k+1}_{\tau} + i\sum_{n=1}^{k-1}\xi^{n}\,d\underset{\sim}{r}^{n}), \tag{4.3}$$

with ξ^{n} being the real scalar

$$\xi^{n} = (I^{\alpha\beta}W^{n}_{\alpha}\,W^{k+1}_{\beta})(I_{\mu\nu}\,Z^{\mu}_{n}\,Z^{\nu}_{k+1}). \tag{4.4}$$

In addition, a straighforward calculation yields the relation [10]

$$Z^{\alpha}_{k}\,d\,W^{k+1}_{\alpha} \wedge Z^{\beta}_{k+1}\,d\,W^{k+1}_{\beta} \wedge Z^{\gamma}_{k+2}\,d\,W^{k+1}_{\gamma} = \frac{(I_{\mu\nu k+1}Z^{\mu}_{k+1}\,Z^{\nu}_{k+2})}{(I^{\alpha\beta}\,W^{k+1}_{\alpha}\,W^{k+1}_{\beta})}\,(Z^{\lambda}_{k}\,W^{k+2}_{\lambda})\Delta\,W^{k+1}, \tag{4.5}$$

where

$$\Delta\,W^{k+1} = 1/3!\,\varepsilon^{\alpha\beta\gamma\delta}\,W^{k+1}_{\alpha}\,d\,W^{k+1}_{\beta} \wedge d\,W^{k+1}_{\gamma} \wedge d\,W^{k+1}_{\delta} \tag{4.6}$$

is the standard dual projective twistor three-form [4,7]. Thus replacing both (2.22) and (4.3) into (4.1), and making use of (2.19),

(2.20) and (4.5), we obtain the SI holomorphic structure

$$\underset{\sim}{\mathcal{K}}^{123\ldots j} = i^{j}\ \frac{I^{\alpha\beta}{}^{1\ 1}W_{\alpha}dW_{\beta} \wedge (\overset{j-1}{\underset{k=1}{\Lambda}}\Delta^{k+1}\ W^{\ }) \wedge I^{\mu\nu}{}^{j+1\ j+1}W_{\mu}d\,W_{\nu}}{\overset{j}{\underset{h=1}{\Pi}}(I^{\rho\sigma}{}^{h\ h+1}W_{\rho}\ W_{\sigma})^{2}}. \qquad (4.7)$$

It is useful to note that the wedge-products actually "annihilate" those terms of (4.3) involving the ξ-scalars when the relevant blocks are fitted together. Evidently, the conjugate of (4.7) is given by

$$\underset{\sim}{\mathcal{K}}^{123\ldots j} = (-i)^{j}\ \frac{I_{\alpha\beta}{}^{1}Z^{\alpha}dZ^{\beta}_{1} \wedge (\overset{j-1}{\underset{k=1}{\Lambda}}\Delta_{k}Z_{1}) \wedge I_{\mu\nu}{}_{j+1}Z^{\mu}_{1}d_{j}Z^{\nu}_{1}}{\overset{j}{\underset{h=1}{\Pi}}(I_{\rho\sigma}{}_{h}Z^{\rho}_{h}\ Z^{\sigma}_{1})^{2}}, \qquad (4.8)$$

where

$$\Delta_{k+1}Z = 1/3!\,\varepsilon_{\alpha\beta\gamma\delta}\ {}_{k+1}Z^{\alpha}\ d_{k+1}Z^{\beta} \wedge d_{k+1}Z^{\gamma} \wedge d_{k+1}Z^{\delta} \qquad (4.9)$$

is the projective three-form corresponding to (4.6). We notice, also, that all the twistors carried by the above Δ-forms are associated with the internal edges of ζ_{j+1}.

The differential form (4.7) can be defined on the product space

$$\mathcal{P}^{*}_{012\ldots j+1} = \mathcal{D}^{*}_{0} \times \overset{j-1}{\underset{n=1}{X}}(\mathcal{D}^{*}_{n} \times \mathcal{D}^{*}_{n+1}) \times \mathcal{D}^{*}_{j+1}, \qquad (4.10)$$

where "X" stands for topological product. Each $\mathcal{D}^{*}_{m}$ is a subset of the Riemann sphere $\mathcal{R}^{*}_{m}$ that represents the (dual) projective line $\mathcal{X}^{*}_{m}$ associated with the vertex $x^{mAA'}$. We thus have $\mathcal{D}^{*}_{m} \subset \mathcal{R}^{*}_{m} \cong \mathcal{X}^{*}_{m}$ and, in the

null portion $\mathbb{PN}^*$ of dual projective twistor space, the product $\mathcal{D}^*_n \times \mathcal{D}^*_{n+1}$ consists only of points representing W^{n+1}_α. For $j > 1$, the number of two-factor products entering into (4.10) is equal to the number $(j-1)$ of internal edges of $E(\zeta_{j+1})$. Each such product actually contributes a three-real-dimensional contour to the integration of any "higher-order" twistorial scattering differential form. This contour is, in effect, involved in the integration of the twistor three-form associated with the internal edge r^{n+1} of the relevant graph (namely ΔW^{n+1}_α). Moreover, it does not appear to be the product $S^2 \times S^1$ associated with $x^{nAA'}$, but picks out the S^1-factor of the structure for this vertex. Its required three-dimensionality turns out to be made up by S^1-contributions coming appropriately from the structures associated with both $x^{nAA'}$ and $x^{n+1AA'}$. Additionally, the subspace in which it lies has to be suitably enlarged so as to accommodate the relevant singularities. For $j = 1$, the subsets $\mathcal{D}^*_0$ and $\mathcal{D}^*_{j+1}$ coincide with those given by Cardoso [8], the product (4.10) being accordingly reduced to $\mathcal{D}^*_{0z} = \mathcal{D}^*_0 \times \mathcal{D}^*_z$. Of course, the former (latter) case appears to be of relevance when we consider massive (massless) elementary fields. In either case, $\mathcal{D}^*_0$ and $\mathcal{D}^*_{j+1}$ consist only of the dual projective twistors $\{W^1_\alpha\}$ and $\{W^{j+1}_\alpha\}$, respectively. Each of these twistors contributes a one-real-dimensional (closed) contour to any integration which is actually an S^1 coming from the splitting of the S^2-parts of the structures for $x^{1AA'}$ and $x^{jAA'}$. For (4.8), a similar prescription can be given. Now the projective lines lie all in $\mathbb{PN}$, the pertinent product-space structure being essentially the same as that for (4.7). In fact, the integration of either of the forms (4.7) and (4.8) does not play any important role here, but the

above prescription will be used to some extent in Sec.5 for defining the explicit contours for the twistorial scattering integrals. There we will have necessarily to take into account the singularities of the integrands when constructing the relevant product spaces.

5. TWISTORIAL MASS-SCATTERING INTEGRALS

Our main aim here is to carry out the actual twistorial transcription of the Minkowskian scattering integrals [1], making explicit use of the formulae exhibited in the foregoing sections. In this connection, we shall first briefly review the prescriptions for building up these RM-integrals, but only the left-handed expressions will be shown. As far as our translation method is concerned, it will suffice once again to carry through explicitly only the procedures yielding the left-handed twistorial integrals. Thereafter the right-handed holomorphic structures will be directly introduced on the basis of trivial handedness rules.

According to what was mentioned earlier, the colored- vertex structures of the graphs representing two elementary contributions of the same order $\{{}^{j-1}\psi_{A}(x), {}_{j-1}\chi_{1}^{A'}(x)\}$ can be built up from one another by applying a simple white-black interchange rule. These contributions are obviously the outgoing fields involved in the scattering processes of order j - 1. It turns out that the scattering integrals for such fields are taken over spaces of MSNZZ's carrying the same number of edges. It is evident that this result amounts to the same thing as saying that the scattering data for both fields carry explicitly the same affine-parameter structures. Indeed the vertex configurations not only

specify the spin-inner products carried by these data but also constitute a label device whereby each field may be clearly identified. The denominator of the expression for either scattering datum actually carries the product of the affine parameters corresponding to the internal edges of some suitable ζ_{j+1} together with the spin-inner products that are set up at the colored vertices of $V(\zeta_{j+1})$. Each of these inner products appears to be unbarred or barred according as the vertex at which it is defined carries the white color or the black color. In the case of either process, the inner product at $x^{1AA'}$ is suitably carried by the appropriate $\hat{\pi}$-NI datum on C_o^+ which enters explicitly into the numerator of the relevant scattering datum along with the mass-factor $(\mu/2\pi)^{j-1}$ and the differential form (4.1). Therefore the numerators carry also the "outgoing" spinors $\{{}^{j+1}o_A, \bar{o}_{j+1A'_j}\}$ which are really taken up by the KAP integrals of the two-form $\underset{\sim}{\mathcal{K}}$. Actually, when j=1 ("zeroth-order processes"), the "scattering" data appear to be nothing else but the $\hat{\pi}$-NID on C_o^+. Consequently, in the even-order left-handed case, the general pattern of the scattering integrals is

$$ {}^{2K}\psi_A(x) \doteq \frac{c_K}{2\pi} \int_{\substack{123\ldots 2K+1 \\ \mathbb{K}}} {}^{2K+2}o_A \frac{\hat{\pi}_{1/2-}\, {}^{o}\psi_L({}^{1}o^{M}; {}^{1}x)\; \underset{\sim}{\mathcal{K}}^{123\ldots 2K+1}}{\left(\prod_{n=1}^{K} {}^{2n+1}z\right)\left(\prod_{m=1}^{K} \bar{z}_{2m}\right)\left(\prod_{p=1}^{2K} {}^{p+1}r\right)}, \quad (5.1) $$

where j=2K+1 and $c_K = (\mu/2\pi)^{2K}$, with $K \in \mathbb{N} \cup \{0\}$. Evidently the denominator of each scattering datum entering into (5.1) carries $\frac{j-1}{2}$ pairs of affine parameters. Hence, using (2.17) and noting that

$$\frac{1}{\left(\prod_{p=1}^{2K} {}^{p+1}r\right)} = \frac{1}{\left(\prod_{\text{even } p=0}^{2K-2} {}^{p+2}r\ {}^{p+3}r\right)}, \tag{5.2}$$

we readily obtain the expression

$$\frac{1}{\left(\prod_{n=1}^{K} {}^{2n+1}z\right)\left(\prod_{m=1}^{K} {}^{\bar{}}z_{2m}\right)\left(\prod_{p=1}^{2K} {}^{p+1}r\right)} = (-1)^{K} \frac{\left(\prod_{h=1}^{2K} I^{\alpha\beta\,h}\ {}^{h+1}W_{\alpha}\ {}^{h+1}W_{\beta}\right)}{\prod_{\text{even } p=0}^{2K-2} \varepsilon^{\mu\nu\lambda\tau}\ {}^{p+1}W_{\mu}\ {}^{p+2}W_{\nu}\ {}^{p+3}W_{\lambda}\ {}^{p+4}W_{\tau}}, \tag{5.3}$$

where the twistors involved belong all to the twistor set for some appropriate $\zeta_{2K+2} \in \mathbb{K}^{123\ldots 2K+1}$. It is obvious that the affine parameters carried by (5.3) belong to $E(\zeta_{2K+2})$ whenever K takes on values in $\mathbb{N}$. The coupling of the left-handed $\hat{\pi}$-datum on C_o^+ with $I^{\mu\nu}\,{}^{1}W_{\mu}\,{}^{1}dW_{\nu}$ can be immediately achieved [8] by using the following formal relation at ${}^{1}x^{AA'} \in V(\zeta_{2K+2})$

$$\overset{2}{o}_{A} I^{\alpha\beta}\,{}^{1}W_{\alpha}\,{}^{1}dW_{\beta} = (I^{\alpha\beta}\,{}^{1}W_{\alpha}\,{}^{2}W_{\beta})\,d\overset{1}{o}_{A} + \underset{\sim}{\nu}\ \overset{1}{o}_{A}, \tag{5.4}$$

which, when combined together with (3.2) and (3.4), yields

$$-\hat{\pi}_{1}\ {}_{1/2-}\overset{0}{\Psi}_{L}(W_{\alpha},W_{\alpha})I^{\mu\nu}\,{}^{1}W_{\mu}\,{}^{1}dW_{\nu} = \underset{\sim}{\overset{0}{\Psi}}_{L}(W_{\alpha},W_{\alpha}) = -\frac{\partial}{\partial\,{}^{2}W_{\lambda}}\overset{0}{\Psi}_{L}(W_{\alpha},W_{\alpha})\,{}^{1}dW_{\lambda}, \tag{5.5}$$

the involved twistor one-form possessing the homogeneity-symmetry property

$$\underset{\sim}{\overset{0}{\Psi}}_{L}(\mu W_{\alpha},\lambda\,{}^{1}W_{\alpha}+\tau\,{}^{2}W_{\alpha}) = \tau^{-3}\,\underset{\sim}{\overset{0}{\Psi}}_{L}(W_{\alpha},W_{\alpha}), \tag{5.6}$$

with $\lambda \in \mathbb{C}$ and $\mu,\ \tau \in \mathbb{C} - \{0\}$. In (5.4), $\underset{\sim}{\nu}$ is a one-form at ${}^{1}x^{AA'}$ which

automatically carries the appropriate spin-weight, but it does *not* enter into (5.5) because of the property (3.2). It should be observed that (5.6) is a massless-free-field property for the case of spin - 1/2. Now, combining (4.7), (5.1), (5.3) and (5.5), we are led to the SI twistorial scattering integral for $^{2K}\psi_A(x)$

$$\frac{c_K}{2\pi i}\oint_{\substack{123\ldots 2K+2\\ \Gamma_L}} {}^{2K+2}O_A \frac{(I^{\lambda\tau}W_\lambda{}^1 W_\tau{}^2)^2\ {}^0\underset{\sim}{\Psi}_L(W_\alpha{}^1, W_\alpha{}^2)\wedge (\overset{2K}{\underset{m=1}{\wedge}}\Delta\ W^{m+1})\wedge I^{\mu\nu}\ W_\mu^{2K+2}\ dW_\nu^{2K+2}}{(I^{\alpha\beta}W_\alpha^{2K+1}\ W_\beta^{2K+2})^2\ (\overset{2K}{\underset{n=1}{\prod}}\ I^{\rho\sigma}W_\rho^{n}\ W_\sigma^{n+1})}$$

$$\times\ \frac{1}{(\overset{2K-2}{\underset{\text{even } p=0}{\prod}}\ \varepsilon^{\mu\nu\lambda\tau}W_\mu^{p+1}\ W_\nu^{p+2}\ W_\lambda^{p+3}\ W_\tau^{p+4})}\ , \qquad (5.7)$$

whose integrand accordingly carries K alternating-twistor pieces. The corresponding RM-integral expressions for the odd-order left-handed fields (j=2K+2) are given by

$$^{2K+1}\psi_A(x) = \frac{C_K}{2\pi}\int_{\substack{123\ldots 2K+2\\ \mathbb{K}}} {}^{2K+3}O_A \frac{\hat{\pi}_1^{1/2+\sigma}R(o_1^{-M'};\overset{1}{x})\ \underset{\sim}{\chi}^{123\ldots 2K+2}}{(\overset{K+1}{\underset{m=1}{\prod}}\ ^{2m}z)(\overset{K}{\underset{n=1}{\prod}}\ \bar{z}_{2n+1})(\overset{2K+1}{\underset{p=1}{\prod}}r^{p+1})}\ , \qquad (5.8)$$

with $C_K = (\mu/2\pi)^{2K+1}$. In order to transcribe these (latter) elementary contributions, we have to modify the NI datum on C_o^+. In fact, there two obvious reasons for carrying through this procedure. The first reason rests upon the fact that each scattering datum in this odd-order case involves explicitly an odd number of affine parameters in its

denominator whence, as the situation stands at this stage, we cannot form any number of r-pairs. The second reason is that, towards building up expressions carrying only independent twistors, it is imperative to convert the information carried by the spinor $\overset{-A'}{o}_1$ into information carried by $\overset{2}{W}^{A'}$. A suitable prescription consists in using the following twistor relation at the element $\overset{1}{x}^{AA'}$ of an appropriate $V(\zeta_{2K+3})$

$$\overset{2}{W}^{A'} = i(I^{\alpha\beta}\overset{1}{W}_{\alpha}\overset{2}{W}_{\beta})\overset{1}{r}\,\overset{-A'}{o}_1 , \tag{5.9}$$

according to which the parameter $\overset{1}{r} \in E(\zeta_{2K+3})$ is effectively brought about. It follows that $\overset{1}{x}^{AA'}$ appears now as a (black) middle vertex in (2.17), and we end up with K+1 pairs of relevant edges provided that

$$\frac{\hat{\pi}_{1/2+\delta}\,\chi_R(\overset{-M'}{o}_1;\overset{1}{x})}{\overset{2}{r}}\,\overset{1}{o}_A d\overset{1}{o}^A = (-i)\frac{(I^{\alpha\beta}\overset{0}{W}_{\alpha}\overset{1}{W}_{\beta})(I^{\mu\nu}\overset{1}{W}_{\mu}\overset{2}{W}_{\nu})^3(I^{\lambda\tau}\overset{2}{W}_{\lambda}\overset{3}{W}_{\tau})}{(\varepsilon^{\alpha\beta\gamma\delta}\,\overset{0}{W}_{\alpha}\overset{1}{W}_{\beta}\overset{2}{W}_{\gamma}\overset{3}{W}_{\delta})}\,\underset{\sim}{X}_R(\overset{1}{W}_{\alpha},\overset{2}{W}_{\alpha}), \tag{5.10}$$

where

$$\underset{\sim}{X}_R(\overset{1}{W}_{\alpha},\overset{2}{W}_{\alpha}) = -\frac{\partial}{\partial\overset{2}{W}_{\lambda}}X_R(\overset{1}{W}_{\alpha},\overset{2}{W}_{\alpha})d\overset{1}{W}_{\lambda}. \tag{5.11}$$

It is of some interest to remark explicitly that this modified one-form possesses the same homogeneity degrees as those for twistor functions generating massless free fields [8,11] of spin -1/2. It thus carries a (holomorphic) homogeneous twistor function on $\mathcal{D}^{*}_{oz}$, satisfying

$$\overset{1}{W}_{\lambda}\frac{\partial}{\partial\overset{2}{W}_{\lambda}}X_R(\overset{1}{W}_{\alpha},\overset{2}{W}_{\alpha}) = 0. \tag{5.12}$$

Hence, invoking (5.10) and adopting a procedure similar to that yielding (5.7), we obtain the SI structure for $\overset{2K+1}{\Psi}_A(x)$

$$\frac{C_K}{2\pi i}\oint_{\substack{123\ldots 2K+3\\ \Gamma_L}} {}^{2K+3}_{O}A\;\frac{(I^{\lambda\tau}\overset{1}{W}_\lambda\overset{2}{W}_\tau)^2\;\underset{\sim}{X}_R(\overset{1}{W}_\alpha,\overset{2}{W}_\alpha)\wedge(\overset{2K+1}{\underset{m=1}{\Lambda}}\Delta\overset{m+1}{W})\wedge I^{\mu\nu}\overset{2K+3}{W}_\mu\;\overset{2K+3}{dW}_\nu}{(I^{\alpha\beta}\overset{2K+2}{W}_\alpha\;\overset{2K+3}{W}_\beta)^2\,(\overset{2K+1}{\underset{n=1}{\Pi}}I^{\rho\sigma}\overset{n}{W}_\rho\,\overset{n+1}{W}_\sigma)}$$

$$\times\;\frac{(I^{\alpha\beta}\overset{0}{W}_\alpha\overset{1}{W}_\beta)}{(\underset{even}{\overset{2K}{\underset{q=0}{\Pi}}}\varepsilon^{\mu\nu\lambda\tau}\overset{q}{W}_\mu\,\overset{q+1}{W}_\nu\,\overset{q+2}{W}_\lambda\,\overset{q+3}{W}_\tau)}\;, \qquad (5.13)$$

which obviously involves twistors belonging to $T(\zeta_{2K+3})$.

The Γ_L's appearing beneath the integral signs in (5.7) and (5.13) mean that all the integrals are taken over suitable closed contours lying in appropriate product spaces. In either massive case, the integration of any "internal" twistor $\overset{M+1}{W}_\alpha$ is performed in three steps. The S^2-part of the factor associated with any colored vertex is suitably replaced by $S^1 \times S^1$. Hence the relevant three-dimensional contour turns out to be $S^1 \times S^1 \times S^1$. Two of these factors are indeed involved in two steps of the integration under consideration which are carried out by holding fixed (one at a time) the vertices $\overset{MAA'}{x}$ and $\overset{M+1AA'}{x}$, one S^1 thus lying in $\mathcal{D}^*_M$ and the other in $\mathcal{D}^*_{M+1}$. The third step is carried out on the product space $\mathcal{D}^*_M \times \mathcal{D}^*_{M+1}$, and involves integrating over a contour ($\cong S^1$) which is associated with the RM- integration along the generator γ_M. At this stage, both $\overset{MAA'}{x}$ and $\overset{M+1AA'}{x}$ move such that this S^1-contour moves continuously without crossing any singularity. The relevant singularity set is essentially provided by

the structure of the denominator occurring explicitly in the integral.

In the even-order massive case ($K \geq 1$), the appropriate product space for the integrations of W_α^1 and W_α^2 is $\mathcal{D}_0^* x \mathcal{D}_1^* x \mathcal{D}_2^* x \mathcal{D}_3^* x \mathcal{D}_4^*$. The W_α^1-integration is taken along a one-real-dimensional closed path $\Gamma_1 \cong S^1$ contained in $\mathcal{D}_0^*$, while the W_α^2-integration is taken over a three-real-dimensional contour $\Gamma_2 \cong S^1 x\ S^1 x\ S^1$ contained in $\mathcal{D}_1^* x\ \mathcal{D}_2^*$. The integrations of W_α^{2K+1} and W_α^{2K+2} are performed over contours lying in the product space

$$\mathcal{P}_K^* = \bigtimes_{n=2K-2}^{2K+2} \mathcal{D}_n^* . \qquad (5.14)$$

For the W_α^{2K+1}-integration, we have the contour $\Gamma_{\substack{2K+1 \\ 2K+2}} \cong S^1 x\ S^1 x\ S^1$ which is contained in $\mathcal{D}_{2K}^* x\ \mathcal{D}_{2K+1}^*$, whereas for the W_α-integration the contour is a one-real-dimensional closed path $\Gamma_{2K+2} \cong S^1$ contained in $\mathcal{D}_{2K+2}^*$. Notice that, for K=1, (5.14) coincides with the product space for the W_α^1- and W_α^2-integrations, but the contour for the W_α^{2K+1}-integral, for instance, is now contained in $\mathcal{D}_2^* x\ \mathcal{D}_3^*$. Whenever K>1, both the W_α^{2N-1}- and W_α^{2N}-integrations are carried out on the space

$$\mathcal{P}_{N-1\ N}^* = \bigtimes_{h=2N-4}^{2N+2} \mathcal{D}_h^* , \quad N=2,3,4,\ldots,K , \qquad (5.15)$$

the contours Γ_{2N-1} and Γ_{2N} being accordingly contained in $\mathcal{D}_{2N-2}^* x \mathcal{D}_{2N-1}^*$ and $\mathcal{D}_{2N-1}^* x\ \mathcal{D}_{2N}^*$, respectively. In particular, for K = 0, we have

$$\overset{o}{\psi}_A(x) = \frac{1}{2\pi i} \oint_{\Gamma_L^{12}} \overset{2}{o}_A \underset{\sim}{\Psi}_L^{o}(W_\alpha^1, W_\alpha^2) \wedge I^{\mu\nu} W_\mu^2 dW_\nu^2 , \qquad (5.16)$$

which is the twistorial integral for the left-handed massless free

elementary contribution. In particular, this integral is taken over a suitable contour $\Gamma^{12}_{L} \cong S^1 \times S^1$ lying in $\mathcal{D}^*_{02}$. General expressions for the case of arbitrary spin are given in Ref.8.

In the case of odd-order massive fields ($K \geq 0$), the vertex prescription given above still applies. The arbitrary (fixed) twistor W^o_α comes now into play through

$$\mathcal{D}^*_{-1} = \{W^o\}, \tag{5.17}$$

where W^o is the point of $\mathbb{PN}^*$ defining the equivalence class $[\lambda W^o_\alpha]$, $\lambda \in \mathbb{C}-\{0\}$. The product space for the W^1_α-integration turns out to be $\mathcal{D}^*_{-1} \times \mathcal{D}^*_{2H} \times \mathcal{D}^*_{1} \times \mathcal{D}^*_{2H+1} \times \mathcal{D}^*_{3}$. For higher odd-order contributions, the integrations of W_α and W_α are taken over contours Γ_{2H} and Γ_{2H+1} ($\cong S^1 \times S^1 \times S^1$) lying, respectively, in the subspaces $\mathcal{D}^*_{2H-1} \times \mathcal{D}^*_{2H}$ and $\mathcal{D}^*_{2H}$ and $\mathcal{D}^*_{2H+1}$ which are contained in

$$\mathcal{P}^*_{H\ H+1} = \bigtimes_{n=2H-3}^{2H+3} \mathcal{D}^*_n, \quad H=1,2,3,\ldots,K. \tag{5.18}$$

The W^{2K+2}_α-integration is taken over a closed contour $\Gamma_{2K+2} \cong S^1 \times S^1 \times S^1$ lying in $\mathcal{D}^*_{2K+1} \times \mathcal{D}^*_{2K+2}$ which enters into

$$\mathcal{P}^*_{K+1} = \bigtimes_{m=2K-1}^{2K+3} \mathcal{D}^*_m, \tag{5.19}$$

while the W^{2K+3}_α-integration is taken along a closed path $\Gamma_{2K+3} \cong S^1$ lying in $\mathcal{D}^*_{2K+3} \subset \mathcal{P}^*_{K+1}$. It is worth remarking explicitly that the subscripts borne by the left-hand sides of (5.14), (5.15), (5.18) and (5.19) can effectively label the alternating-twistor pieces carried by the integrands of (5.7) and (5.13).

In either case, all the integrations involved in the actual evaluation of any contribution are carried out independently of one another. The viability of this procedure is due to the fact that the RM-integration along a suitable edge $\overset{k}{r}$ is expressed as an integral of the twistor $\overset{k+1}{W}_{\alpha}$ (see (4.3)). To any order, the contours suitably avoid the singularities of the integrand, separating them into (closed) subsets of the relevant product spaces. These contours cannot be continuously shrunk to a point without crossing some singularity. In addition, we should emphasize that the singularities of both twistor-datum one-forms appear to be relevant only to the integrations of the twistors $\overset{1}{W}_{\alpha}$ and $\overset{2}{W}_{\alpha}$.

It has become manifest that the Minkowskian integral expressions for right-handed contributions can be at once derived from those for the corresponding left-handed fields by taking a complex conjugation and replacing adequately the $\hat{\pi}$-data on C_o^+. In accordance with this result, explicit calculations show us that the right-handed twistorial integrals can be obtained from (5.7) and (5.13) by making the simultaneous replacements

$$\overset{o}{\Psi}_L \longrightarrow \underset{oR}{X}, \quad X_R \longrightarrow \Psi_L, \quad \overset{n}{W}_{\alpha} \longrightarrow \underset{n}{Z}^{\beta}, \qquad (5.20)$$

where n runs over the values 1,2,3,...,2K+2 in the case of even-order contributions, and over the values 0,1,2,...,2K+3 in the case of odd-order fields. We thus have for $\underset{2K}{\chi}^{A'}(x)$

$$\frac{c_K}{2\pi i}\oint_{\substack{123\ldots 2K+2\\ \Gamma_R}} \overset{-A'}{\underset{2K+2}{\circ}} \frac{(I_{\lambda\tau}Z_1^{\lambda}Z_2^{\tau})^2\ \underset{\sim}{\overset{\vee}{\circ}}R(Z_1^{\beta},Z_2^{\beta})\wedge(\overset{2K}{\underset{m=1}{\wedge}}\Delta Z_{m+1})\wedge I_{\mu\nu 2K+2}Z_{2K+2}^{\mu}\,dZ_{2K+2}^{\nu}}{(I_{\alpha\beta 2K+1}Z_{2K+1}^{\alpha}Z_{2K+2}^{\beta})^2\ (\overset{2K}{\underset{n=1}{\prod}} I_{\rho\sigma n}Z_{n+1}^{\rho}Z_{n+1}^{\sigma})}$$

$$\times\ \frac{1}{(\underset{even}{\overset{2K-2}{\underset{p=0}{\prod}}}\varepsilon_{\mu\nu\lambda\tau}Z_{p+1}^{\mu}Z_{p+2}^{\nu}Z_{p+3}^{\lambda}Z_{p+4}^{\tau})}, \qquad (5.21)$$

and for $\chi^{A'}_{2K+1}(x)$

$$\frac{C_K}{2\pi i}\oint_{\substack{123\ldots 2K+3\\ \Gamma_R}} \overset{-A'}{\underset{2K+3}{\circ}} \frac{(I_{\lambda\tau}Z_1^{\lambda}Z_2^{\tau})^2\ \underset{\sim}{\overset{\Psi}{\circ}}L(Z_1^{\beta},Z_2^{\beta})\wedge(\overset{2K+1}{\underset{m=1}{\wedge}}\Delta Z_{m+1})\wedge I_{\mu\nu 2K+3}Z_{2K+3}^{\mu}\,dZ_{2K+3}^{\nu}}{(I_{\alpha\beta 2K+2}Z_{2K+2}^{\alpha}Z_{2K+3}^{\beta})^2\ (\overset{2K+1}{\underset{n=1}{\prod}} I_{\rho\sigma n}Z_{n+1}^{\rho}Z_{n+1}^{\sigma})}$$

$$\times\ \frac{(I_{\alpha\beta 0}Z_1^{\alpha}Z_1^{\beta})}{(\underset{even}{\overset{2K}{\underset{q=0}{\prod}}}\varepsilon_{\mu\nu\lambda\tau}Z_q^{\mu}Z_{q+1}^{\nu}Z_{q+2}^{\lambda}Z_{q+3}^{\tau})}\ . \qquad (5.22)$$

The right-handed massless free contribution is particularly given by

$$\chi_0^{A'}(x) = \frac{1}{2\pi i}\oint_{\substack{12\\ \Gamma_R}} \overset{2A'}{\underset{2}{\circ}} \underset{\sim}{\overset{\chi}{\circ}}R(Z_1^{\beta},Z_2^{\beta})\wedge I_{\mu\nu 2}Z_2^{\mu}dZ_2^{\nu}\ . \qquad (5.23)$$

The Γ_R's bear a meaning similar to that of the left-handed case. All the basic prescriptions are essentially the same as the previous ones, but the relevant projective lines lie now in $\mathbb{PN}$.

6. CONCLUDING REMARKS AND OUTLOOK

The twistorial transcription presented here exhibits some remarkable features. One of these is the correspondence between the handedness of the fields and the valence of the twistors involved in the respective field integrals. All the left-handed contributions are, in effect, given as integrals carrying only $[\,{}^{o}_{1}\,]$-twistors, while the field integrals for all the right-handed elements involve only $[\,{}^{1}_{o}\,]$-twistors. It is believed that this feature would eventually play an important role in a quantum description of the fields [5]. Another feature of the holomorphic differential structures occurring in the explicit twistorial scattering integrals is their invariance under both Poincaré transformations and arbitrary rescalings of the elements of the relevant forward spin-basis sets.

Most noteworthy is the relationship between the nullity of the graphical Minkowskian structures that describe the scattering processes and the total skew-symmetry of the holomorphic scattering differential forms. This insight has actually emerged from the transcription procedures given here. Moreover, it seems to indicate that standard sets of twistor formulae arising directly from the actual transcription of NID expressions must consist of SI integrals that involve skew-symmetric holomorphic projective structures.

In respect of the desirable independence of the W_{α}- and Z^{β}-twistor subsets involved in the definition of the twistor set for some MSNZZ, it is worth pointing out that the inner products carrying the elements of the associated spin-basis set can be effectively introduced regardless of whether they are held fixed at the outset.

Indeed this result appears to be an immediate consequence of the fact that the spinors entering into their definition are not solutions of the underlying field density equations. In case we had initially held them fixed, we might think of each corresponding twistor inner product as a (holomorphic) two-variable twistor function after carrying through the pertinent procedures.

The existence of the (closed) contours over which the scattering integrals appear to be taken, has indeed been assumed from the beginning. This assumption rests upon the fact that our scattering forms are intimately associated with essentially null graphs in $\mathbb{RM}$. A formal proof of the relevant statement is still required, however. We believe, also, that a representation of the scattering integrals in terms of twistor diagrams will afford us new insights into the theory of twistors. It should be emphazised that our prescription for specifying the topology of the contours was based only upon the simplicity of all poles occurring in the integrands of the twistorial field integrals. In particular, this has allowed us to carry out the splitting of the space-like S^2-spheres in a trivial way. Nevertheless, we must observe that an alternative contour prescription can well be used without making it necessary to call for other product-space structures.

ACKNOWLEDGMENTS

I am deeply indebted to Professor Roger Penrose for providing me with the techniques upon which this work is essentially based. I would like to acknowledge Dr. Asghar Qadir for some useful suggestions. My warmest thanks go to the World Laboratory for financial support.

REFERENCES

1. Cardoso J G 1991 Intern. Jour. Theor. Phys. Vol.30 12, 1566-1588.

2. Penrose R 1980 General Relativity and Gravitation 12, 225.

3. Penrose R and Rindler W 1984 "*Spinors and Space-Time*", Vol.1 (Cambridge : CUP).

4. Penrose R 1975 "*Twistor Theory: Its Aims and Achievements*" (Quantum Gravity: An Oxford Symposium) eds. C J Isham, R Penrose and D W Sciama (Oxford, Clarendon) pp. 268-407.

5. Penrose R 1975 "*Twistor and Particles*" (Quantum Theory and the Structures of Time and Space) eds. L Castell, M Drieschner and C F Weiszacker (Verlag, München, 1975), pp. 129-145.

6. Penrose R 1977 Reports on Mathematical Physics 12, 65.

7. Penrose R and MacCallum MAH 1972 Physics Reports 6C, 241.

8. Cardoso J G 1991 Intern. Jour. Theor. Phys. Vol.30 4, 447-461.

9. Penrose R and Rindler W 1986 "*Spinors and Space-Time*", Vol.2 (Cambridge: CUP).

10. Cardoso J G 1988 M.Sc.Thesis (University of Oxford).

11. Penrose R. and Ward R.S. 1980 "*Twistors for Flat and Curved Spacetime*" (General Relativity and Gravitation, One Hundred Years After the Birth of Albert Einstein) ed. A Held (New York: Plenum), pp. 283-328.